CORE
Metadata, citation and similar papers at core.ac.uk
Provided by Chalmers Publication Library

CHALMERS

Towards Active Car Body Suspension in Railway Vehicles

JESSICA FAGERLUND

Department of Signals and Systems
CHALMERS UNIVERSITY OF TECHNOLOGY
Göteborg, Sweden 2009

THESIS FOR THE DEGREE OF LICENTIATE OF ENGINEERING

Towards Active Car Body Suspension in Railway Vehicles

JESSICA FAGERLUND

Department of Signals and Systems
CHALMERS UNIVERSITY OF TECHNOLOGY
Göteborg, Sweden 2009

Towards Active Car Body Suspension in Railway Vehicles

JESSICA FAGERLUND

Technical Report No R009/2009
ISSN 1403-266X

Department of Signals and Systems
Mechatronics Research Group
Chalmers University of Technology
SE-412 96 Göteborg, Sweden
Telephone +46 (0) 31 772 10 00

© 2009 Jessica Fagerlund
All rights reserved

Printed by Chalmers Reproservice
Göteborg, Sweden 2009

Typeset by the author with the LaTeX Documentation System

abstract

Towards Active Car Body Suspension in Railway Vehicles
Jessica Fagerlund

Department of Signals and Systems
Chalmers University of Technology

Today, most railway suspension systems are passive. The most wide-spread exception is active car body tilt systems, which are mounted in some high-speed trains. Replacing some of the passive suspension components with active could reduce the weight and cost of the vehicle. It may also improve passenger comfort without increasing the deflections within the suspension, or, similarly, allow the vehicle to be run at higher speeds or on less smooth tracks, with comfort and deflection kept at today's levels.

This thesis deals with background studies of a model of a railway vehicle, aiming towards actively controlling its vertical secondary suspension, i.e. the part of the suspension that is fitted vertically between the bogie frame and the car body.

First, some requirements on the actuator, e.g. maximum forces, are studied, for some cases of replacing passive components with active. Those cases are: removing the anti-roll bars, removing the pneumatic systems of the air-spring, and both combined, in all cases adding 2 actuators in the vertical direction for each bogie. The forces the actuators have to be able to deliver are high, but still within reason to implement.

Also, the possibility to use a single-input single-output (SISO) control design is studied. It is found that neither input/output pairing, nor using stationary decoupling matrices, gives any promising results that a SISO control design could be based on. The coupling between the inputs and outputs is found to be both very high, and very frequency dependent.

To make multiple-input multiple-output (MIMO) control design a feasible choice, the original nonlinear model with 330 states is linearized, and different methods of reducing this model are studied. A model reduction algorithm was developed, that was better suited to this problem than the two standard methods it was compared to. The new algorithm is both less computationally demanding, and for this model produces reduced models, that have gain curves that are closer to those of the full linear model, within the interesting frequency region.

Finally, an attempt is made at designing a linear quadratic (LQ) control, and the difficulties with that control strategy on this particular model are discussed.

Additional work is needed to fully understand the model, and to find a control law that offers an advantage over the fully passive system.

KEYWORDS: Active suspension, Decoupling, MIMO systems, Model reduction, LQ control, Railway vehicles

acknowledgments

I want to thank my supervisor and examiner, Jonas Sjöberg, as well as Thomas Abrahamsson, who was my co-supervisor during parts of the project. Thank you Thomas Abrahamsson, Jonas Sjöberg, and Tomas McKelvey for initiating the project.

Thanks to Bombardier Transportation and the center of excellence CHARMEC for sponsoring the work in this thesis, and to Bombardier Transportation for providing me with a model of a train.

Thank you Madeleine Persson and Lars Börjesson, and other administrative and technical staff, for help within those areas.

Finally, I want to thank my present and former colleagues and superiors, and Anna-Karin Christiansson, for valuable discussions on and off topic.

Göteborg, May 2009
Jessica Fagerlund

contents

chapters

chapter i

introduction

Today, most railway suspension systems are passive. The most wide-spread exception is active car body tilt systems, which are mounted in some high-speed trains, (Zolotas, Pearson and Goodall 2006). Replacing some of the passive suspension components with active could reduce the weight and cost of the vehicle, (Ågren 2004–2005). It may also improve passenger comfort without increasing the deflections within the suspension, or, similarly, allow the vehicle to be run at higher speeds or on less smooth tracks, with comfort and deflection kept at today's levels, (Goodall and Mei 2006).

This thesis is a preliminary study, dealing with the questions if it is reasonable to use active secondary suspension, and investigating further which issues that needs to be addressed for the developing of a control strategy.

1.1 Main Contributions

- Estimation of requirements on actuators in Chapter 5.
- Studies of coupling and decoupling in Chapter 7.
- Development of a model reduction technique in Chapter 8.
- Pointing out issues with linear quadratic control for this application in Chapter 9.

1.2 Publications

- Jessica Fagerlund, Jonas Sjöberg and Thomas Abrahamsson: *Passive Railway Car Secondary Suspension - Force, Power, Deflection, Roll and Comfort*, Technical Report, Chalmers University of Technology, 2005.
- Jessica Fagerlund, Jonas Sjöberg and Thomas Abrahamsson: *Briefly on Passive Railway Car Secondary Suspension - Force, Power, Deflection, Roll and Comfort*, Mekatronikmöte (Mechatronics Conference), Halmstad, November 2005.
- Jessica Fagerlund, Jonas Sjöberg, *Active secondary suspension in railway vehicles*, S2 Research Day - Poster Exhibition Abstracts, p. 12, Chalmers: Department of Signals and Systems, October 2008.

The conference paper is a significantly abbreviated version of the internal report. The internal report makes up the basis for Chapter 5, Appendix A, and Appendix D, as well as

parts of Chapter 2 and Chapter 4. The poster abstract briefly introduces the work in this thesis.

1.3 Thesis Outline

Chapter 2 gives a brief overview of background theory regarding railway vehicles in general as well as comfort calculations. In Chapter 3 the research objective is stated, the method is described, and the flow between the chapters is described in more detail than here. Chapter 4 describes the particular model used in this thesis. Chapter 5 deals with the question if it is at all reasonable to use actuators in the vertical secondary part, by estimating what would be required by the actuators. In Chapter 6 deals with if the linear model used is adequate for the task. In Chapter 7, 8, and 9 analysis and preparations regarding control laws are carried out. In those chapters, Chapter 7 deals with whether SISO design is reasonable, 8 deals with model reduction, which is necessary for the use of state feedback, and 9 deals with issues with LQ design. Finally, conclusions and recommendations for future work are found in Chapter 10.

chapter ii

background theory

This chapter introduces the reader to some generally known facts about railway vehicles, active suspension, and how to calculate ride comfort. Other algorithms, that are only used in a single chapter, are introduced in the chapters they are used.

2.1 Introduction to Railway Vehicles

This section offers a very brief introduction to railway vehicles. Significantly more detailed descriptions can be found in for example (Andersson and Berg 1999) and (Andersson, Berg and Stichel 2004).

Railway vehicles are guided by a rail. In the case studied in this thesis, wheels of steel are rolling on steel rails. This is also by far the most common technique for rail vehicles in the world, (Andersson and Berg 1999). By using this technique, the vehicle is generally automatically steered. (The exception is if the wheel axle is removed and the wheels individually steered.) The steering works in the following way: The wheels are shaped in a way that makes the running circle longer if the wheel is moving outwards on the rails. At the same time the wheel on the other side moves inwards (assuming the distance between the rails, called gauge, is constant). This way the wheels on the left and the right side travel different far during one revolution, and this way the wheelset is steering towards centering over the rails, see Figure 2.1.

In many cases, including in this thesis, the wheelsets are connected (by a suspension) two by two to a bogie (wheel truck). The bogies are then connected (by a suspension) to the car body. Using bogies improves the curving performance and decreases the risk of derailment, compared to using a suspension directly between the wheelsets and car body, (Andersson et al. 2004). Also, using bogies makes it possible to reduce car body vibrations as well as wheel-rail forces, (Andersson et al. 2004).

2.1.1 Suspension

This subsection briefly introduces the suspension areas the reader needs to be familiar with to understand this thesis.

In general, the suspension is the set of elastic elements (springs), dampers and associated components which connect the wheelsets to the car body, (Orlova and Boronenko 2006). The suspension can be divided into primary and secondary suspension. The primary suspension is the suspension between the wheelset and the bogie frame. The secondary suspension is the suspension between the bogie frame and the car body, (Andersson and Berg 1999). See

Figure 4.1. The springs are used to equalize the vertical loads between the wheels, stabilize the motion of the vehicle on the track, and to reduce the dynamic forces and accelerations due to track irregularities, (Orlova and Boronenko 2006). Dampers are used to dampen the oscillations in the suspension, (Orlova and Boronenko 2006).

Specific components of the suspension, mentioned in this thesis, are the anti-roll bar, the secondary vertical dampers, and the air-spring with its pneumatic system. A schematic view of an anti-roll bar is shown in Figure 2.2. The anti-roll bar counteracts roll between car body and bogie frame. This is achieved by the design where the long bar acts as a torsional spring. A difference in deflection between bogie frame and car body, between the two sides where the anti-roll bar is attached, will cause a torque in the long bar of the anti-roll bar. Through the levers this torque will transfer into forces, F, acting on the car body, which oppose roll.

The secondary vertical dampers' main task is to dampen roll movement, (Ågren 2004–2005), but they will also dampen vertical movement.

The pneumatic system of the air-spring is intended to keep the car body at the same vertical position regardless of the amount of payload. This is achieved by adding pressurized air through a levelling valve, (Andersson and Berg 1999). The levelling valve can be controlled either passively, (Andersson and Berg 1999), or actively (Ågren 2004–2005).

2.2 Active Suspension in Theory and Practice - Other Research

When the suspension is active, actuators, sensors, and electronic controllers are used, (Goodall and Mei 2006). As a comparison, the conventional, passive, suspension is purely mechanical, (Goodall and Mei 2006). There are three major categories of active suspension that are studied for railway vehicles: active tilting, active secondary suspensions, and active primary suspensions, (Goodall and Mei 2006).

Tilting of the car body is used to reduce the lateral acceleration experienced by the passengers in curves, and by this improving passenger comfort, (Goodall and Mei 2006). Active tilting is a standard technology for railway vehicles, (Goodall and Mei 2006).

Secondary active suspension is intended to improve the vehicle dynamic response and provide a better isolation of the vehicle body to the track irregularities, compared to a fully passive suspension, (Goodall and Mei 2006). The improved performance could for instance be used to improve the comfort for the passengers, (Goodall and Mei 2006). The first commercial use of active secondary suspension was in the Japanese high speed trains (Shinkansen). It was introduced in 2002, and the actuators were installed in the lateral direction, (Goodall and Mei 2006).

Active primary suspension is intended to improve running stability and curving performance, (Goodall and Mei 2006). There is a trade-off between those issues, and it is difficult to further improve both simultaneously with passive techniques, (Goodall and Mei 2006). When using active primary suspension, the wheelsets can be either independently rotating, or connected by a solid axle, (Goodall and Mei 2006). The idea of active primary suspension is relatively new, but has been successfully tested on a full size roller rig in Germany, (Goodall and Mei 2006).

2.3 Human Sensitivity for Accelerations at Different Frequencies

Human beings are sensitive to shaking and can find that unpleasant. The amount of discomfort experienced varies with the frequency of the acceleration. It is possible to weigh the accelerations for a compound motion together and form a single number, that can be used to compare the level of discomfort. This number is called *ride index* or *Wertungszahl (Wz)*. The higher the number is, the worse is the comfort. How to evaluate comfort is described in this section since one of the criterions on if the secondary suspension is good, is passenger comfort.

2.3.1 Ride index

The ride indexes (Wz-numbers) are calculated using the ISO-standard 2631, (*Mechanical vibration and shock - Evaluation of human exposure to whole-body vibration – Part 1: General requirements* 1997). This standard contains different weighing curves for calculation of Wz-numbers depending on position of human and direction of vibration. The transfer functions used to weigh the signals (comfort filters) can be found later in this section. The Wz-number is calculated as follows, (Intec GmbH 2005):

$$Wz = (100 \cdot \sqrt{\sigma_{\mathrm{w}}^2})^{0.3}, \tag{2.1}$$

where σ_{w} is the variance of the output from the comfort filter. The input to the comfort filter is car body accelerations.

Transfer Functions (Comfort Filters)

The transfer functions used to weight the accelerations are

$$H_{\mathrm{W,z}}(s) = \frac{(s + 2\pi \cdot 16)(s^2 + \frac{2\pi \cdot 2.5}{0.8}s + (2\pi \cdot 2.5)^2) \cdot 32.768\pi}{(s^2 + \frac{2\pi \cdot 16}{0.63}s + (2\pi \cdot 16)^2)(s^2 + \frac{2\pi \cdot 4}{0.8}s + (2\pi \cdot 4)^2)} \tag{2.2}$$

in the vertical direction,

$$H_{\mathrm{W,xy}}(s) = \frac{(s + 2\pi \cdot 4)4\pi}{(s^2 + \frac{2\pi \cdot 2}{0.63}s + (2\pi \cdot 2)^2)} \tag{2.3}$$

in the lateral and longitudinal directions, and

$$H_{\mathrm{o}}(s) = \frac{(2\pi \cdot 100)^2}{s^2 + \frac{2\pi \cdot 100}{0.71}s + (2\pi \cdot 100)^2} \tag{2.4}$$

and

$$H_{\mathrm{u}}(s) = \frac{s^2}{s^2 + \frac{2\pi \cdot 0.4}{0.71}s + (2\pi \cdot 0.4)^2} \tag{2.5}$$

for all directions, (Intec GmbH 2005).

The total transfer function of the comfort filter is calculated by $H_{\mathrm{C},i}(s) = H_{\mathrm{W},i}(s) \cdot H_{\mathrm{u}}(s) \cdot H_{\mathrm{o}}(s)$, where $H_{\mathrm{W},i}(s)$ is the weighting filter, and $H_{\mathrm{u}}(s)$ and $H_{\mathrm{o}}(s)$ together makes up the band limiting filter, (Intec GmbH 2005). The subscript i could be either xy or z. When the subscript is xy, the filter is valid in the lateral and longitudinal directions of the vehicle when the passengers are seated or standing. When the subscript is z, the filter is valid in the vertical direction of the vehicle when the passengers are seated or standing. The magnitudes of the total transfer functions, in the frequency interval 0.1–100 Hz, are plotted in Figure 2.3 and Figure 2.4. The accelerations are causing most discomfort in the frequency interval where the magnitude of the comfort filters are largest.

Crest Factors

To check whether it is correct in a specific case to calculate the comfort values using Wz-numbers, the crest factors are studied. The crest factor is defined as the quotient between the maximum acceleration and the rms-value of the acceleration, $a_{\max}/a_{\mathrm{rms}}$. When the maximum and rms-value are determined on the weighted signal, the crest factor should be no higher than 9. If the crest factor is higher than 9, the effect of the motion may be underestimated. Otherwise it is normally sufficiently accurate. The calculation and interpretation of the crest factor are described in the ISO-standard 2631-1:1997(E), (*Mechanical vibration and shock - Evaluation of human exposure to whole-body vibration – Part 1: General requirements* 1997).

Motion Sickness

There is also a weighting curve in the vertical direction for motion sickness (not shown here). This has it peak just below 0.2 Hz, (Andersson et al. 2004). It will however be seen in Chapter 6, that this is outside the range of the validity of the linear model used in this thesis. The motion sickness aspect has therefore not been considered in this thesis.

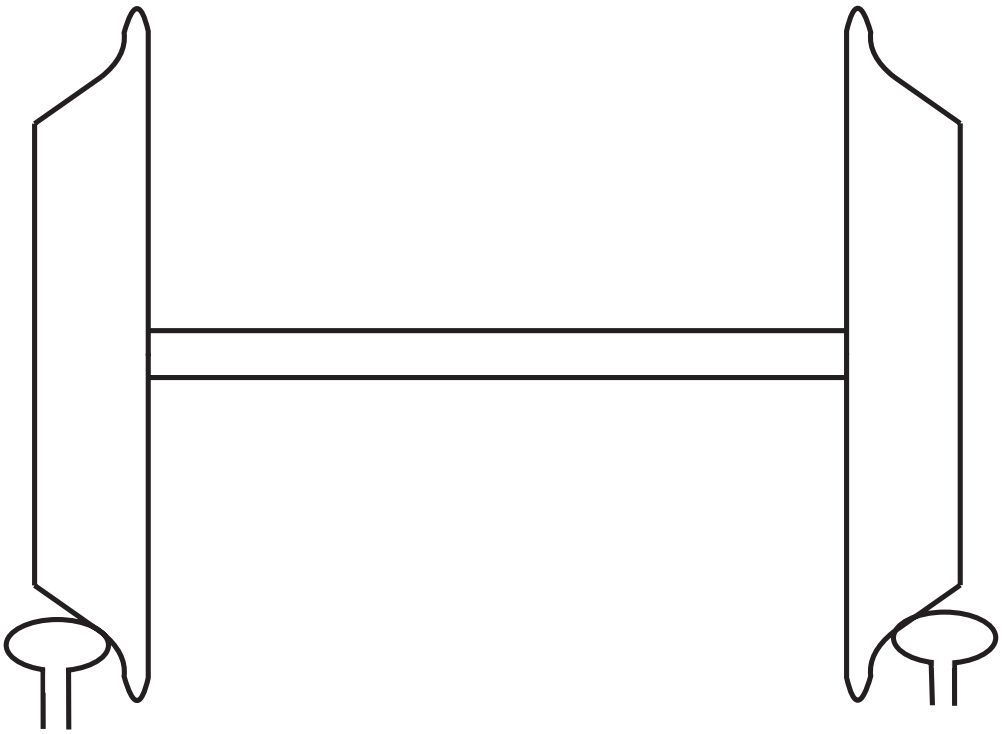

Figure 2.1: Principal sketch of how wheel and rail are designed for automatic steering. (Disproportional and exaggerated for illustrative purposes.)

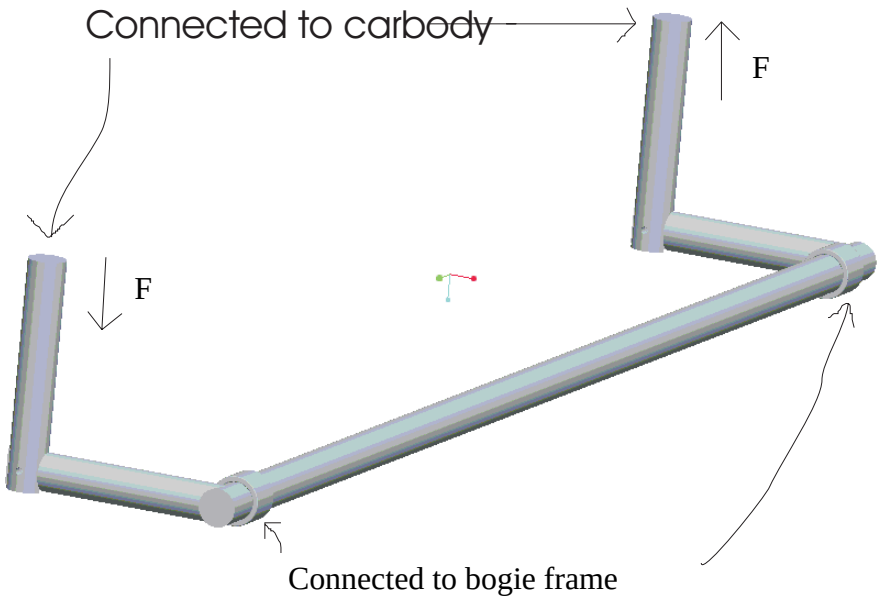

Figure 2.2: Principle of anti-roll bar.

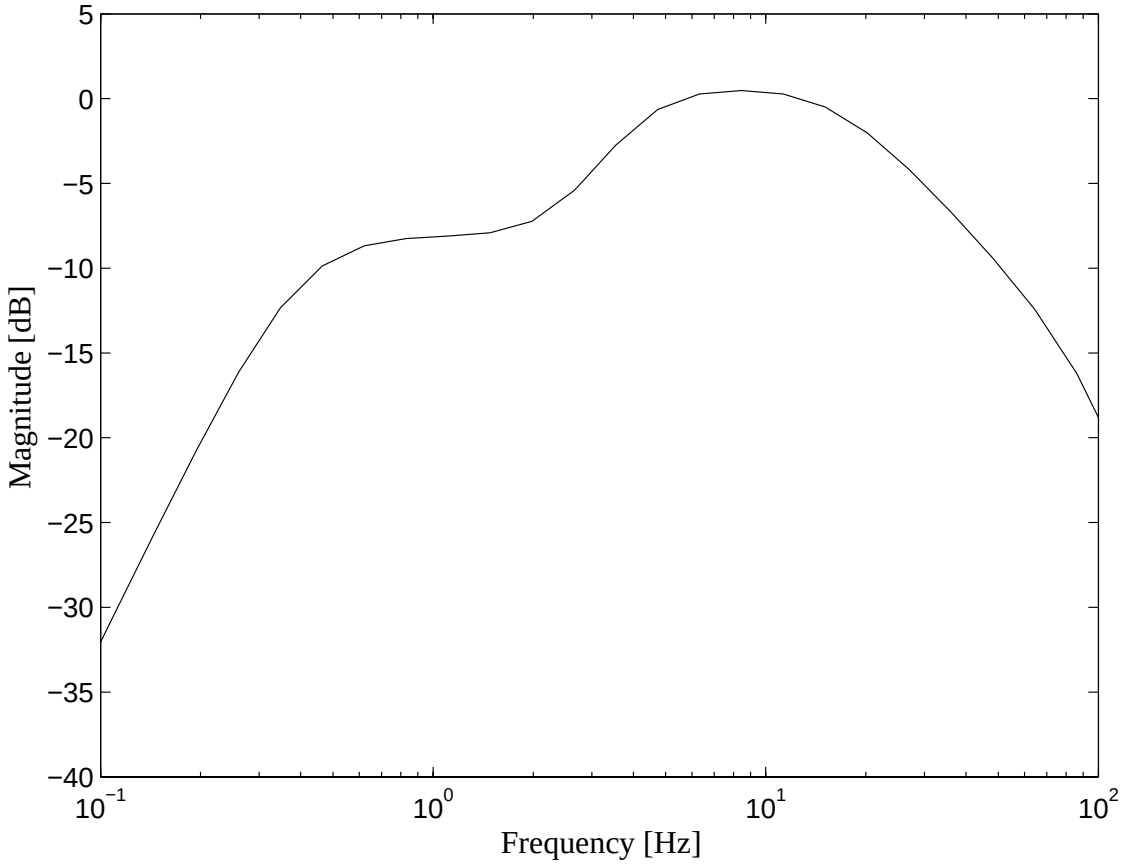

Figure 2.3: Magnitude of total transfer function of the comfort filter, $H_{\mathrm{C,z}}(s)$.

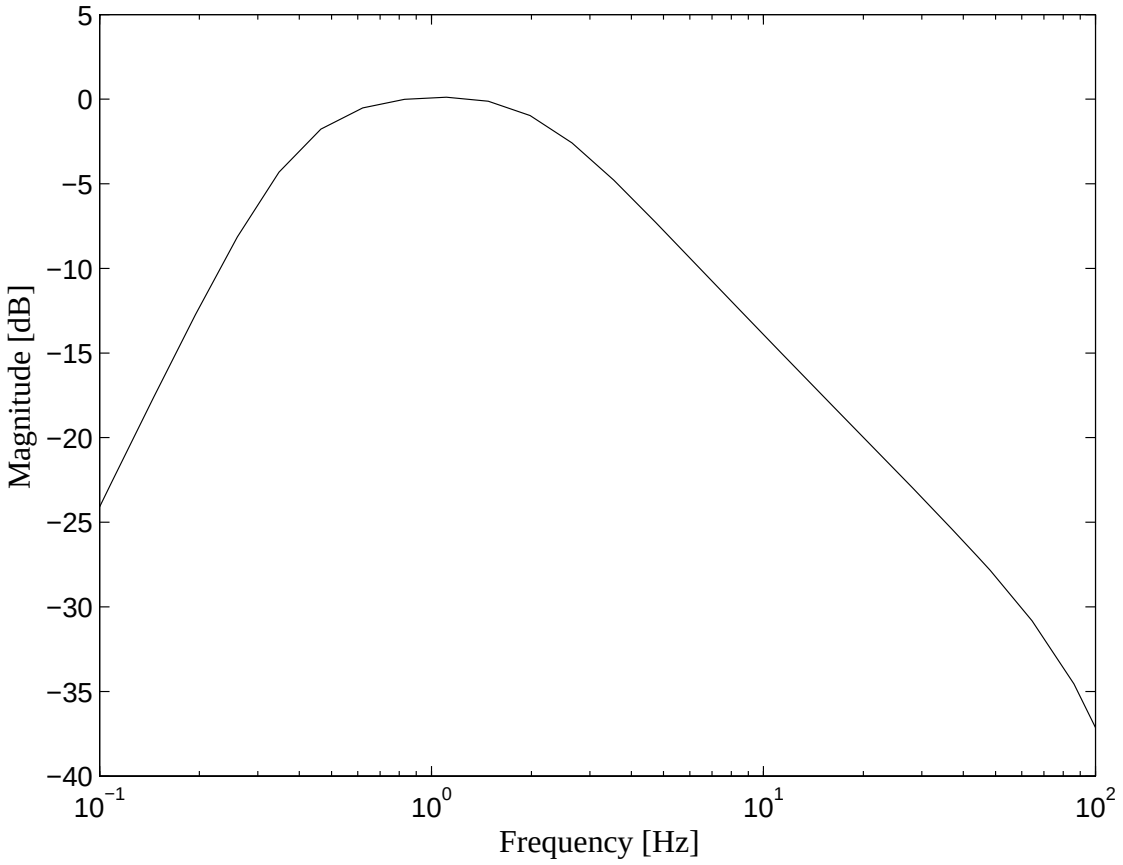

Figure 2.4: Magnitude of total transfer function of the comfort filter, $H_{\mathrm{C,xy}}(s)$.

chapter iii

research objective, methodology and thesis structure

In this chapter the research objectives are stated, an overview on how the work has been carried out is presented, and it is described how the different chapters connect to each other.

3.1 Research Objective

The long term goal is to replace passive suspension components with active, while at the same time improving vehicle performance. Replacing some passive suspension components with active could reduce the weight and cost of the vehicle, (Ågren 2004–2005). Adding active suspension may also improve passenger comfort without increasing the deflections within the suspension, or, similarly, allow the vehicle to be run at higher speeds or on less smooth tracks, with comfort and deflection kept at today's levels, (Goodall and Mei 2006).

The active suspension design can be divided into four areas: which passive components that are replaced with active, where the active components are placed, which control strategy that is used, and which active components, such as sensors and actuators, that are used. In this thesis, only control strategy is considered. Other factors are decided without investigating other options. The sensors and actuators are assumed to be ideal, which means that they have no dynamics in themselves, and are without error or noise.

In this thesis, there is no intention to actually remove any components. It is assumed, that the forces exerted by the passive components, can be calculated approximately and added to the control law, once a control law has been found.

The research objective in this thesis is to analyze a model of a railway vehicle, and to do background studies to prepare for the developing of a control law to be used in an active suspension. The active suspension should be fitted in the vertical direction, between the bogie frames and the car body.

3.1.1 Evaluation Criteria

The main criterion has been chosen as passenger comfort. Passenger comfort is decided by the accelerations, in a way which is described in detail in Section 2.3. Improving comfort tends to increase (worsen) the deflection, which also must be kept under control. Therefore, also deflection is an evaluation criterion. More specifically, the choice has fallen on studying the maximum deflection, since the space available is critical. Also, the requirement on force, power, and speed of the actuator needs to be kept an eye on.

3.2 General Methods

The work has been purely theoretical. The focus has been on computer simulations and analysis. For simulation purposes a large, non-linear model has been used. For analysis and design, linear, and for some cases reduced, models have been used. Those have all been derived from the large, non-linear model.

3.2.1 Software Tools

The model is modeled in the software Simpack, which is a multibody simulation tool, from INTEC GmbH, Weßling, Germany. Simpack is used with the module Simpack Rail, which supports railway simulations. Also, linear state matrices are exported from Simpack to Matlab. In Matlab analysis and control design are carried out. Matlab is used with Control Systems Toolbox and Simulink, also from MathWorks, and with Slicot. Slicot is a subroutine library based on BLAS and LAPACK routines and further developed, partly in the framework of the European project NICONET[1], (Benner, Mehrmann, Sima, Huffel and Varga 1998). Simulations are carried out in Simpack, using the solver SODASRT, and in Simulink, using ODE45 (Dormand-Prince).

3.2.2 Linearization

In the software Simpack, there is a build-in support to create and export linear models. A velocity is set, inputs and outputs are chosen, the wheel-rail contact is linearized, the vehicle is put at (or as close as possible to) equilibrium. Then a linear state space model is created and exported in a format that can be read by Matlab.

During the linearization, the vehicle is positioned on a straight, flat (not leaning) track without any disturbances, and is running at approximately 1 km/h. This velocity is set because zero velocity cannot be used with tangential forces (Intec GmbH 2003). Also, a margin is kept to high velocities, which could induce instability and worsen numerical issues.

3.3 Work Flow and Thesis Structure

In this section, the work flow is described, together with references to in which chapter each part of the work can be found. An overview of the work flow can be seen in Figure 3.1. A more detailed description, that refers to that figure, follows below.

The first main box in Figure 3.1 is labeled ”Configuration”. The more general configurations, regarding choices of model parameters and where the active suspensions is fitted, are described in Chapter 4. In the same chapter the vehicle is briefly described. Also, the measured disturbances are plotted and analyzed. More specific choices of running scenario are described in respective chapter, most notably in Chapter 5.

The second main box in Figure 3.1 is labeled ”Feasibility Studies”. Here it is investigated whether or not it is reasonable to go on with finding a control strategy. In this box, the first box is labeled ”Hardware”. This is referring to the work in Chapter 5, where it is estimated what is required by the actuators in an active secondary suspension, if fitted

[1] http://www.icm.tu-bs.de/NICONET/

as desired. The purpose is to estimate if it is feasible to implement physically, and in that way make the basis of the decision to move on with trying to find a control strategy for this configuration. The second box is labeled ”Model Validity”. This is referring to the work in Chapter 6, where the validity of the linear model is estimated, in order to check that the model can be used in the frequency region that is important from a comfort point of view.

The third main box in Figure 3.1 is labeled ”Control Design”. This term is used here for some background work aiming towards finding a control. (The actual design is left as future work.) In this box, the first box is labeled ”Coupling”. This is referring to the work in Chapter 7, of which the purpose is to investigate the possibilities of splitting the problem into several problems with one input and one output each (SISO design). Here the coupling between different inputs and outputs are studied, and attempts are made at decoupling. This fails. The second box is labeled ”Model Reduction”. This is referring to the work in Chapter 8. Since the attempts at SISO design were unsuccessful, it is desired to try design a control system for using all input and outputs at once (MIMO design). However, to make that task more reasonable, the system needs to be simplified (reduced). The last box is labeled ”MIMO Design Aspects”. Here some issues with MIMO design, concentrating on linear quadratic (LQ) design, are explored.

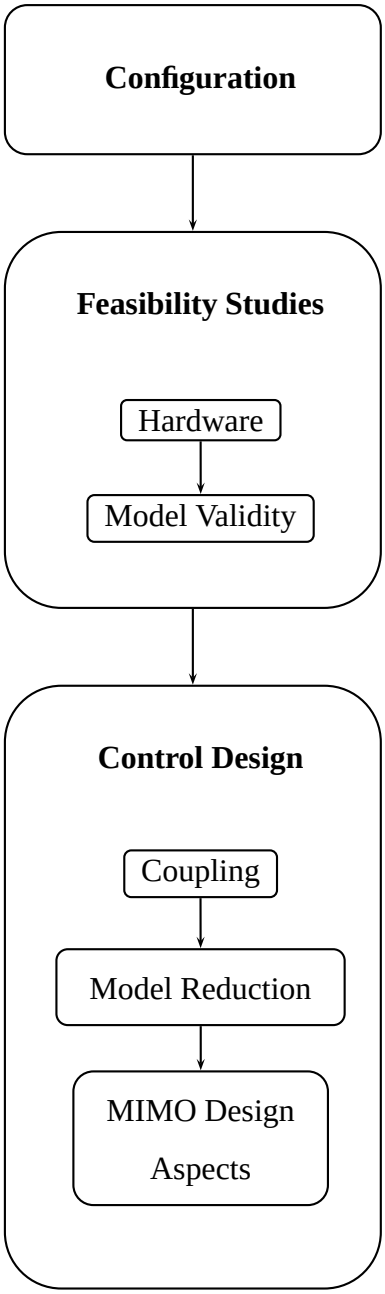

Figure 3.1: Work flow.

chapter iv

model

4.1 Model Structure

All vehicle models used in this report are based on the same three-dimensional, non-linear model of a railway vehicle, obtained from Bombardier Transportation, modeled by Björn Roos. That model is modeled in an MBS (Multi Body Systems) program, and is described in this chapter.

4.1.1 Vehicle

The vehicle is a passenger vehicle. However, where nothing else is noted in this thesis, the passengers are not included in the model. Without passengers the model has 330 states. In some cases passengers are modeled. This is described in Appendix A. The maximum allowed velocity for the vehicle is 200 km/h.

The railway vehicle consists of a single car. It is modeled using rigid bodies, which are connected with various joints and force elements. The car is not quite symmetric in any direction.

4.1.2 Active Suspension

The active suspension (force inputs) has been positioned in the secondary suspension in the vertical direction. The secondary suspension is the suspension between the car body and the bogie frame, as shown in Figure 4.1. To be able to handel both vertical and roll disturbances, there has to be control inputs on both sides of the vehicle.

Four actuators are used. The actuators are placed in the same spots as the vertical secondary dampers. This is not a problem in simulations, and won't be in reality either, since it's assumed that the secondary dampers will be removed before any physical implementation will be attempted.

4.1.3 Inputs and Outputs

The control inputs are actuator forces.

The outputs are car body acceleration as well as the distances between car body and bogie frames. The disturbance inputs have their origin in rail imperfections, which are described as deviations in lateral, vertical, and roll directions. For the simulations (not linear analyzes), there are also deviations in gauge (distance between the rails).

The location of control inputs, disturbances, and outputs are shown in Figure 4.2. The numbering is described below. The control inputs are the following:

$$u = \begin{pmatrix} u_1 \\ u_2 \\ u_3 \\ u_4 \end{pmatrix} = \begin{pmatrix} \text{Actuator force front right} \\ \text{Actuator force front left} \\ \text{Actuator force rear right} \\ \text{Actuator force rear left} \end{pmatrix} \tag{4.1}$$

The outputs are the following:

$$y = \begin{pmatrix} y_1 \\ y_2 \\ y_3 \\ y_4 \\ y_5 \\ y_6 \\ y_7 \\ y_8 \end{pmatrix} = \begin{pmatrix} \text{Acceleration front right} \\ \text{Acceleration front left} \\ \text{Deflection front right} \\ \text{Deflection front left} \\ \text{Acceleration rear right} \\ \text{Acceleration rear left} \\ \text{Deflection rear right} \\ \text{Deflection rear left} \end{pmatrix} \tag{4.2}$$

The disturbances are the following, where the wheelsets are numbered from front to back:

$$w = \begin{pmatrix} w_1 \\ w_2 \\ w_3 \\ w_4 \\ w_5 \\ w_6 \\ w_7 \\ w_8 \\ w_9 \\ w_{10} \\ w_{11} \\ w_{12} \\ \vdots \\ w_{36} \end{pmatrix} = \begin{pmatrix} \text{Lateral deflection first wheelset} \\ \text{Lateral velocity first wheelset} \\ \text{Lateral acceleration first wheelset} \\ \text{Vertical deflection first wheelset} \\ \text{Vertical velocity first wheelset} \\ \text{Vertical acceleration first wheelset} \\ \text{Roll angle first wheelset} \\ \text{Roll angle velocity first wheelset} \\ \text{Roll angle acceleration first wheelset} \\ \text{Lateral deflection second wheelset} \\ \text{Lateral velocity second wheelset} \\ \text{Lateral acceleration second wheelset} \\ \vdots \\ \text{Roll angle acceleration fourth wheelset} \end{pmatrix} \tag{4.3}$$

The disturbances are repeated in the same order for all wheelsets, from first to fourth.

4.2 Measured Input Data

This section deals with the track irregularities exciting the vehicle. The irregularities have been obtained from Bombardier Transportation, and have been measured with 0.5 m interval. That means that if, for example, disturbances up to 20 Hz are desired, the vehicle needs to be run at at least 72 km/h. (The model itself is valid also at lower velocities, but would need other inputs to enable evaluation of the entire interesting frequency region.)

4.2.1 Track Irregularities in Spatial Domain

The measured track irregularities used in this report are shown in Figure 4.3 – Figure 4.6. Note that the scale on the y-axis is not the same in all figures.

4.2.2 Track Irregularities in Frequency Domain

Figure 4.7 – Figure 4.10 show the spatial frequency content of the track irregularities. The frequency content in the time domain depends on vehicle velocity. The dependency of the velocity is due to the fact that when the spatial irregularities are traversed faster or slower, the vehicle will, for the same spatial irregularities, feel different frequencies in Hz. Note that the scale on the y-axis is not the same in all figures.

The frequency content is calculated, using the Welch's method for power spectral density estimate, with a Hamming window, 8 sections, and 50% overlap. Welch's method is chosen, because the PSD is very noise if calculated directly, and Welch's method smoothes this out a bit.

The data is, as previously mentioned, sampled at 0.5 meters interval. The peaks in the irregularities at approximately 0.32 m^{-1} (in Figure 4.7 – Figure 4.10) could be due to an alias phenomenon from the sleeper passage, which in itself has a too high frequency to render properly with those measurement data. The sleeper distance is usually 0.60–0.65 meters at the main railway lines in Sweden, (Andersson and Berg 1999). This corresponds to a spatial frequency of 1.54–1.67 m^{-1}. With the sampling frequency 2 m^{-1}, this shows up as 0.33–0.46 m^{-1}. (A sleeper distance of 0.595 m would look like 0.32 m^{-1})

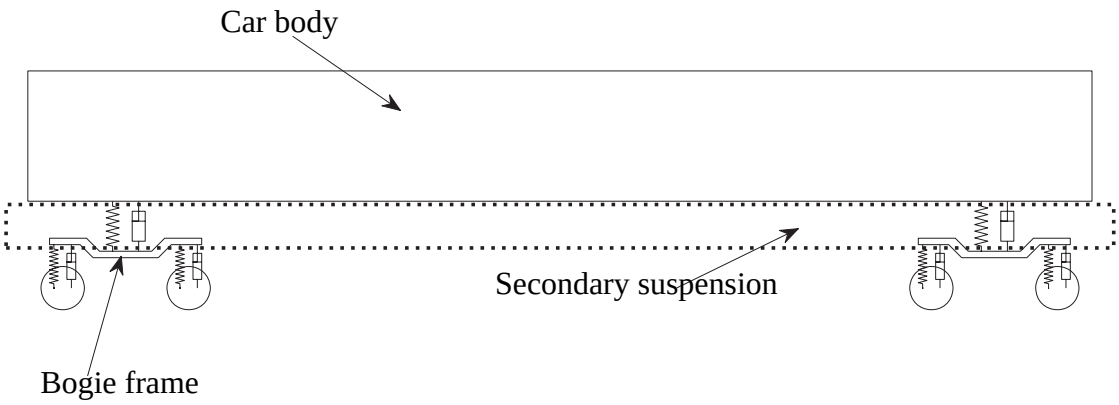

Figure 4.1: Schematic picture of where the secondary suspension is located. (It is within the dotted box.)

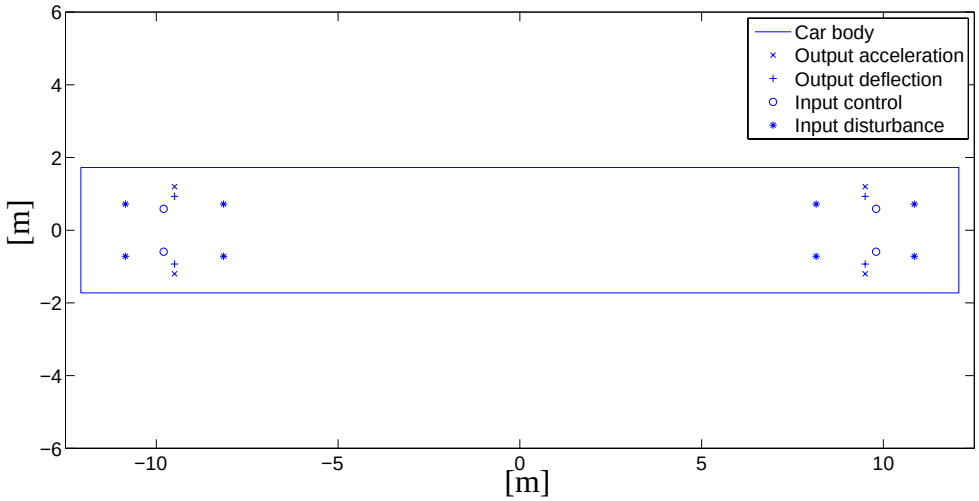

Figure 4.2: Location of inputs and outputs, top view.

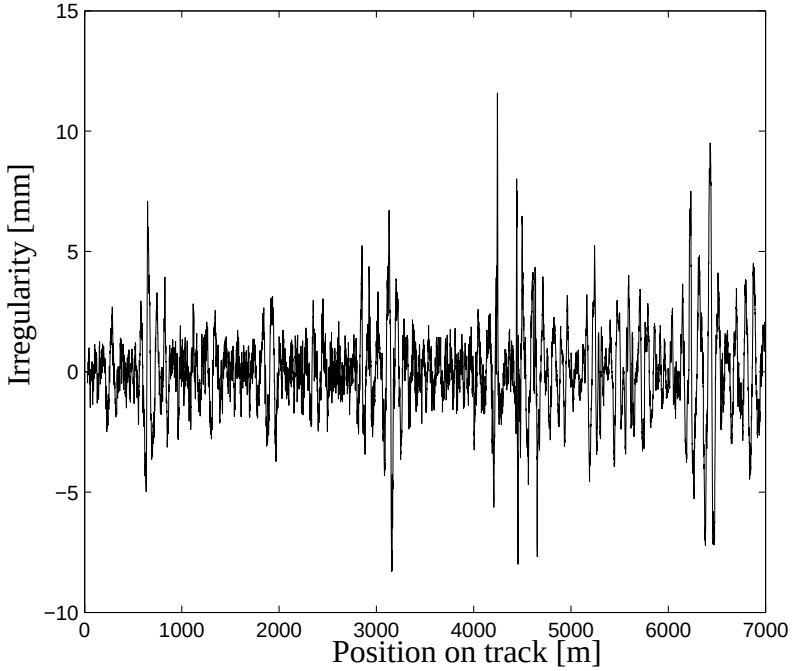

Figure 4.3: Lateral track irregularities.

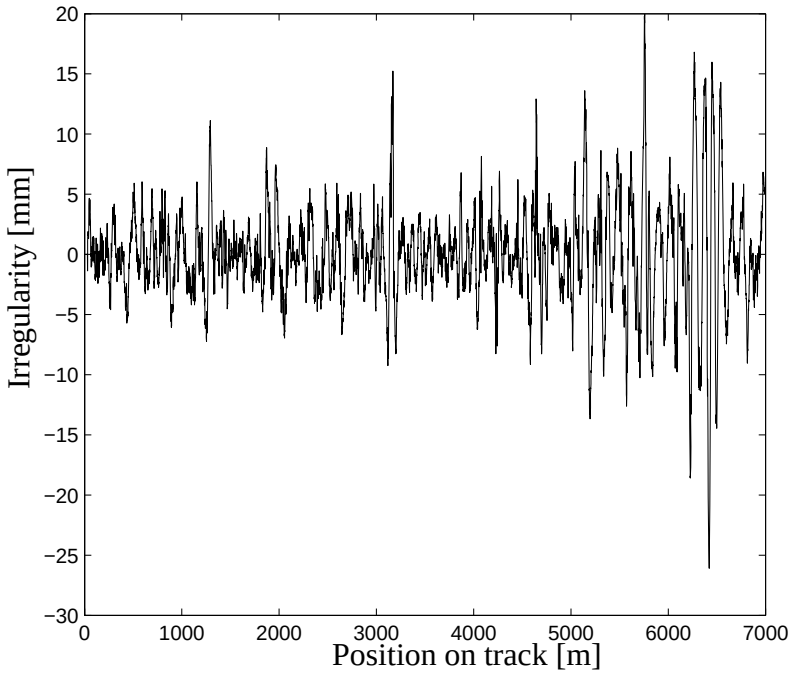

Figure 4.4: Vertical track irregularities.

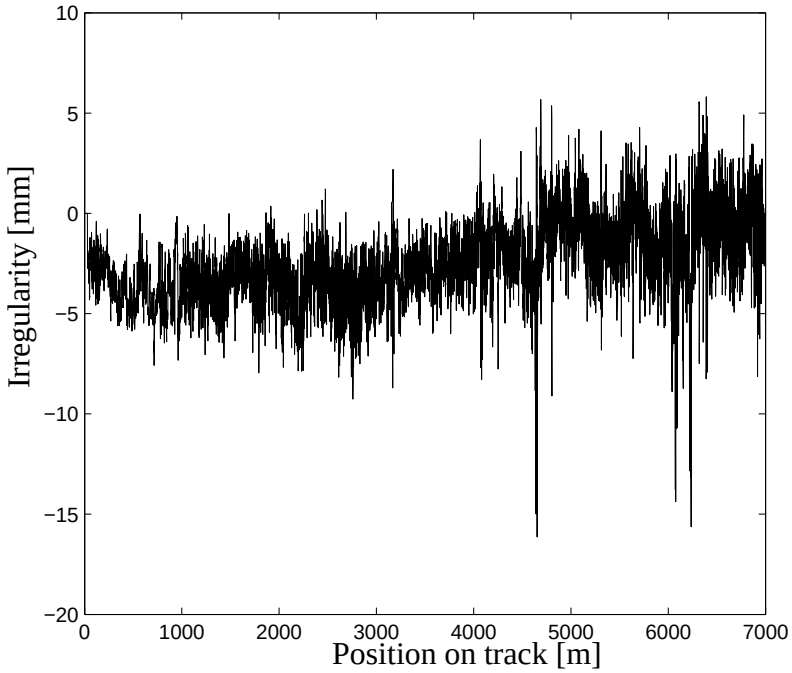

Figure 4.5: Gauge track irregularities.

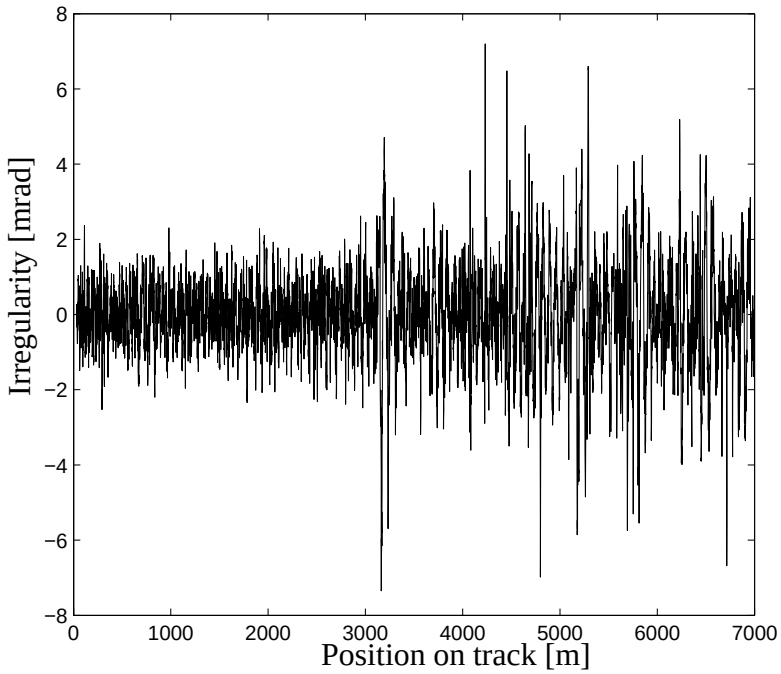

Figure 4.6: Roll track irregularities.

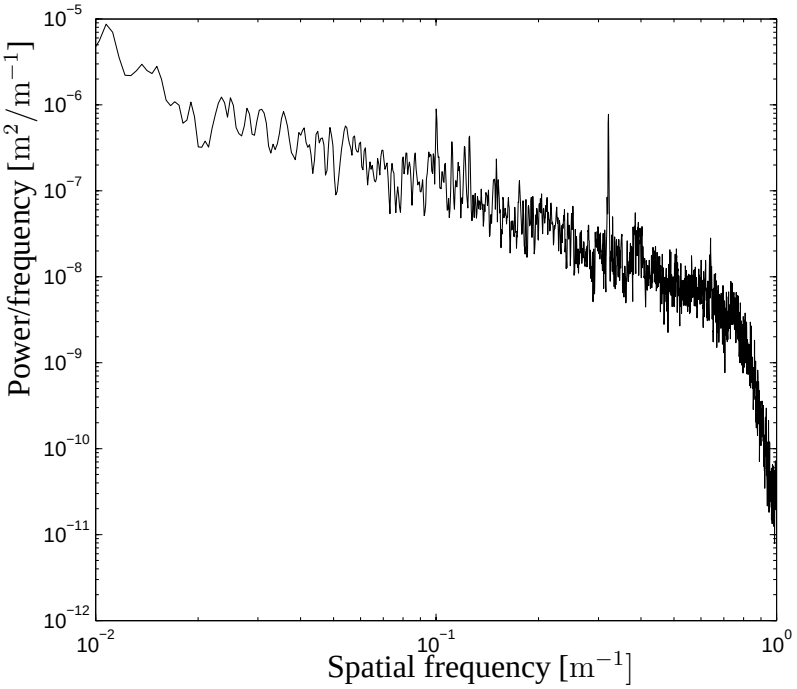

Figure 4.7: Frequency content of lateral track irregularities, by Welch power spectral density estimate.

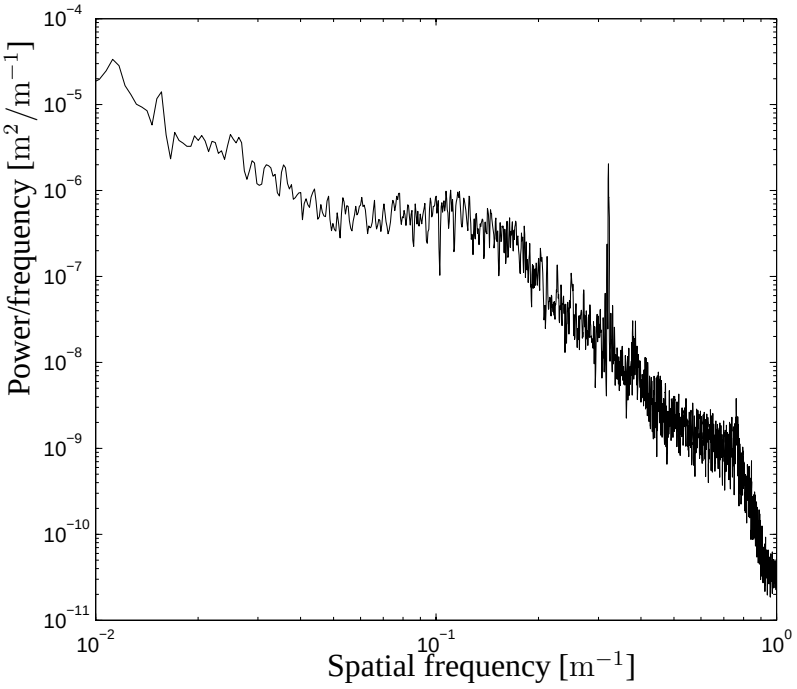

Figure 4.8: Frequency content of vertical track irregularities, by Welch power spectral density estimate.

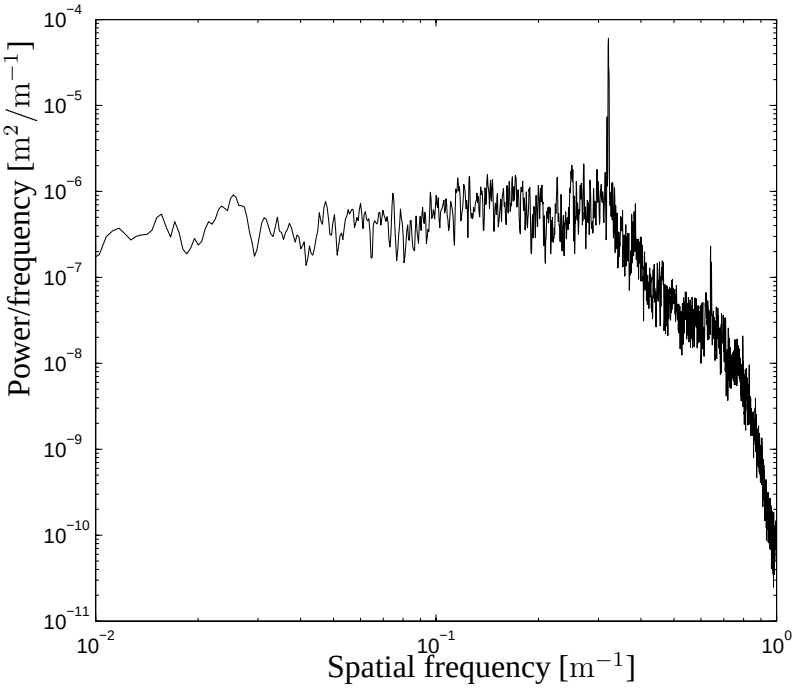

Figure 4.9: Frequency content of gauge track irregularities, by Welch power spectral density estimate.

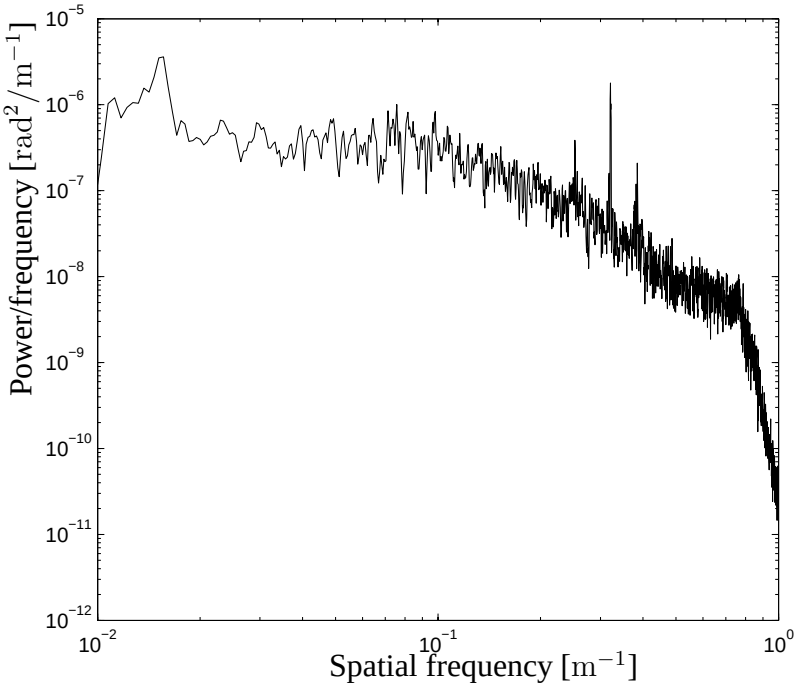

Figure 4.10: Frequency content of roll track irregularities, by Welch power spectral density estimate.

chapter v

feasibility considerations

The purpose of this chapter is to investigate if it seems reasonable to use active suspension to replace some of the passive components. This is from the point of view if it is reasonable to assume that it is possible to construct actuators that are able to deal with the task of active secondary vertical suspension. More specifically, the purpose of this chapter is to decide whether it is reasonable to switch to one of the active designs described in Section 5.2.1.

For this purpose, requirements on forces that need to be delivered by an active secondary railway suspension system are investigated, as well as the active system's estimated power consumption. This is done by calculating the corresponding properties for a specific passenger train with passive suspension system from Bombardier Transportation, for the different scenarios. Although the future choice of control strategy will affect the requested forces and effective powers from the actuators, and thus the requirements on actuator performance, the passive behavior is used as an approximation of what is required.

Both quasi-static and dynamic conditions are studied. Through this quasi-static forces, dynamic forces, and powers, that need to be delivered by an actuator, are obtained.

5.1 Background Theory

This section describes the theoretical background that choices and conclusions in this chapter are based on.

5.1.1 Railway Vehicle

Speed Limitations

If the vehicle is run through a curve, the maximum allowed velocity, $v_{\max}$, is limited also by the maximum allowed lateral acceleration, $a_{\mathrm{y,max}}$ by the following equation:

$$v_{\max} = \sqrt{R(a_{\mathrm{y,max}} + g\frac{h_{\mathrm{t}}}{2b_{\mathrm{o}}})}, \tag{5.1}$$

where R is the curve radius, g is the acceleration of gravity, h_{t} is the cant (distance that the outer rail is raised in a curve), and $2b_{\mathrm{o}}$ is the distance between the nominal wheel-rail contact points on the left and right rail, (Andersson et al. 2004). The maximum allowed lateral (track plane) acceleration is 0.98 m/s^2 for vehicles of category B is Sweden, (Andersson et al. 2004). This is the category the vehicle studied in this thesis belongs to.

Friction

If the track, rail, and wheel properties, and vehicle speed are such that there will be no flange contact with any of the reasonable friction values between the wheel and the rail, high friction is worse regarding the transmission of disturbances to the vehicle due to a stiffer coupling between the rail and the wheel. However, as the track, rail, and wheel properties, and vehicle speed are such that flange contact is likely, a low friction will cause more severe disturbances since flange contact will then occur more often, and flange contact causes disturbances. A normal value of the friction is 0.3. A reasonable value for low friction is 0.1, and for high friction 0.5, (Ågren 2004–2005).

5.1.2 Actuators

Peter Kjellqvist has written a doctoral thesis about the design of electromechanical actuators for active suspension in rail vehicles, for the lateral direction. The final actuator in his report has a rated (average) force of 13 kN and a peak force of 37 kN. However, those data origin from the requirements on an active lateral suspension, and an earlier version of the actuator design had a rated force of 20 kN. In the lateral case, he found that the high peaks are short compared to the permitted overload time, which causes the average force requirement to be critical. During the design there is a trade-off between actuator size, its dynamic properties, and temperature, (Kjellqvist 2002). The rated power is 4.2 kW.

5.2 Quasi-Static Analysis

Quasi-static analyses are performed in order to find the maximum quasi-static forces that arise in the secondary suspension. The maximum quasi-static forces are obtained at the worst allowed conditions. From the results, conclusions are drawn about in which way passive components can be replaced with active components. The results comes from either simulation in SIMPACK, or from analytic calculations. For the simulation results, simulations are performed without track irregularities, since those would introduce dynamic forces. The simulation properties are further described below. For the analytic calculations, simplified models are used. One of them has one, and the other with two, degrees of freedom.

5.2.1 Considered Scenarios

Quasi-static worst case conditions are studied in order to obtain the quasi-static forces required by each actuator. The obtained quasi-static suspension forces are used to assess requirements on the actuators in three different, possible, active systems. All active systems assume four actuators for each railway car. What differs is which passive components that are replaced with active.

The conditions are quasi-static when all forces and relative displacements within the vehicle and between vehicle and track are constant in time, (Andersson et al. 2004). To get this, there can be neither track irregularities nor transient curves. Irrespective of which control strategy that is used, the quasi-static forces in the suspension will be the same, for any given placement of the actuators. There is however a condition for this to be true: the roll and deflection have to be kept the same for all control strategies.

For the quasi-static forces, three different scenarios where currently used components will be replaced with active, are studied. Those are

Scenario 1. Remove anti-roll bar and secondary vertical damper. (Studied in infinite curve.) This scenario is studied by passive simulations in Section 5.2.2, and by analytic calculations in Section 5.2.3. The models for the analytic calculations are more simplified than those for the simulations. Another difference is that the analytical calculations deals with a tougher condition on the quasi-static roll performance, namely that the car body should be kept parallel to the bogie. The passive simulations will give the quasi-static forces needed to keep the same quasi-static roll performance as of the current passive vehicle, which does not require the car body to be quite parallel to the bogie.

Scenario 2. Remove pneumatic system of the air-spring (not the air-spring itself). (Studied for payload deviations.) This scenario is studied in Section 5.2.4.

Scenario 3. Combine the two scenarios above. This scenario is studied in Section 5.2.5.

The quasi-static forces are studied since the force that an actuator can deliver during a long period of time is lower than the peak force it can deliver, and specifications need thus to be stated for quasi-static forces. The limit for quasi-static forces is lower than the limit for peak forces, since temperature is a limiting factor in actuator design, (Kjellqvist 2002). The temperature will not reach its maximum value for a given force instantly. Also, the quasi-static forces can be decided exactly when the running conditions and performance requirements are known, which makes it easy to find a requirement for quasi-static conditions.

5.2.2 Force to Control Roll, Passive Simulations (Scenario 1)

In the passive case, the quasi-static forces that are controlling the roll, are exerted by the anti-roll bars and the air-springs. The maximum quasi-static forces on the anti-roll bar are obtained in the worst allowed curves at maximum vehicle load. The worst possible case would be, when the lateral (track plane) acceleration is at its maximum allowed value.

A simple way to imitate the worst case curve, is to do a simulation using a straight track, with a fictitious component of gravity pointing in the lateral direction. Such simulations are run until initial transients decay and the forces are stabilized.

Simulation data are as follows:

- Mass AW3 (100 seated passengers in the car and 2 standing passengers per square meter. Carbody and passengers weighs 53052 kg together, where the payload part is 10776 kg. Each person weighs 80 kg.) (Roos 2005).
- Vehicle velocity 0.1 m/s. (The velocity needs to be greater than zero for simulation purposes, (Intec GmbH 2003).)
- Simulation time is 40 s, which suffices to let the transients decay.
- Pre-loaded forces (nominal forces) of the model's preloaded force elements are calculated analytically outside of SIMPACK, to get static equilibrium at straight track with no cant deficiency or cant excess. These are not consistent with the fictitious skewed gravity vector, which implies that the vehicle is not initially at equilibrium.

- Fictitious gravity vector:
  either
  $g_{\mathrm{x}} = 0\ \mathrm{m/s^2}$, $g_{\mathrm{y}} = 0.98\ \mathrm{m/s^2}$, $g_{\mathrm{z}} = 9.76\ \mathrm{m/s^2}$, corresponding to the case when the entire lateral part of the gravity comes from the true acceleration of gravity. Here the resultant gravity is $9.81\ \mathrm{m/s^2}$.
  or
  $g_{\mathrm{x}} = 0\ \mathrm{m/s^2}$, $g_{\mathrm{y}} = 0.98\ \mathrm{m/s^2}$, $g_{\mathrm{z}} = 9.81\ \mathrm{m/s^2}$, corresponding to the case when no part of the lateral part of the gravity comes from the true acceleration of gravity, but comes from the centripetal force instead. Here, the resultant fictitious gravity is $9.86\ \mathrm{m/s^2}$.

The simulation results yield that the resulting force in each anti-roll bar is 32.3 kN, for both cases of fictitious gravity vector. Also, each air-spring contributes to limit the roll. However, since there is no intention to remove the air-springs here (see Section 3.1), this contribution is assumed to remain also for a modified system, and is therefore not considered here.

5.2.3 Force to Control Roll, Carbody Parallel with Bogie (Scenario 1)

As opposed to the previous section, this section does not deal with the passive system. Instead, an active system is studied. Here, the assumption is made that quasi-statically, the car body should be kept parallel to the bogie. That is a requirement for better performance regarding roll than in the passive case. If the roll is to be compensated in a way that keeps the car body parallel to the bogie, higher forces than what is required to imitate the passive system will be needed. See the calculations below. For the following calculations, regarding components, it is assumed that the air-springs are kept at their current positions in the suspension design, but the anti-roll bar and secondary dampers have been removed from the original model. Instead, actuators are introduced at the former position of the dampers.

In Figure 5.1, all variables that are not explicitly defined in this section, are defined. α is the angle between the bogie frame and the wheelset. This angle is assumed to be small. θ is defined in Equation 5.12 – Equation 5.14. COG means center of gravity. g_{tot} is the total acceleration caused by the combination of the maximum allowed lateral acceleration, $a = 0.98\ \mathrm{m/s^2}$, see Section 5.2.2, and the acceleration of gravity, $g = 9.81\ \mathrm{m/s^2}$. The lateral acceleration, a, could origin from either a centripetal force, or, if the track has a cant, the acceleration of gravity. It could also be a combination of both. The remaining part of the acceleration of gravity, that is pointing in the vertical direction, is called g_{z}. The Pythagorean theorem yields

$$g_{\mathrm{tot}} = \sqrt{g_{\mathrm{z}}^2 + a^2}. \tag{5.2}$$

Force equilibrium in the vertical direction, with positive direction upwards, gives for the car body

$$F_{\mathrm{sl}} + F_{\mathrm{al}} + F_{\mathrm{ar}} + F_{\mathrm{sr}} - mg_{\mathrm{tot}} \cos\theta = 0. \tag{5.3}$$

Since the car body is kept parallel to the bogie, the displacements of the left and right air-spring are the same, and thus their forces are the same. In order to minimize the need of active force, the air-springs should carry the load of the car body. Thus

$$F_{\mathrm{sl}} = F_{\mathrm{sr}} = \frac{mg_{\mathrm{tot}}}{2} \cos\theta \tag{5.4}$$

and

$$F_{\mathrm{al}} + F_{\mathrm{ar}} = 0. \tag{5.5}$$

Moment equilibrium clockwise around the connection point of the left actuator to the car body yields

$$F_{\mathrm{sl}}(d-e) + emg_{\mathrm{tot}}\cos\theta + hmg_{\mathrm{tot}}\sin\theta - 2F_{\mathrm{ar}}e - F_{\mathrm{sr}}(d+e) = 0. \tag{5.6}$$

Using Equation 5.4 and Equation 5.6, and solving for F_{ar} yields

$$F_{\mathrm{ar}} = \frac{mg_{\mathrm{tot}}h}{2e}\sin\theta. \tag{5.7}$$

The force required by an actuator is increased with increased car body mass, increased total acceleration acting on the car body, increased distance to the center of gravity of the car body, and increased angle between the resultant force from the accelerations and the bogie. The force needed is decreased with increased distances from the lateral center of the car body and the connection points of the actuators.

To find out the additional angle, α, caused by the deflections in the primary suspensions, equilibrium for the primary suspension was set up, see Equation 5.8 – Equation 5.12.

$$F_{\mathrm{pl}} + F_{\mathrm{pr}} - F_{\mathrm{sl}} - F_{\mathrm{al}} - F_{\mathrm{ar}} - F_{\mathrm{sr}} = 0, \tag{5.8}$$

$$F_{\mathrm{sl}}(f-d) + F_{\mathrm{al}}(f-e) + F_{\mathrm{ar}}(f+e) + F_{\mathrm{sr}}(f+d) - F_{\mathrm{pr}}2f = 0 \tag{5.9}$$

$$x_{\mathrm{l}} = \frac{F_{\mathrm{pl}}}{k_{\mathrm{p}}} \tag{5.10}$$

$$x_{\mathrm{r}} = \frac{F_{\mathrm{pr}}}{k_{\mathrm{p}}} \tag{5.11}$$

$$\alpha = \arctan\frac{x_{\mathrm{r}} - x_{\mathrm{l}}}{2f} \tag{5.12}$$

k_{p} is the vertical spring value of the primary suspension, and the other variables are defined in Figure 5.1. The angle α is then added to the angle from the track plane acceleration, θ_0. Thus

$$\theta = \theta_0 + \alpha, \tag{5.13}$$

where

$$\theta_0 = \arcsin\frac{a}{g_{\mathrm{z}}}, \tag{5.14}$$

where a is the maximum allowed lateral acceleration, 0.98 m/s^2, see Section 5.2.2, and g_{z} is the vertical part of the acceleration of gravity. g_{z} can vary between 9.76 m/s^2 and 9.81 m/s^2, depending on how much from the gravity that will be a part of a. The calculations were iterated until the angles and forces did not change anymore. The resulting force in each actuator is 39.3 kN, for all allowed values of g_{z}, at maximum payload. This can be compared with the result from Section 5.2.2, which was that the quasi-static force needed from each actuator is 32.3 kN. Thus a higher quasi-static force is needed to keep the car body parallel to the bogie, than for keeping the roll at the level of today's passive suspension.

5.2.4 Air-Spring Deviation from Equilibrium (Scenario 2)

The quasi-static forces that hold the vehicle in place vertically, are only calculated for the deviation from equilibrium that the load variations introduce. That is done since the purpose is to study the possibilities to remove the pneumatic system that keeps the car body level as passengers are moving on and off, Scenario 2 in Section 5.2.1. The air-springs will still take a static load, but usually not the entire static load.

To minimize the maximum quasi-static forces needed, equilibrium are assumed at half of the maximum payload. Thus the active system never needs to compensate for more than half of the payload. It it assumed that 4 actuators will be used. The result is then that the maximum quasi-static force for the load control, $F_{\mathrm{q,lc}}$, will be

$$F_{\mathrm{q,lc}} = \frac{m_{\mathrm{load}} g}{2 \cdot 4} = \frac{10776\ \mathrm{kg} \cdot 9.81\ \mathrm{m/s^2}}{8} \approx 13.2\ \mathrm{kN}, \tag{5.15}$$

where the number 4 comes from the assumption that 4 actuators will be used, and the number 2 from that the system never needs to compensate for more than half of the load due to the chosen load of equilibrium. The result is that the force that each actuator need to deliver, if the pneumatic system of the air-springs are replaced by actuators, is approximately 13 kN. This maximum force will occur both when the payload is at its maximum and when there is no payload. At any payload in between those limits, the actuator will need to deliver less force.

5.2.5 Active Roll and Level Control (Scenario 3)

When the anti-roll bar, secondary damper, and pneumatic levelling control system for the air-springs, are all removed at the same time, the quasi-static forces for Scenario 1 and Scenario 2 are superposed. Since at maximum payload, both Scenario 1 and Scenario 2 experiences a worst case condition, maximum payload becomes the worst case for the combined scenario. When the total quasi-static forces are calculated, the different contributions are added with sign. The levelling control (Scenario 2) will have equal sign and value on both side of the suspension, and the roll control (Scenario 1) will have opposite sign and equal value on either side of the suspension. Thus on one side, both quasi-static forces have the same sign, and their absolute values can thus be added to obtain the total maximum quasi-static force, see Figure 5.2. The result is that each actuator needs to be able to deliver approximately 46 kN quasi-statically.

5.3 Dynamic Simulations

During normal operation of the vehicle, the conditions are not quasi-static, but dynamic. Using some control law, the forces from the actuators will differ from those in the passive suspension. Still, the passive forces will indicate roughly how large the forces might be. In order to see what forces that are exerted by the passive system under dynamic conditions, the passive system is simulated during some different conditions. The system is exited by track irregularities. For some of the simulated cases also the track topology will vary, with the track being composed of straight track sections, curves, and transition curves.

For the dynamic studies of forces and powers, only Scenario 1 is considered. The results are the forces and delivered powers that would be needed to imitate the passive system. Those

indicate roughly what will be required from an active system. The reason that the results are not exact is, as mentioned above, that the forces and powers will depend on control strategy.

The dynamic studies also yield the vehicle performance in the passive system, concerning deflections, roll, and comfort. These results can be used as requirements for an active system.

5.3.1 Simulated Cases

To obtain the dynamic forces in the secondary suspension, simulations are run at some certain circumstances according to the list below. Some circumstances are chosen to be normal, other to be as bad as possible. Some parameters for the simulation that might need further explanation are explained here:

- Velocity
  For all cases listed below, the velocity is the maximum allowed for the vehicle, considering the curve radius.
- Track irregularities
  For all cases, measured track irregularities are used. In some cases, the amplitude of the irregularities are multiplied with some factor. Then the irregularities will correspond to a track with larger irregularities, since the factors are greater than 1.
- Friction
  Where the friction is not chosen as normal friction, the friction is chosen to cause maximum disturbance. In curves the friction are chosen to maximize the risk of flange contact.

The following cases were evaluated:
Case 1 (straight track)

- Straight track.
- Velocity 200 km/h.
- No payload – this will give the worst comfort, since then the quotient between the unsprung and sprung mass reaches its highest value.
- Measured track irregularities multiplied with 1.5.
- Friction 0.5 (high friction).

Case 2 (tight curve)

- Curve radius 300 m.
- Cant 150 mm.
- Velocity 87 km/h.
- No payload.
- Measured track irregularities multiplied by 2.

- Friction 0.1 (low friction).

Case 3 (tight curve, same as case 2 but with full payload)

- Curve radius 300 m.
- Cant 150 mm.
- Velocity 87 km/h (maximum to stay within allowed lateral acceleration (Andersson and Berg 1999)).
- Full payload.
- Measured track irregularities multiplied by 2.
- Friction 0.1 (low friction).

Case 4 (measured track)

- Measured track.
- Velocity 200 km/h.
- No payload.
- Measured track irregularities.
- Friction 0.3 (normal friction).

Case 5 (measured track, same as case 4 but with full payload)

- Measured track.
- Velocity 200 km/h.
- Full payload.
- Measured track irregularities.
- Friction 0.3 (normal friction).

5.3.2 Simulation Results

This section describes the simulation results. The forces and powers can be used to estimate what will be required by the actuators if active suspension is used.

Simulations are run for the 5 different conditions described in Section 5.3.1. In the following sub-sections, maximum and minimum values come from varying force elements and simulation conditions. For a complete list of results, see Appendix D.

Forces in Anti-Roll Bar and Damper

The maximum peak force in the anti-roll bar is 41 kN. This occurs in case 3 (curve with full load). The maximum mean of the absolute value of the force in the anti-roll bar is 32.0 kN. This also occurs in case 3.

The maximum peak force in the vertical damper in the secondary suspension is smaller, 6.1 kN. This occurs in case 1 (straight track).

Ideal Power Dissipation or Consumption in Anti-Roll Bar and Damper

The power dissipation in the secondary damper is, naturally, modelled as force times velocity ($P = \boldsymbol{F} \cdot \boldsymbol{v}$, (Nordling and Österman 1996)). This yields a maximum peak power of 1.9 kW, which occurs in case 1.

The power that corresponds to the anti-roll bar is calculated in a less intuitive way. The force in the anti-roll bar is (for each component x, y, and z) multiplied with the velocity between the connection between the anti-roll bar and the car body, and a point on the bogie that is originally right below the connection point. The reason of this choice is that this yields the power needed if the anti-roll bar is replaced by an actuator placed in that position. The maximum absolute value of the power derived from the anti-roll bar is 4.4 kW, also this is occurring in case 1.

The differences in powers in the anti-roll bars and dampers are larger than the differences in forces in the anti-roll bars and dampers. This indicates that the velocity is low near the maximum deflection. That is as expected, since that is where the movement change direction.

5.4 Concluding Remarks

First, the quasi-static conditions are discussed:

For Scenario 1, the active suspension replaces the anti-roll bar and the secondary vertical damper. Then the results show that each actuator must be able to deliver quasi-static forces of roughly 32 kN.

For Scenario 2, the pneumatic pump system for the air-springs, which adapts the air pressure to compensate for payload variations, is removed. Instead, the active suspension will be used to keep the car body at the same vertical position regardless of the amount of payload. This requires a quasi-static force from each actuator of about 13 kN, for the worst case.

Scenario 3 combines Scenario 1 and Scenario 2. The resulting quasi-static forces that the actuators might need to deliver is the sum of the quasi-static forces from the two different systems mentioned above, 46 kN.

Comparing the requirements in Kjellqvists's thesis with the results in this section leads to the following conclusion: The actuator prototype developed by Kjellqvist is strong enough to handle load variations, scenario 2, but not strong enough to handle roll, scenario 1, or the combination of these two scenarios.

Then, the dynamic conditions are discussed:

For the dynamic simulation, which corresponds to Scenario 1 in the quasi-static case, the results are, that over the running conditions the largest men force is 32 kN, the largest peak force is 42 kN, the largest mean power is 0.64 kW, and the largest peak power is 4.6 kW.

Comparing this to what the prototype developed by Kjellqvist yields similar results as in the quasi-static case. Regarding the forces, the mean values are most critical, and that was the same as in the quasi-static case. The powers are more difficult to make conclusions about, since the losses are unknown.

Finally, a final conclusion for both quasi-static and dynamics conditions:

The actuator developed by Kjellqvist does not seem to be able to handle neither the quasi-static, nor the dynamic, conditions studied here. However, the forces required are of the same order of magnitude as those from the actuator. Also, powers are of the same size order. This makes it reasonable to expect that an actuator, which is able to handle the required

forces, could be developed. To study the subject from a theoretical point does seem to make sense.

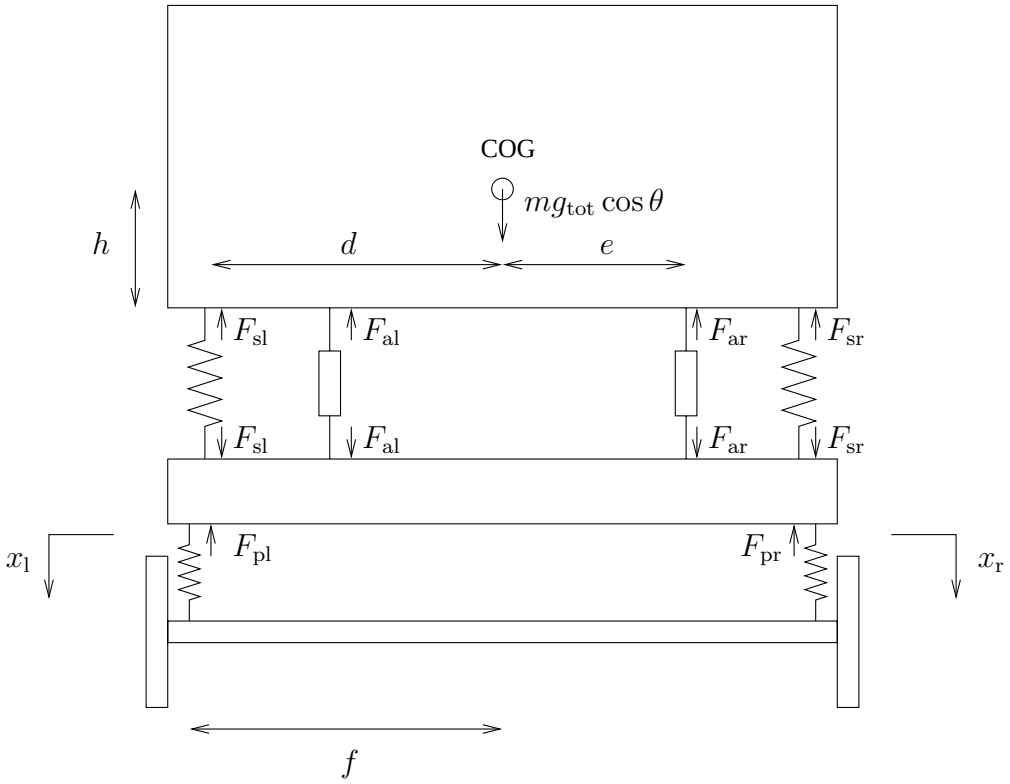

Figure 5.1: Simplified 2D model for equilibrium calculations.

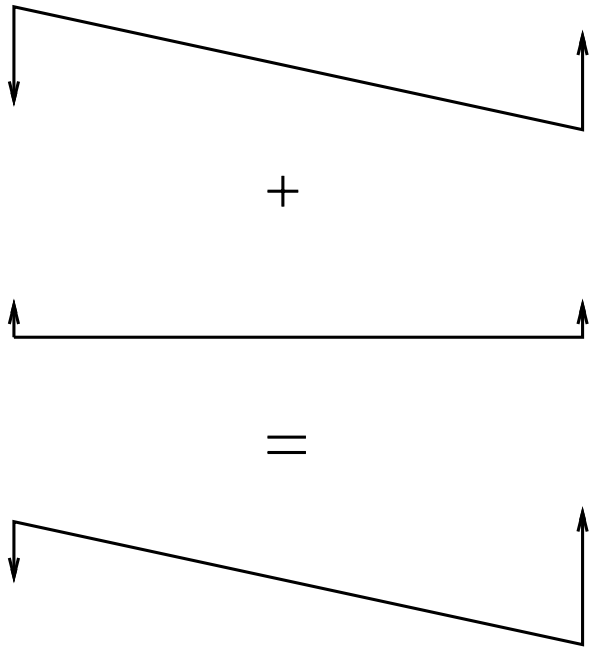

Figure 5.2: Illustration of superposition of quasi-static forces.

chapter vi

frequency range for linear model validity

The purpose of this chapter is to estimate in which frequency range the linear model, extracted from the original nonlinear model as described in Section 3.2.2, is valid. To do that, the model has been compared to what physical insight tells us, and has also been validated against the nonlinear model, as well as against itself using the redundant information it contains.

6.1 Comparison of Same Transfer Function Obtained in Different Ways

The linear system matrices have been generated using more outputs than the ones really wanted, to allow comparisons. The interesting outputs are car body acceleration and bogie-to-carbody deflection (position). However, for each interesting output location, the position, velocity and acceleration all been chosen as outputs. Any one of those would be enough to calculate all three transfer functions, using integration or differentiation. The transfer functions not corresponding to the initial interesting outputs have either been integrated (divided by s or $j\omega$), or the derivative has been taken on the function (it has been multiplied with s or $j\omega$), to also give the interesting input-output relation. In theory those three versions should give identical transfer functions. They do in some frequency range. However, at low and high frequencies they don't. This means that the linearized models cannot be trusted outside this mid frequency range. In Figure 6.1–Figure 6.5 the transfer functions have been studied from vertical acceleration disturbances at the first wheelset, to different outputs. In Figure 6.6–Figure 6.9 the transfer functions have been studied from actuator force in the same way. As can seen in those figures, the transfer functions are approximately the same for all ways to compute them, for frequencies from approximately 1 Hz.

6.2 Gain Plots Compared to Physical Insight

It can be seen that the transfer functions are incorrect at low frequencies by studying the low frequency asymptote when the vehicle is excited with all excitations in phase with each other. Physical insight tells that a constant vertical acceleration in the rail should give the same constant vertical acceleration in the car body. That is, this transfer function should tend to 1, or 0 dB, at low frequencies. That is not the case when the transfer function is calculated directly from input acceleration to output acceleration. However, if that transfer function is re-calculated with the position, differentiated twice, it comes close. See Figure 6.10. For

the same disturbance, the distance between the car body and bogie frame should reach a constant value. That is not obtained from any of the ways to calculate a transfer function, see Figure 6.11.

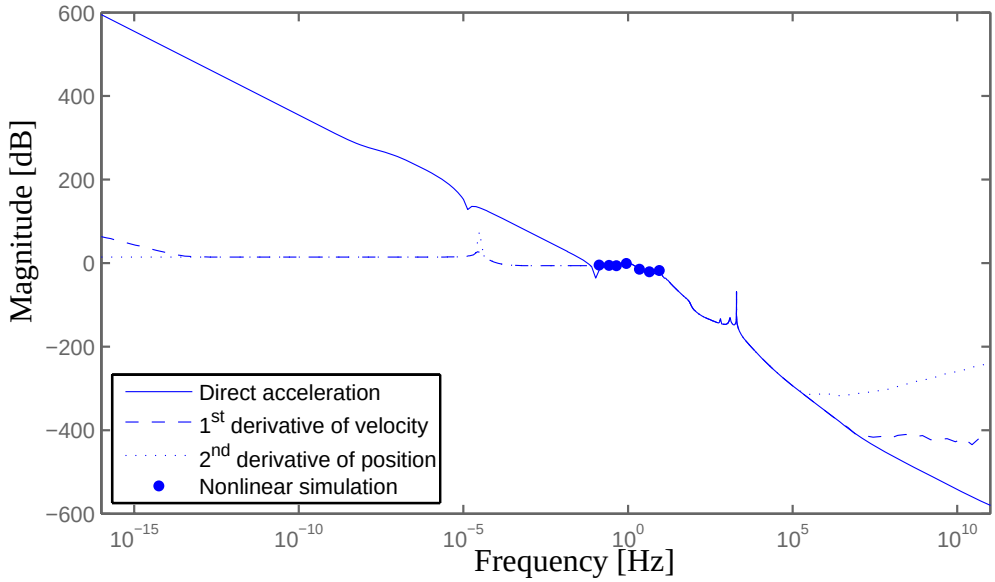

Figure 6.1: Acceleration in car body, front right. Input acceleration of vertical disturbances.

6.3 Comparison with Nonlinear Simulations

The linear model is compared with nonlinear simulations with disturbances at a single frequency for each simulation.

The disturbances are chosen as sinus signals, which are applied only on the front wheelset. This is to enable a direct comparison with the corresponding bode plots. Disturbance amplitudes are chosen to give an output that looks as much as possible as a sinus, to resemble linear behavior. This is difficult to achieve at low or high frequencies, but works well in a mid frequency range. All the points plotted in Figure 6.1–Figure 6.5 are in that mid frequency range. It might be possible to measure gains at higher frequencies than can be seen in those figures, but then the disturbance amplitude has to be very small in order to get approximately linear behavior, which leads to a very long time until the transients decay. Also, the nonlinearities tend to increase with increased frequency. Thus the linear model might not be useable for high frequencies anyway.

When a simulation output is obtained, it is run through a bandpass filter with the following transfer function:

$$\frac{s^3}{(s^2+s+\omega_0^2)^3}, \tag{6.1}$$

where ω_0 is the frequency, in rad/s, that is singled out, while other frequencies are depressed. The filter magnitude is plotted in Figure 6.12. This bandpass filter is a modified version of a bandpass filter found in (Sedra and Smith 1998). The bandpass filter in that book is

$$\frac{a_1 s}{s^2 + s\frac{\omega_0}{Q} + \omega_0^2}. \tag{6.2}$$

Q has been chosen as ω_0, and a_1 has been chosen as 1. This makes the maximum gain equal to 1, which is desired to keep the magnitude of the signal studied. Then the entire filter has been taken to the power of 3, since this makes the peak narrower, and without that there were too much of other frequencies left in the output.

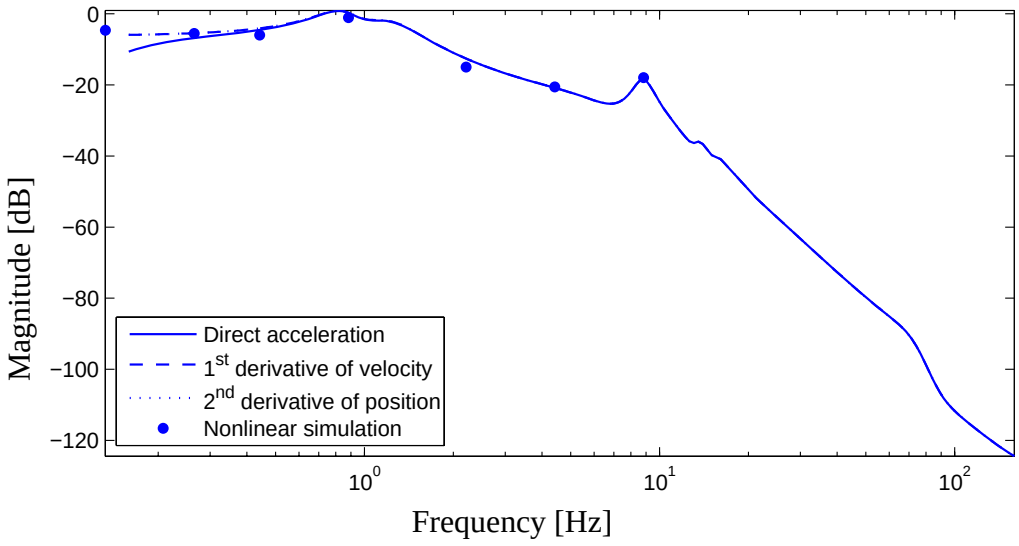

Figure 6.2: Acceleration in car body, front right. Input acceleration of vertical disturbances.

6.4 Concluding Remarks

The different methods of generating linear input-output relationships results in the same frequency responses in a mid range of frequencies. The differences between the nonlinear and linear cases could be a source of concern though, especially for the rear part of the vehicle. For low frequencies, lower than approximately 1 Hz, the model is inconsistent. That is definitely the case also for very high frequencies (above approximately 10^5 Hz), but those are too high to matter for comfort, see Section 2.3. Medium high frequencies are more difficult to make absolute conclusions about. It has proven difficult to confirm the model with nonlinear simulations above approximately 10 Hz, but this could be due to that the gains of the transfer functions are small there. There are no data to indicate that the linear models are neither correct nor incorrect. For the range 1–10 Hz, the nonlinear simulations approximately matches the linear models, although the differences are too big to feel confident the linear model is a good approximation. Also, the outputs from the nonlinear

simulations were nonlinear, and needed to be filtered with a very narrow bandpass filter to give a linear output, which makes it even more difficult to make a comparison.

In brief, the linear model should not be used below 1 Hz or above 10^5 Hz. For 1–10 Hz, it seems reasonable to make an attempt to use the linear model. In the remaining frequency interval, the model may or may not be sufficiently accurate. This means that the linear model is not suitable for studies of motion sickness, where low frequencies are important, see Section 2.3. For comfort studies, where the most interesting frequency region is 2–40 Hz, with the peak at 6–10 Hz, it is more reasonable to use the linear model, although there is some doubt about this usage also.

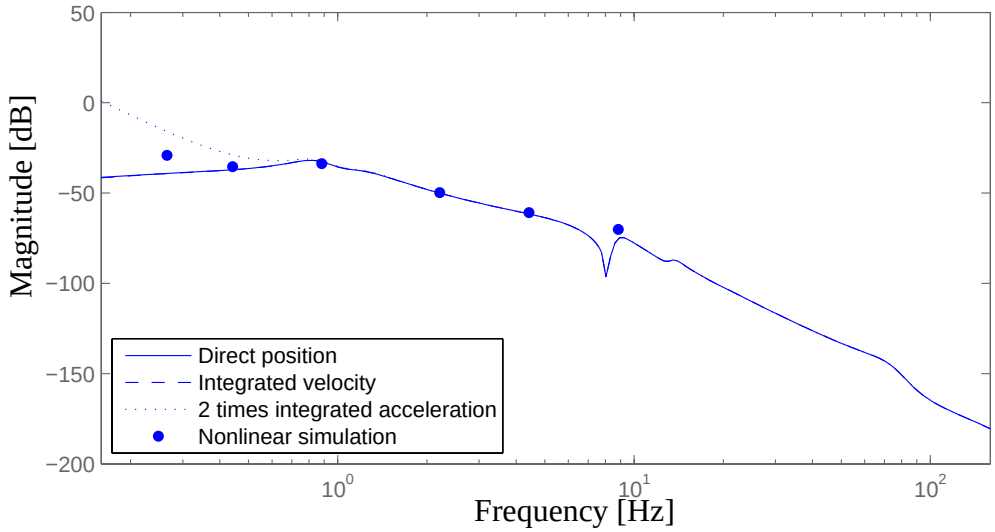

Figure 6.3: Deflection between car body and bogie frame, front right. Input acceleration of vertical disturbances.

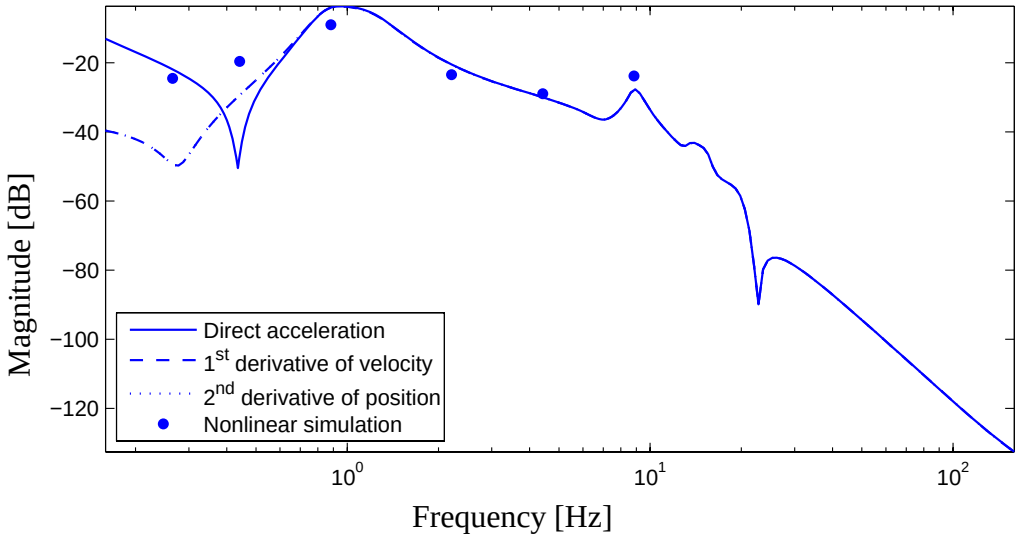

Figure 6.4: Acceleration in car body, rear left. Input acceleration of vertical disturbances.

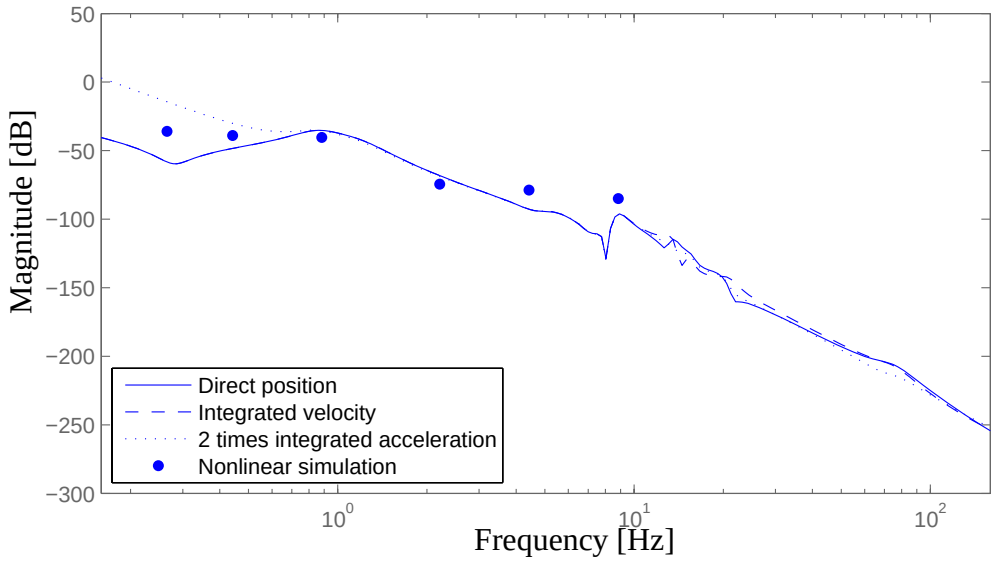

Figure 6.5: Deflection between car body and bogie frame, rear left. Input acceleration of vertical disturbances.

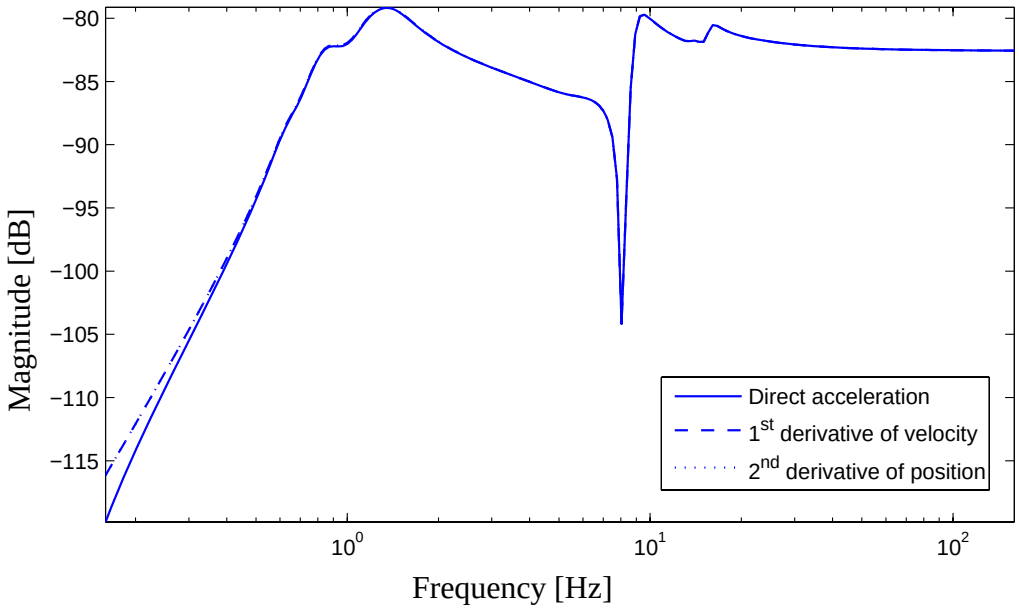

Figure 6.6: Acceleration in car body, front right. Input actuator force.

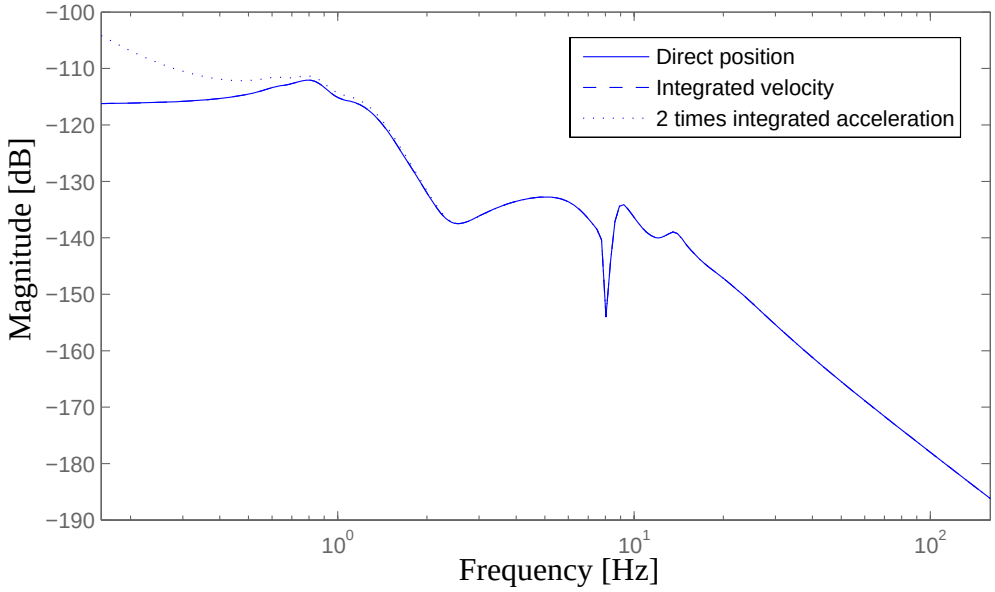

Figure 6.7: Deflection between car body and bogie frame, front right. Input actuator force.

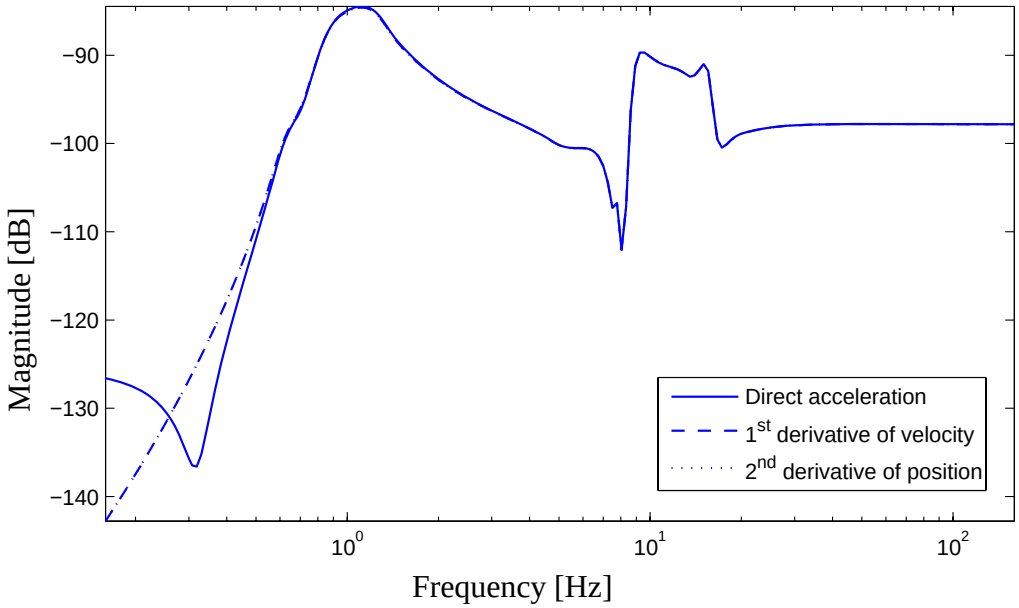

Figure 6.8: Acceleration in car body, rear right. Input actuator force.

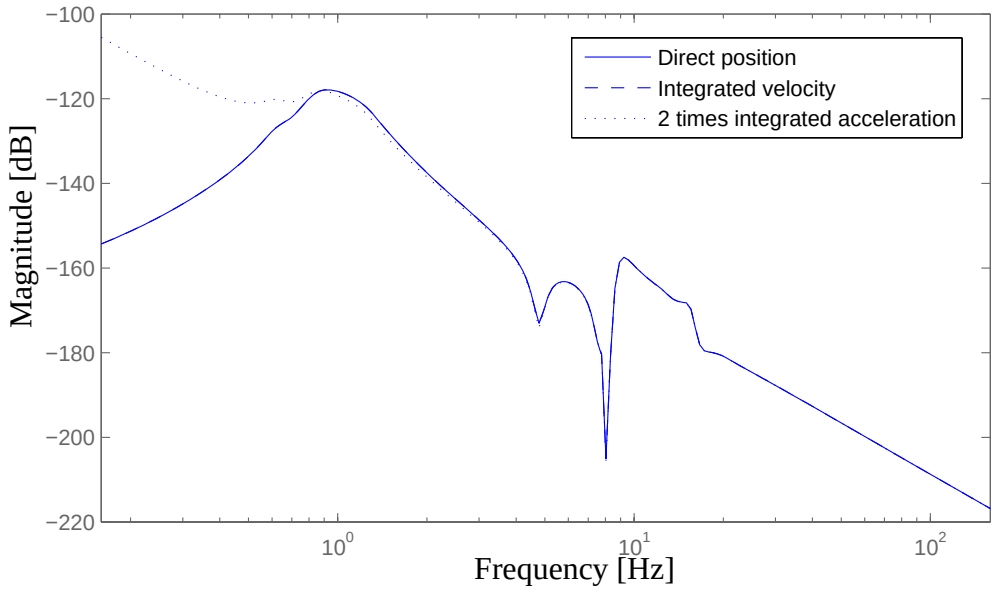

Figure 6.9: Deflection between car body and bogie frame, rear right. Input actuator force.

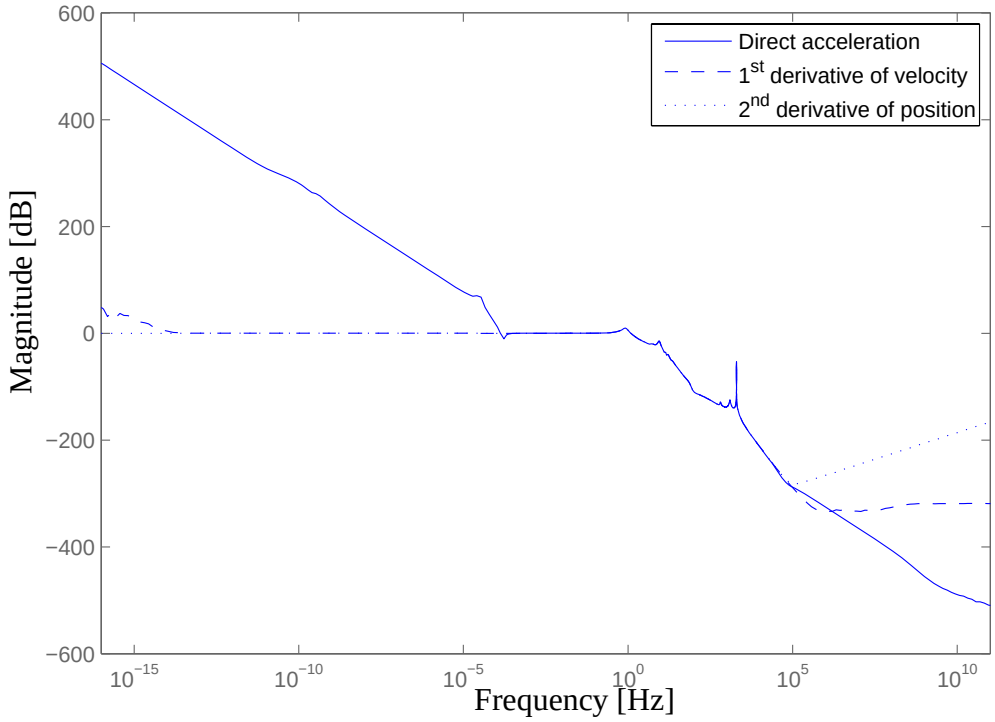

Figure 6.10: Acceleration in car body, front right. Input acceleration of vertical disturbances. All inputs in phase.

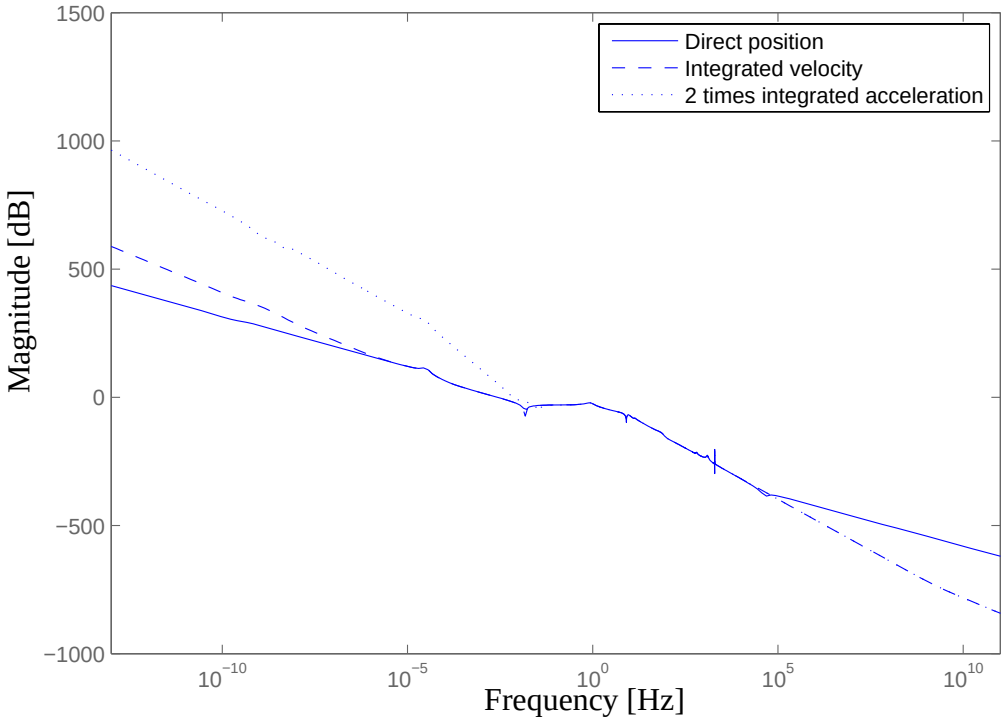

Figure 6.11: Deflection between car body and bogie frame, front right. Input acceleration of vertical disturbances. All inputs in phase.

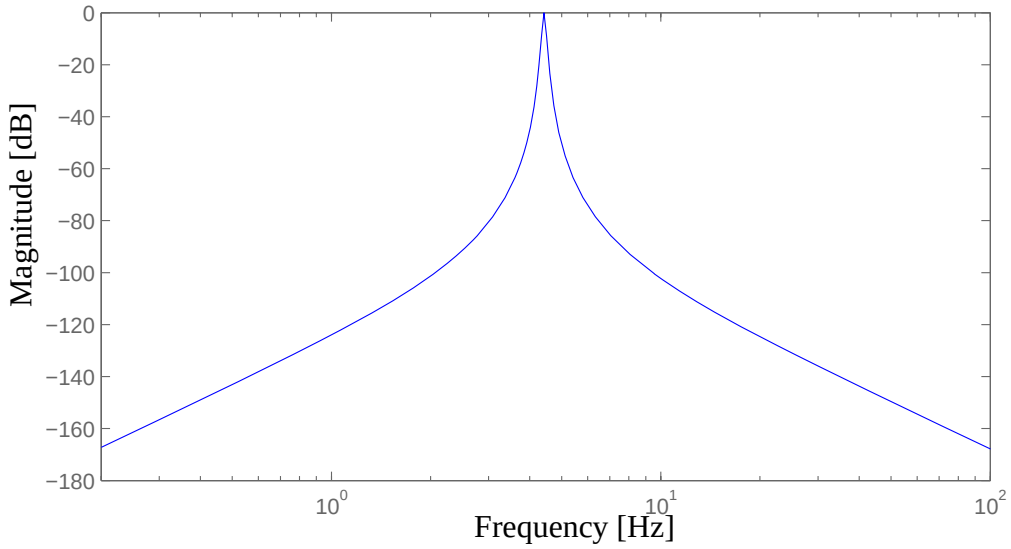

Figure 6.12: Bandpass filter used to get sinus from simulation output. Example for $f_0 = 4.4$ Hz.

chapter vii

coupling between inputs and outputs

A single-input single-output (SISO) controller is easier to construct and analyze, and could be made less complex, than a multiple-input multiple-output (MIMO) controller. Therefore, it is interesting to study how each output depend on each input. It is also interesting to see if the system can be divided into smaller sub-systems.

The simplest solution would be, if one physical input (actuator force) could be connected to the nearest output. That would allow for SISO design. If that is not possible, it might still be possible to decouple the system. That would also allow for SISO design, only the control and/or output signals used in the SISO design, would not correspond to any physical signal. Instead, they would have to be calculated from a combination of physical signals. It will however be shown below that neither version is possible.

7.1 Background Theory

This section describes formal methods to divide a system with multiple inputs and outputs, into several systems with a single input and output, for control purposes.

7.1.1 Relative Gain Array

To measure the amount of interaction between different inputs and output of a system, a special matrix called the *Relative Gain Array*, RGA, can be used, (Glad and Ljung 2000). For an arbitrary quadratic, invertible matrix A, this is defined as

$$\mathrm{RGA}(A) = A. * (A^{-1})^T, \tag{7.1}$$

and for an arbitrary complex matrix A as

$$\mathrm{RGA}(A) = A. * (A^{\dagger})^T, \tag{7.2}$$

where .* denotes elementwise multiplication, (Glad and Ljung 2000). In this chapter, RGA will be used for the case when $A = G(j\omega)$, where $G(j\omega)$ is a matrix of transfer functions.

If RGA is used for a matrix of transfer functions, an input-output relation is not much affected by the other inputs, for RGA-elements near 1. If it is not near one for an output that is supposed to be controlled by a certain input, there are significant cross couplings, (Glad and Ljung 2000). A perfectly decoupled system, where the inputs and outputs are numbered such that input number i controls output number i, for all i, has the unity matrix as its RGA, as can be seen from Equation 7.1.

7.1.2 The Pairing Problem

The pairing problem deals with deciding which output signals should be controlled by which control signals, (Glad and Ljung 2000). Two main rules are given in (Glad and Ljung 2000) to pair the signals using the RGA matrix.

1. Pair the signals in a way that will make the diagonal elements in $\mathrm{RGA}(G(j\omega_c))$, where ω_c is the the intended bandwidth for the controlled system, as close to $1+0j$ as possible.

2. Avoid pairings that will make the diagonal elements in $\mathrm{RGA}(G(0))$ negative.

When the relative gain is negative, there will be positive feedback in this loop, either when the other loops are open, or when they are closed, depending on controller configuration, (Shinskey 1996). Furthermore, if the relative gain is infinity, the loops are completely dependent, (Shinskey 1996).

7.1.3 Decoupling

If the inputs and outputs cannot be paired into pairs that dominate the dynamics, it might be possible to use variable changes to find such pairs, (Glad and Ljung 2000). Let $\tilde{y} = W_2 y$ and $\tilde{u} = W_1^{-1} u$. Then the transfer function from $\tilde{u}$ to $\tilde{y}$ will be

$$\tilde{G}(s) = W_2(s)G(s)W_1(s). \tag{7.3}$$

W_1 and W_2 should be chosen to make $\tilde{G}(s)$ as diagonal as possible, which would make it possible to make a diagonal controller F_y^{diag} for the new variables, (Glad and Ljung 2000). In the original variables the controller will then be

$$u = -W_1 F_y^{diag} W_2 y, \tag{7.4}$$

which is a decoupled controller, (Glad and Ljung 2000).

To get the system truly decoupled (diagonal), the matrices W_1 and W_2 would have to be complex and dynamic (depending on s). Normally, this cannot be implemented, and thus constant, real matrices have to be used instead as an approximation. This approximation is made by choosing a frequency at which the decoupling is made, (Glad and Ljung 2000).

7.2 Signal Coupling and Pairing

To pair each input with one output it is necessary to have the same number of outputs and inputs. (The input and outputs and their numbering were described in Section 4.1.3.) As the main choice, only the acceleration outputs are chosen. This is since the accelerations are the outputs that are related to comfort, which is what is aimed at to optimize in this thesis, see Section 3.1. Since deflection would have to be kept under control, some other control law would have to be superimposed to keep it within boundaries, though. Therefore, the coupling of the deflections are also studied.

7.2.1 Gain Plots

In this subsection gains between inputs and outputs are plotted. If one output is influenced much more by one input than by the others, the gain from that input will be much larger, and will be a natural choice for SISO pairing. The advantage of using this method, compared to using the RGA as in the next subsection, is that the entire interesting frequency range can be studied at once. Thus, the risk of not noticing interaction that is limited to a small frequency range, is minimized.

To allow comparison, the magnitudes of the transfer functions from input number i to output number k, G_{ik}, have been plotted in Figure 7.1–Figure 7.2. Then, to make it easier to see how much the actuators influence the output relative to each other, the quotient of the gains have been calculated. Those quotients, plotted in Figure 7.3–Figure 7.6, are calculated as

$$G_{\mathrm{rel},ik}(j\omega) = \frac{|G_{ik}(j\omega)|}{|G_{kk}(j\omega)|}. \tag{7.5}$$

When $i = k$ it is the same function in the numerator as in the denominator. Thus the value of $G_{\mathrm{rel},ik}(j\omega)$ is 1 for all ω. This is the transfer function from the actuator closest to the measured output, which is the most natural choice of input-output pairing. That is, the input actuator force, front right, is paired with the output car body acceleration, front right, and so on. It is desirable that the transfer functions from the other actuators to the same output are small. However, as can be seen in Figure 7.3–Figure 7.6, they are not. In some cases there are some frequency ranges in which they are even higher. The influence from other actuators are thus substantial, and could hardly be neglected. This is true also when interest is directed to only the most important region, which would be approximately 2–40 Hz for the acceleration, according to Figure 2.3, or maybe with an upper limit for model validity at 10 Hz according to the discussion in Section 6. The locations of inputs and outputs are illustrated in Figure 4.2. The vehicle is almost symmetric, and the plots for left and right side are almost identical. Therefore only one side is plotted.

The reason for plotting both $G_{ik}(j\omega)$ and $G_{\mathrm{rel},ik}(j\omega)$ is that studying both those simultaneously makes it easier to see if there are significant interaction from other actuators than the one that is supposed to control a certain output. It is easier to see the relative influences in $G_{\mathrm{rel},ik}(j\omega)$, but if the coupling is strong only where the magnitude $G_{ik}(j\omega)$ has a notch frequency, it might be of less importance, or even due to numerical errors. The highest, sharp peak in Figure 7.3 admittedly is at the frequency where there is a notch in the gain (see Figure 7.1), but there are comparatively high influence from other actuators also at frequencies where the gain is high.

7.2.2 Relative Gain Array

A more formal way to show that there is no way to pair the inputs and outputs into SISO controlled loops is by using the relative gain array (RGA). The relative gain array is calculated according to Section 7.1.1. (All the cases below turn out to have full rank. Thus the inverse exists, and is therefore used in the equations.) Relative gain arrays are calculated at steady state as well as two different suggested bandwidths (10 Hz and 40 Hz). This since those are needed to make the pairing according to Section 7.1.2. RGA has also been calculated for 5 Hz, since this is about in the middle of the most interesting frequency region. If the system is split into SISO systems, it is important to know that nothing strange happens there.

When accelerations are used as outputs the following relative gain arrays are obtained:

$$\mathrm{RGA}(G(0)) = 10^7 \cdot \begin{pmatrix} \text{-4.2} & \text{5.4} & \text{-5.6} & \text{4.5} \\ \text{4.3} & \text{-5.5} & \text{5.8} & \text{-4.6} \\ \text{3.4} & \text{-4.3} & \text{4.5} & \text{-3.6} \\ \text{-3.5} & \text{4.4} & \text{-4.7} & \text{3.7} \end{pmatrix} \tag{7.6}$$

$$\mathrm{RGA}(G(5 \cdot 2\pi j)) = 10^{10} \cdot \begin{pmatrix} \text{-6.4-28j} & \text{5.6+22j} & \text{1.9-1.6j} & \text{-1.1+7.5j} \\ \text{5.6+22j} & \text{-6.4-28j} & \text{-1.0+7.5j} & \text{1.9-1.5j} \\ \text{-1.0-5.5j} & \text{1.8+11j} & \text{1.6-16j} & \text{-2.5+9.8j} \\ \text{1.8+11j} & \text{-1.0-5.5j} & \text{-2.5+9.8j} & \text{1.7-1.6j} \end{pmatrix} \tag{7.7}$$

$$\mathrm{RGA}(G(10 \cdot 2\pi j)) = 10^{11} \cdot \begin{pmatrix} \text{4.0+5.3j} & \text{-3.7-4.78j} & \text{1.1+1.2j} & \text{-1.4-1.7j} \\ \text{-3.7-4.8j} & \text{4.0+5.3j} & \text{-1.4-1.7j} & \text{1.1+1.2j} \\ \text{1.2+1.7j} & \text{-1.5-2.2j} & \text{3.8+3.8j} & \text{-3.4-3.3j} \\ \text{-1.5-2.2j} & \text{1.2+1.7j} & \text{-3.4-3.3j} & \text{3.8+3.8j} \end{pmatrix} \tag{7.8}$$

$$\mathrm{RGA}(G(40 \cdot 2\pi j)) = 10^{12} \cdot \begin{pmatrix} \text{-9.1+19j} & \text{7.3-15j} & \text{-1.5+3.1j} & \text{3.3-6.9j} \\ \text{7.3-15j} & \text{-9.1+19j} & \text{3.3-6.9j} & \text{-1.5+3.1j} \\ \text{-1.5+3.2j} & \text{3.3-6.9j} & \text{-9.1+19j} & \text{7.2-15j} \\ \text{3.3-6.9j} & \text{-1.5+3.2j} & \text{7.2-15j} & \text{-9.1+19j} \end{pmatrix} \tag{7.9}$$

In the matrices above it is clearly seen that no element is anywhere near 1, which was needed for pairing. Instead, they are very large, which means that the loops are very dependent of each other. Thus, there is no pairing possible. This is the same conclusion as in the previous section, where the same interactions were studied in a different way.

When deflections are used as outputs the following relative gain arrays are obtained:

$$\mathrm{RGA}(G(0)) = \begin{pmatrix} \text{4.4} & \text{-3.2} & \text{-0.05} & \text{-0.1} \\ \text{-3.3} & \text{4.4} & \text{-0.09} & \text{-0.05} \\ \text{0.0001} & \text{-0.15} & \text{4.6} & \text{-3.4} \\ \text{-0.15} & \text{0.007} & \text{-3.4} & \text{4.6} \end{pmatrix} \tag{7.10}$$

$$\mathrm{RGA}(G(5 \cdot 2\pi j)) = \begin{pmatrix} \text{1.3-0.65j} & \text{-0.26+0.65j} & \text{-0.0006+0.0001j} & \text{0.001-0.001j} \\ \text{-0.26+0.65j} & \text{1.3-0.65j} & \text{0.001-0.001j} & \text{0.0006+0.0001j} \\ \text{-0.0007+0.0003j} & \text{0.001-0.001j} & \text{1.3-0.66j} & \text{-0.31+0.67j} \\ \text{0.001-0.001j} & \text{-0.0007+0.0003j} & \text{-0.31+0.67j} & \text{1.3-0.66j} \end{pmatrix} \tag{7.11}$$

$$\mathrm{RGA}(G(10 \cdot 2\pi j)) = \begin{pmatrix} \text{0.63-0.67j} & \text{0.38+0.67j} & \text{-0.002-0.001j} & \text{-0.002+0.0002j} \\ \text{0.38+0.67j} & \text{0.63-0.67j} & \text{-0.002+0.0002j} & \text{-0.002-0.001j} \\ \text{-0.002-0.001j} & \text{-0.002+0.0002j} & \text{0.89-0.55j} & \text{0.12+0.55j} \\ \text{-0.002+0.0002j} & \text{-0.002-0.001j} & \text{0.12+0.55j} & \text{0.89-0.55j} \end{pmatrix} \tag{7.12}$$

$$\mathrm{RGA}(G(40 \cdot 2\pi j)) = \begin{pmatrix} \text{1.0-0.002j} & \text{-0.002+0.002j} & \text{-0.0005} & \text{-0.002} \\ \text{-0.002+0.002j} & \text{1.0-0.002j} & \text{-0.002} & \text{-0.0005} \\ \text{-0.0005} & \text{-0.002} & \text{1.0-0.0006j} & \text{0.001+0.0006j} \\ \text{-0.002} & \text{-0.0005} & \text{0.001+0.0006j} & \text{1.0-0.0006j} \end{pmatrix} \tag{7.13}$$

This is better than for acceleration, since those are much close to the identity matrix, and in all cases the numbers on the diagonal are positive. Here, if studying only those RGA:s, chosen according to the suggestions in Section 7.1.1, it would be possible to pair the signals according to the rules in that same section. Then input number 1 would be paired with output number 1, 2 with 2, 3 with 3 and 4 with 4. That means that each actuator would control the output closest to itself, see Chapter 4.1. The interaction from the nearest actuator is however high at low and medium frequencies. Therefore it might be better to divide the system into two 2×2 systems. However, as already mentioned, neither solution would be able to control the acceleration, which is important to comfort. Therefore, such a solution is impossible for the purposes of this thesis.

The conclusion that if only deflections were interesting, it would be possible to divide the system into two 2×2 systems, is not the same as in the previous subsection. Studying Figure 7.4 and Figure 7.6 tells us that there are quite a lot of influences from all actuators at some frequencies. Looking at those figures, for instance 1 Hz could be interesting to study.

Now we get

$$\mathrm{RGA}(G(1\cdot 2\pi j)) = \begin{pmatrix} \text{2.2-4.4j} & \text{-1.4+4.3j} & \text{1.6-0.93j} & \text{-1.4+0.96j} \\ \text{-1.4+4.3j} & \text{2.3-4.4j} & \text{-1.4+0.98j} & \text{1.6-0.91j} \\ \text{1.5-0.79j} & \text{-1.3+0.82j} & \text{1.0-5.0j} & \text{-0.19+5.0j} \\ \text{-1.3+0.84j} & \text{1.4-0.77j} & \text{-0.18+5.0j} & \text{1.0-5.1j} \end{pmatrix}. \tag{7.14}$$

Here it is no longer obvious which actuator should control which output. The influences are high not only between left and right side, but also between front and rear bogie. This example serves as a warning to accept a pairing suggested by the RGA without checking intermediate frequencies.

7.3 Decoupling

Since input-output pairing didn't work, an attempt is made at decoupling. An attempt is made at exact decoupling at a single frequency. That is, complex matrices has been allowed. According to Section 7.1, normally real matrices are needed for implementation. Such approximations have not been reported here, since already the complex decoupling matrices have been found insufficient, as seen below. The weighing matrices W_1 and W_2 have been chosen as $G(j\omega_{dc})^{-1}$ and the identity matrix, respectively, inspired by an example in (Glad and Ljung 2000). This corresponds to weighing of the input (control) signal. ω_{dc} is the frequency that is chosen for decoupling, here $5\cdot 2\pi$ rad/s (5 Hz). The inverse of G does exist at this frequency. With those choices of weighing matrices, the decoupled system, $\tilde{G}(j\omega)$, will be the identity matrix at ω_{dc}. Thus $\tilde{G}(j\omega_{dc})$ is perfectly diagonal, as desired. With this choice, also $\mathrm{RGA}(\tilde{G}(j\omega_{dc}))$ will be unity. The system is perfectly decoupled at the selected frequency. However, even a minor change in frequency will make the system heavily coupled again. Shown below is the RGA for 4.9 Hz, where we even get negative elements on the diagonal, which indicates positive feedback.

$$\mathrm{RGA}(\tilde{G}(4.9\cdot 2\pi j)) = 10^{13}\cdot \begin{pmatrix} \text{-1.4-1.4j} & \text{-0.89-1.5j} & \text{0.46+1.6j} & \text{1.8+1.3j} \\ \text{-0.9-1.6j} & \text{-0.47-1.6j} & \text{0.05+1.6j} & \text{1.4+1.6j} \\ \text{0.55+1.8j} & \text{0.09+1.6j} & \text{0.32-1.6j} & \text{-0.97-1.8j} \\ \text{1.8+1.2j} & \text{1.3+1.4j} & \text{-0.82-1.7j} & \text{-2.2-1.0j} \end{pmatrix} \tag{7.15}$$

Similarly, for decoupling at 2 Hz. The decoupling is perfect at 2 Hz, but unacceptable at 1.9 Hz, see below.

$$\mathrm{RGA}(\tilde{G}(1.9\cdot 2\pi j)) = 10^{13}\cdot \begin{pmatrix} \text{1.0-0.34j} & \text{1.0-0.31j} & \text{-1.0+0.30j} & \text{-1.0+0.35j} \\ \text{1.0-0.31j} & \text{1.1-0.28j} & \text{-1.1+0.26j} & \text{-1.0+0.32j} \\ \text{-1.0+0.30j} & \text{-1.1+0.27j} & \text{1.1-0.25j} & \text{1.0-0.31j} \\ \text{-1.0+0.35j} & \text{-1.1+0.32j} & \text{1.0-0.31j} & \text{1.0-0.36j} \end{pmatrix}$$

(7.16)

Those frequencies would have to work for decoupling to work in application in this thesis. No further investigations are needed to turn down the idea of decoupling with the use of those weighing matrices. However, another choice that would also make $\tilde{G}(j\omega_{dc})$ equal to the identity matrix is switching W_1 and W_2 with each other. This corresponds to weighing of the output signal. For that choice, and decoupling at 5 Hz, we get at 4.9 Hz

$$\mathrm{RGA}(\tilde{G}(4.9{\cdot}2\pi j)) = \begin{pmatrix} \text{1.3-0.10j} & \text{-0.25+0.07j} & \text{-1.23+0.75j} & \text{1.2-0.71j} \\ \text{-0.25+0.07j} & \text{1.2-0.03j} & \text{0.70-1.0j} & \text{-0.66+0.96j} \\ \text{-1.5+0.55j} & \text{0.94-0.92j} & \text{5.0-5.8j} & \text{-3.5+6.1j} \\ \text{1.4-0.52j} & \text{-0.90+0.87j} & \text{-3.5+6.0j} & \text{4.0-6.4j} \end{pmatrix} \tag{7.17}$$

which is not sufficient, since it is no longer obvious which input that should belong to which output. For decoupling at 2 Hz, we get at 1.9 Hz

$$\mathrm{RGA}(\tilde{G}(1.9 \cdot 2\pi j)) = \begin{pmatrix} \text{1.2-0.12j} & \text{-1.2-0.17j} & \text{0.36-0.04j} & \text{-0.19-0.02j} \\ \text{-0.13+0.15j} & \text{2.2+0.20j} & \text{-0.37+0.02j} & \text{0.18+0.006j} \\ \text{-0.14+0.17j} & \text{1.3+0.17j} & \text{0.64+0.07j} & \text{0.19+0.02j} \\ \text{0.13-0.19j} & \text{-1.3-0.19j} & \text{0.40-0.04j} & \text{0.84+0.02j} \end{pmatrix} \tag{7.18}$$

which already is quite far from the identity matrix, and lowering the frequency further to 1 Hz, without redoing the decoupling, will make the system unstable.

$$\mathrm{RGA}(\tilde{G}(1.9{\cdot}2\pi j)) = 10^2{\cdot}\begin{pmatrix} \text{0.39+2.2j} & \text{-0.17-2.2j} & \text{-1.9-0.45j} & \text{1.7+0.46j} \\ \text{-0.07-2.6j} & \text{-0.20+2.6j} & \text{2.1+1.5j} & \text{-1.8-1.5j} \\ \text{-0.30+0.58j} & \text{0.33-0.39j} & \text{-0.23-0.86j} & \text{0.21+0.67j} \\ \text{-0.01-0.13j} & \text{0.05-0.0005j} & \text{0.04-0.21j} & \text{-0.07+0.34j} \end{pmatrix} \tag{7.19}$$

Another common choice of decoupling matrices, which are generally more robust solutions than to make the decoupled system diagonal, is to choose either $W_1 \cdot G = P$ or $G \cdot W_2 = P$, where P is a diagonal matrix with the diagonal elements of G on its diagonal, (Breitholtz 2009). (As a comparison, for the decoupling matrices attempted above, $P = I$.)

With $G \cdot W_2 = P$, and decoupling at 2 Hz, RGA is the identity matrix at 2 Hz as expected, but the following RGA is obtained at 4.9 Hz. (Outputs are accelerations.)

$$\mathrm{RGA}(\tilde{G}(4.9{\cdot}2\pi j)) = 10^2{\cdot}\begin{pmatrix} \text{0.63-0.63j} & \text{-0.51+0.75j} & \text{-1.0+0.09j} & \text{0.92-0.20j} \\ \text{-0.56+0.74j} & \text{0.44-0.86j} & \text{1.2-0.15j} & \text{-1.0+0.27j} \\ \text{-2.5+0.16j} & \text{2.7-0.42j} & \text{2.2+1.9j} & \text{-2.5-1.7j} \\ \text{2.4-0.27j} & \text{-2.7+0.53j} & \text{-2.3-1.9j} & \text{2.6+1.6j} \end{pmatrix}$$

(7.20)

Here the elements are large and it is also unclear which input-output pairs are dominating. Thus this decoupling matrix did not work either.

A final attempt is made with $W_1 \cdot G = P$. With decoupling at 2 Hz, we get already at 1.9 Hz:

$$\mathrm{RGA}(\tilde{G}(1.9 \cdot 2\pi j)) = 10^{12} \cdot \begin{pmatrix} \text{-1.2+2.0j} & \text{-1.3+2.0j} & \text{1.3-2.0j} & \text{1.2-2.0j} \\ \text{-1.3+2.0j} & \text{-1.4+2.0j} & \text{1.4-2.0j} & \text{1.3-2.0j} \\ \text{1.3-2.0j} & \text{1.4-2.0j} & \text{-1.4+1.9j} & \text{-1.3+2.0j} \\ \text{1.2-2.0j} & \text{1.3-2.0j} & \text{-1.3+2.0j} & \text{-1.2+2.1j} \end{pmatrix} \tag{7.21}$$

This is very large and the loops are therefore almost completely dependent.

The conclusion is that decoupling does not work with neither input nor output weighing, for any of the decoupling matrices studied for this system. Generally the output weighing deteriorates slower though, as the RGA is studied further away from the decoupling frequency.

7.4 Concluding Remarks

Unfortunately the coupling between all input-to-output relations is very high, and no pairing that can be used for control design can be found. Decoupling with stationary weight matrices does not look promising either, not even over a small frequency interval. This is probably due to the strong frequency dependence of the coupling. Therefore, MIMO design has been chosen.

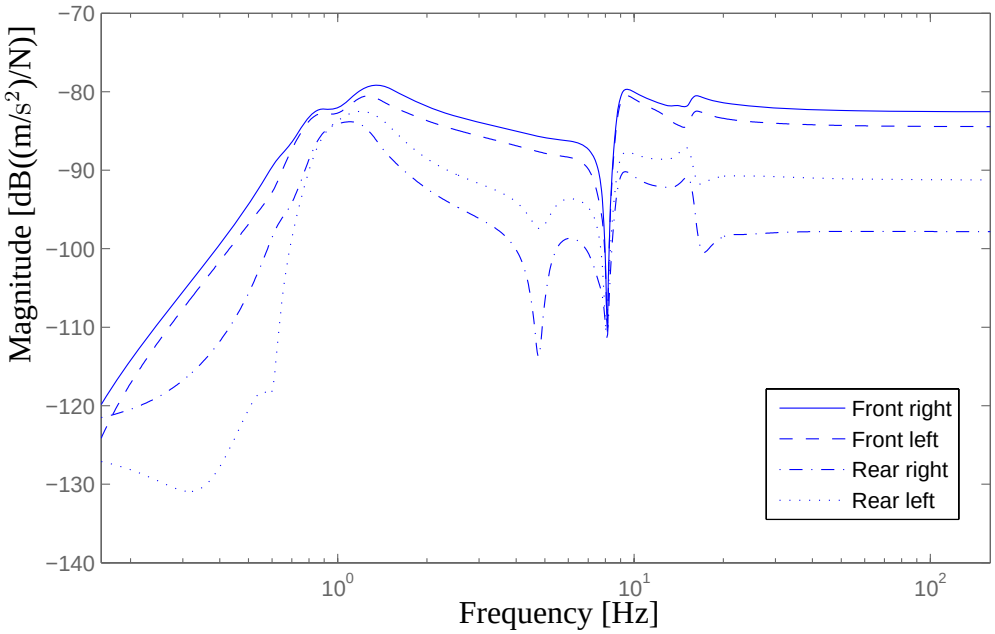

Figure 7.1: Gain plot of transfer function from all actuator forces to acceleration in car body, front right. Train velocity 1 km/h, passive suspension.

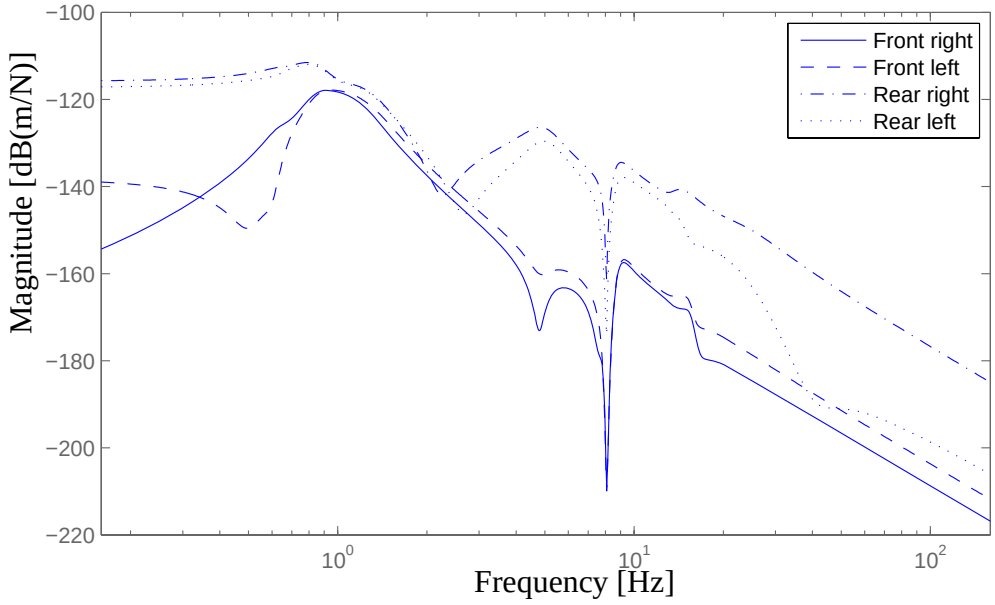

Figure 7.2: Gain plot of transfer function from all actuator forces to bogie-to-carbody deflection, rear right. Train velocity 1 km/h, passive suspension.

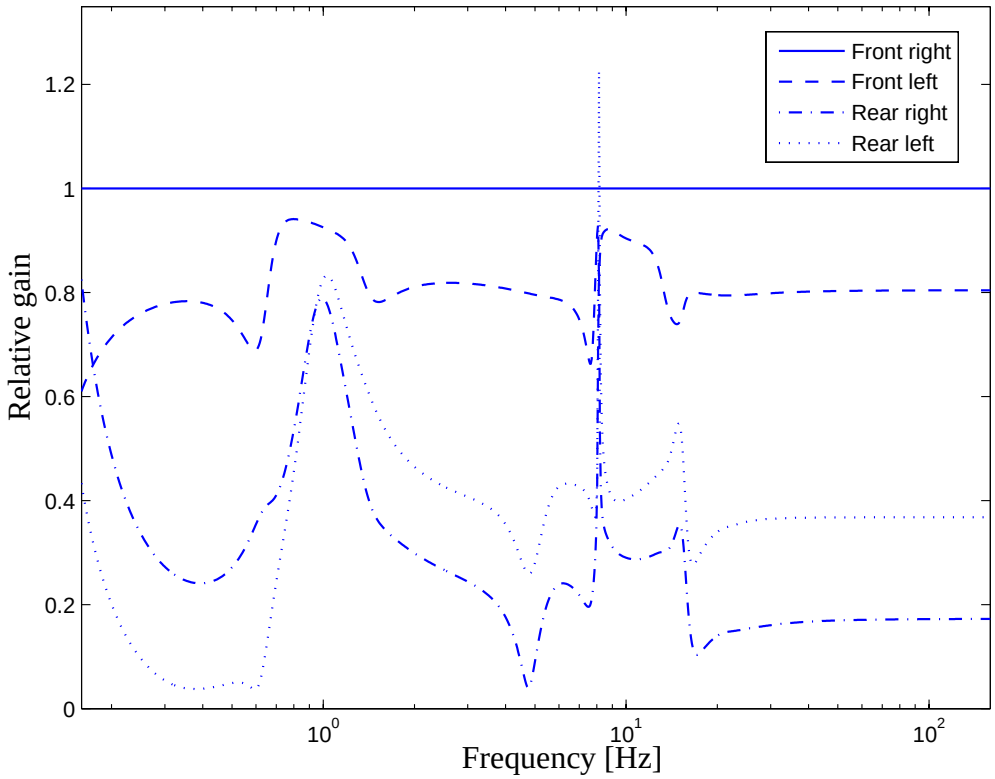

Figure 7.3: Magnitude of transfer function from each actuator (force) to car body acceleration front right, divided by magnitude of transfer function from the front right actuator. Normalized according to Equation 7.5.

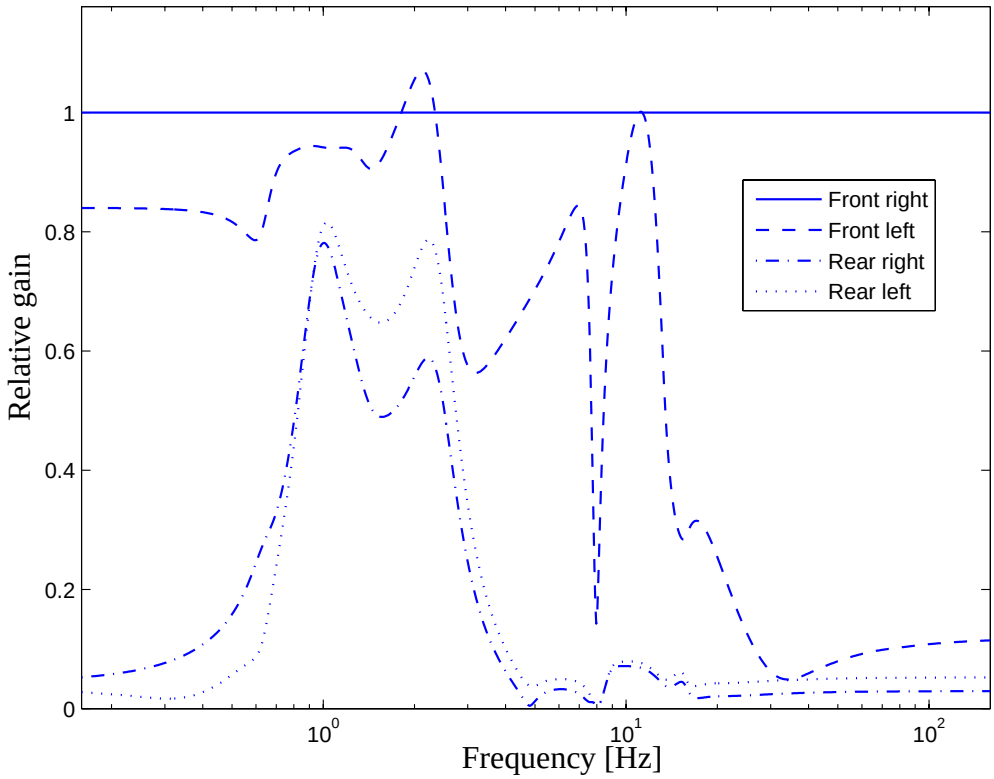

Figure 7.4: Magnitude of transfer function from each actuator (force) to bogie-to-carbody deflection front right, divided by magnitude of transfer function from the front right actuator. Normalized according to Equation 7.5.

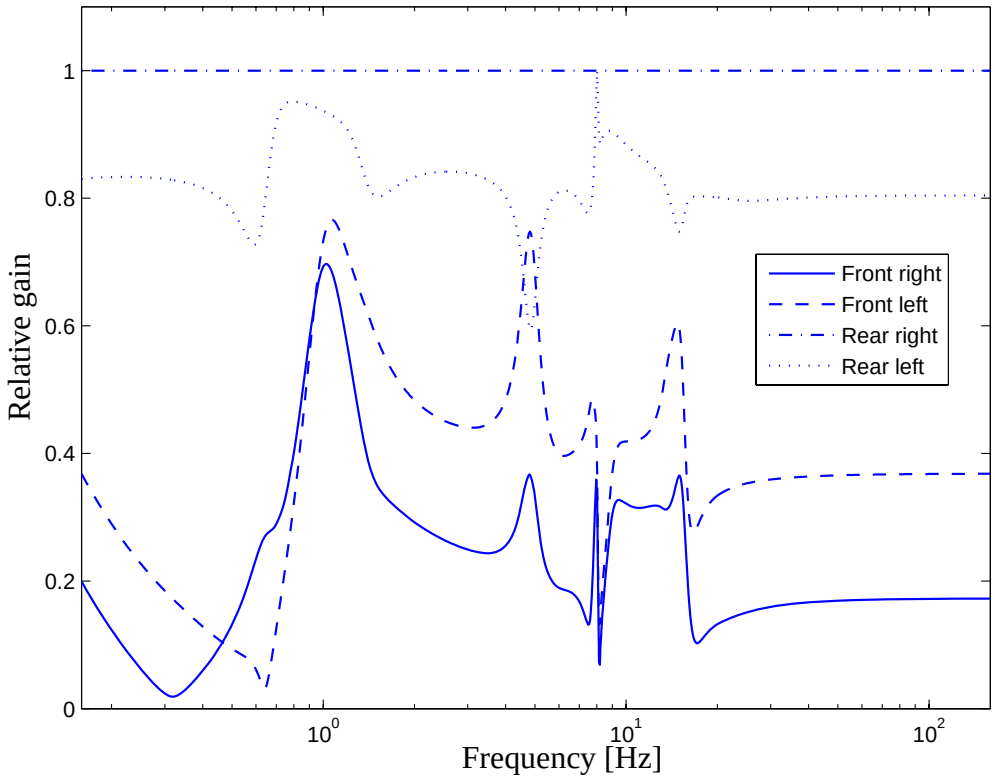

Figure 7.5: Magnitude of transfer function from each actuator (force) to car body acceleration rear right, divided by magnitude of transfer function from the rear right actuator. Normalized according to Equation 7.5.

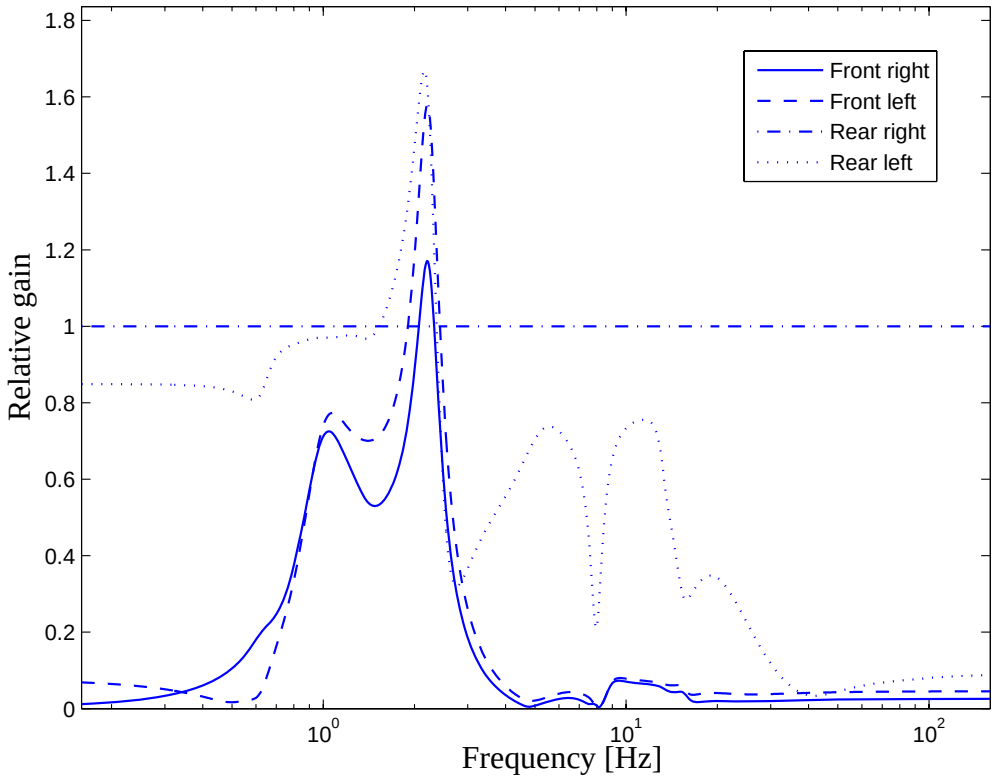

Figure 7.6: Magnitude of transfer function from each actuator (force) to bogie-to-carbody deflection rear right, divided by magnitude of transfer function from the rear right actuator. Normalized according to Equation 7.5.

chapter viii

model reduction

Since Chapter 7 showed that SISO control design wasn't feasible, the choice will have to fall on MIMO control design. Modern methods of controller design, such as $\mathcal{H}_\infty$ and LQG, produce controllers of equal or higher order than the plant, (Skogestad and Postlethwaite 1996). (Both $\mathcal{H}_\infty$ and LQG are methods that can be used with MIMO systems, (Glad and Ljung 2000).) If a system can be approximated with one of a lower order, it makes analysis, control design, and implementation easier, (Glad and Ljung 2000).

This approximation is what is referred to as model reduction or model simplification. One starts with a higher order model, and reduces it to a model with a lower order than the initial model.

Assuming that not all states can be measured, it is necessary to use an observer if some kind of state feedback is to be used. (Which is the case for instance when using LQ control.) The Kalman filter requires a model both from disturbances and control signals (with the same states and outputs), (The MathWorks 2007). Thus the goal of the model reduction is to calculate a reduced model from both the control signals and disturbances, with both the same states and outputs. The models should be as much reduced as possible while still being "good enough".

In this chapter an algorithm, tailored for model reduction of the railway vehicle model studied in this thesis, is developed and compared with two commercial methods. The model used as a starting point for all reductions in this chapter, is a linear time-invariant model on state space form, the same as in Chapter 6.

8.1 Background Theory

This section describes commercial methods of model reduction and their basis, as well as the theoretical basis for another method suggested in this chapter.

Assume a system on the following form:

$$\dot{x} = Ax + Bu \tag{8.1}$$
$$y = Cx + Du, \tag{8.2}$$

where x represents the states, u the inputs, and y the outputs.

8.1.1 State Transform

With the state transform $\xi = Tx$, if the inverse of T exists, the state space model will turn into

$$\dot{\xi} = TAT^{-1}\xi + TBu \tag{8.3}$$
$$y = CT^{-1}\xi + Du, \tag{8.4}$$

(Lennartson 2002).

8.1.2 Diagonalization

An $n \times n$ matrix A is diagonalizable if and only if A has n linearly independent eigenvectors. If it is diagonalizable it can be written on the form $A = vA_{diag}v^{-1}$, where v is an $n \times n$-matrix consisting of the eigenvectors to the diagonal matrix A_{diag}, (Bengtsson and Weisstein 2008).

8.1.3 Controllability and Observability

A state vector x^* is *controllable* if there is an input signal that brings the state from the origin to x^* in finite time. A system is controllable if all its state vectors are controllable. A state vector $x^* \neq 0$ is *unobservable* if the output signal is identically zero when the initial value is x^* and the input signal is identically zero. The system is *observable* if none of its state vectors are unobservable, (Glad and Ljung 1989).

When a system is on a diagonal form, a mode x_i with corresponding row vector $B_i = 0$ is not affected by the input, and is thus uncontrollable, (Glad and Ljung 2000). In the same way, a mode x_i with corresponding column vector $C_i = 0$, does not affect the output, and is thus unobservable, (Glad and Ljung 2000).

The Controllability Gramian can be written as

$$S_x = \int_0^\infty e^{At}BB^T e^{A^T t}dt, \tag{8.5}$$

and the Observability Gramian as

$$O_x = \int_0^\infty e^{A^T t}C^T C e^{At}dt, \tag{8.6}$$

(Glad and Ljung 2000)

8.1.4 Balanced Realization

A balanced realization is an asymptotically stable minimal realization in which the controllability and observability Gramians are equal and diagonal, (Skogestad and Postlethwaite 1996).

8.1.5 Softwares for Model Simplification

Two software programs with support for model simplification, both based on balancing techniques, have been used. Those are briefly described below.

Slicot

SLICOT is a subroutine library based on BLAS and LAPACK routines and further developed, partly in the framework of the European project NICONET[1], (Benner et al. 1998). The SLICOT routines are written in Fortran 77, but they can also run from Matlab and Scilab, (Varga 2000).

According to the Slicot manual, its command `fwbred` is a function for frequency-weighted balancing related model reduction. It has support for input and output weighing. `fwbred` also handles unstable models, and will then always keep the unstable parts, (Niconet 2005). There are two methods available for the reduction: the Balanced Truncation Approximation and the Singular Perturbation Approximation, (Niconet 2005).

Matlab

In a paper published the year 2000, (Varga 2000), Varga showed that `balreal`, which is a method for balanced realization in Matlab that is used for model reduction, systematically fails at high order systems, which Slicot handles. However, since this paper was published, Mathworks have improved their algorithms. It still indicates that there are numerical issues to deal with when reducing large models, though.

According to the Matlab manual, its command `balred` uses implicit balancing techniques to compute a reduced-order approximation. `balred` also handles unstable models, and will then always keep the unstable parts, (The MathWorks 2007). As opposed to the Slicot routine described above, there is however no support for neither input nor output weighing. With `balred`, there are two choices of how to reduce the model. One is to enforce matching DC gains, and the other to discard the states associated with small Hankel singular values. The latter method, that is referred to as the 'Truncate' method, tends to produce a better approximation in the frequency domain, but the DC gains are not guaranteed to match, (The MathWorks 2007).

8.2 Evaluation Method

The reduced model is good enough if it can be used to design a controller which, with an acceptable outcome, can be placed in the un-reduced model. This is difficult to see without actually doing so, but there are some indications. The un-reduced and reduced models are compared in Bode plots. The Bode plots where the outputs are accelerations are multiplied with the comfort filter, described in Section 2.3, before evaluation. The reason for this is that comfort is one of the evaluation criterions, which acceleration in itself isn't, see Section 3.1. If the frequency weighted Bode plots from the reduced model seem to follow the unreduced rather well in the selected area, 1–40 Hz, the reduced model is a candidate for controller design. The frequency range is chosen based on the vertical comfort filter in Section 2.3, and the frequency range of model validity in Chapter 6, with some added margin in the upper frequency region.

The Bode plots are compared for accurateness using visual inspection. More weight is put on the control signal to output relationship, than to the disturbance to output relationship. The reason for this is that if you cannot control a state it does not help much to model it. Also, there could be other, unknown, disturbances not modeled.

[1] http://www.win.tue.nl/niconet/niconet.html

When studying the Bode plots, the state space matrices have been rewritten to only have the second derivative of the track irregularities as inputs. The dynamics of the disturbances and its derivatives have been included in the model. The details can be found in Appendix B.

8.3 Methods of Model Reduction

In this section, the algorithm of a method of model reduction, tailored for the application in this thesis, is described. Also described is how two commercial algorithms have been used, and the additional calculations necessary for application here.

8.3.1 Preparatory Manipulations

Removing Unstable States – Motivation

When simplifying the model, some methods will either keep all unstable states, or not work at all if there are unstable states. (Though the latter case is not presented here.) When there is a wish to remove unstable states, those have to be removed before running such a method. (After would sometimes be a possible option also. They do need to be removed sometime, though.)

Physical insight tells that there should not be any unstable states in this model (at 1 km/h). Also, when simulating the non-linear model, it is stable, and without disturbances it rapidly moves to equilibrium and stays there. However, the model has 330 states with eigenvalues distributed between the order of magnitude 10^{-4}, and the order of magnitude 10^{10}, disregarding the eigenvalues that are zero in Simpack (but not in Matlab). This indicates that the problem is difficult to handle from a numerical point of view. As mentioned, there are some eigenvalues that are zero in Simpack. It is some of those that are small and positive in Matlab. By studying the mode shapes it can be seen that the zero eigenvalues corresponds to modes in the wheelsets and other rotating objects attached to those. (There is a build-in feature to study this in Simpack.) In this project, only vertical and roll directions are studied. Those directions are orthogonal to the rotations of the wheelsets, and thus should not be part of the transfer functions studied. An analysis in Matlab shows, as expected, that the unstable states are not observable. (Save for some numerical errors.) See Chapter 8.3.2. Also, it can be seen in the Bode plots, after diagonalization and removal of unstable states and states close to the stability limit (y-axis) that the transfer function are barely affected. See Figure 8.1.

Diagonalization

To be able to easily remove unstable states, and to allow further model reduction by the method described in Section 8.3.2, the model is diagonalized. That is, a state transform is applied on the state space matrices to make the A matrix diagonal. Then the entries in the A matrix with a positive real part corresponds to an unstable state.

In this case, the matrix A, which is a 330×330-matrix, has eigenvectors which, when put together in a matrix, has full rank. That is, rank 330. Thus it has 330 linearly independent eigenvectors, and the matrix A is diagonalizable, according to Section 8.1.

To get a linear state space model with a diagonal A-matrix, the following state transform is applied:

$$A_{new} = v^{-1} A_{old} v \tag{8.7}$$
$$B_{new} = v^{-1} B_{old} \tag{8.8}$$
$$C_{new} = C_{old} v \tag{8.9}$$
$$D_{new} = D_{old}. \tag{8.10}$$

In practice though, the eigenvector matrix v and the diagonal matrix A_{diag} with eigenvalues on the diagonal, are calculated simultaneously with the Matlab command `eig`. A_{new} is set to be A_{diag}. This way A_{new} will really be diagonal, and round-off errors on the off-diagonal elements will be avoided. In theory $A_{diag} = v^{-1} A_{old} v$.

State Removal

Since the system is now on diagonal form, the rows and columns corresponding to a certain state, that has been found unimportant, can simply be deleted. This is also the method chosen. Another choice would have been to match the DC-gain (0 Hz), but this worsens the accuracy in other frequency intervals. The DC-gain is not considered the primary concern here, since if needed that could be taken care of by a slower loop containing integration, acting on the error in the outputs. Also, it is outside of the chosen range, as mentioned above. And as seen in Chapter 6, the model is not valid below 1 Hz anyway.

8.3.2 Tailored Algorithm

When using the tailored algorithm described here, the model is reduced based on a combination of observability, controllability from the actuators and (sometimes) controllability from the disturbances, as well as frequency concerns.

The original reason for developing a tailored algorithm was that the balancing methods in Matlab could not handle sufficiently large models. After improvements in recent versions of Matlab, Matlab's build-in functions for model reduction can be used. The algorithm described here yields significantly better results, though. See Section 8.4.

An overview of the tailored algorithm can be found in Figure 8.2. A more detailed description can be found in the enumerated list that follows. For clarifying reasons, the inputs have been divided into control inputs u, and disturbance inputs w. The syntax used is

$$\dot{x} = Ax + Bu + Nw \tag{8.11}$$
$$y = Cx + Du + Mw. \tag{8.12}$$

1. To make it easy to see which states corresponds to high frequencies and which are controllable or observable, the model is written on diagonal form, as described in Section 8.3.1. Then the eigenvalues can be found on the diagonal.

2. Then, parts of the state space representation that correspond to high frequencies are selected for removal. Those are selected since the high frequency accelerations are not important for human comfort, and the deflections are small in those regions anyway. The choice has fallen on removing states with eigenvalues corresponding to frequencies higher than 40 Hz.

3. Then, parts of the model that are close to unobservable have been removed. To select modes that are close to unobservable, the absolute values of the elements in each column in C are summed and normalized, see Figure 8.3. The modes corresponding to a small sum in any of these are selected for removal. This removes all unstable states, and is done before the removal of uncontrollable states, to make it easier to set the limit of removal of not controllable states. The reason for this is that some of the states that are unstable influence some states very much, and the limit of state removal is set as a quotient of the maximum. After normalizing the C matrix to give equal weight to all outputs, and then normalizing again to make the maximum column sum equal to 1, the maximum column sum for an unstable state is $1.5 \cdot 10^{-8}$. Thus the unstable states are basically unobservable. With this normalization, any state corresponding to a column sum smaller than 1/100 is removed.

4. This step has the option of two different versions. The first version only takes the controllability from the actuator into account. The second version combines controllability from the disturbances with controllability and observability from the actuators.

   To select modes that are close to uncontrollable from the actuators or uncontrollable from the disturbances, the absolute values of the elements in each row in B and N are summed. Figure 8.4 shows the absolute values of the row sums for the B and N matrices. Since the system is on diagonal form, those sums show the effect of the input on the states. If a sum is zero (each element is zero) that state is not controllable. If it is very small it is close to not controllable. Since there is a few orders of magnitude difference between the row sums from the actuators and from the disturbances (the units are also different), the sums are divided by a value to make each maximum sum equal to 1.

   Version a) In this version, parts of the model that are close to uncontrollable from the actuator is removed. That is, only the row sums of the B matrix are studied. Modes corresponding to a small sum here, are selected for removal. With the normalization explained above, removal of states corresponding to row sums of 1/10 gives 21 states, 1/5 gives 15 states, and 1/2 gives 9 states.

   Version b) In this version, both the controllability from the actuators, and from the disturbances, are used when selecting modes to remove. The motivation for not disregarding the disturbances in the reduction, although the possibility to handle disturbances where the actuator has low influence is limited, is that a disturbance might heavily affect a state that had *just* bad enough controllability to be removed. Then it will still be important for the performance of the system to keep that state and do the best to control it. Looking at the controllability there aren't very heavy influences from the disturbances where it is not controllable though, see Figure 8.4, and the approach in the previous version has been used only in some cases.

   The states that are kept in this version, but not in the previous, are those who are well controllable from the disturbances, and at the same time reasonable well controllable from the actuators. Written with the symbols from set theory, the states that are kept from the version where only high frequency content has been removed are:

$$S_1 \cup (S_2 \cap (S_3 \cap S_4)), \tag{8.13}$$

where S_1 contains the states that are well controllable from the control signals, S_2 contains the states that are well controllable from the disturbance signals, S_3 contains the states that are reasonable well controllable from the control signal, and S_4 contains the states that are well observable.

5. The model has been on complex diagonal form during the reduction. However, to be able to do simulations in Simulink, the model has to be on real form. Therefore the model is transformed back into real block-diagonal form. This is the form that is finally compared with the original model.

Discussion and Future Work

Different limits on observability and controllability have been tried. This naturally results in different sized reduces models, where the accuracy of the reduced model deteriorates with increased reduction.

Unstable states are not removed before using this method. They disappear automatically since they are unobservable.

Due to the diagonalization (state transform), the states in the reduces models do not correspond to specific physical states, but are linear combinations of those.

When using the described method, it is necessary with some caution. The transfer function from input number *i* to output number *j* can be calculated as

$$g_{ij} = \sum_{n=1}^{N} \frac{c_{in} b_{nj}}{\mathrm{s} - a_{nn}} + d_{ij}, \tag{8.14}$$

where *N* is the number of states, s is the Laplace variable, and *a*, *b*, *c*, *d* and *g* are single elements in the corresponding matrices. G is here the matrix of transfer functions. All matrices have complex numbers. This equation is derived in Appendix C. From this it can be seen that the same input-output relationships can be described in different ways, by moving influences between the B and C matrices. In this particular application the described method works, although lowering the demands on observability deteriorates the system accuracy significantly faster than lowering the demands on controllability. The system here is generated from physical data, consistently using SI-units, which might have helped. It is important to evaluate the system in each step to see if the suggested algorithm works, and where to put the limits for reduction. For applications on other systems, the suggested algorithm may or may not work, and it is recommendable to compare the results with those from an other method as well.

The described algorithm does not offer much of a frequency weighting. It simply regards high frequencies all together, and considers the remaining equal. It would be straight-forward to add frequency weighing though. When it is considered whether a state should be removed or not, the sum used to decide this could first be multiplied with a frequency dependent weight. The problem is that it is not so straight-forward to add *different* frequency dependent weights to acceleration and deflection outputs. Thus either acceleration or deflection would be weighted wrong.

Another possible way to improve the reduced model is to manipulate the D matrix. As seen in Equation 8.14, each element in D influences one single transfer function. The gain is influenced independent of frequency, and the phase is not influenced at all. Thus for cases

where the entire gain function of the simplified model is too high or too low, this could be a way to improve the simplification algorithm.

How to weigh the disturbances is another thing that is not optimized. Equal weight have been put to track irregularities and its derivatives. Putting some clever weights on those might improve the result, in the cases disturbances are at all taken into account.

8.3.3 Commercial Software

The two commercial softwares used for model reduction are Matlab and Slicot, where Slicot is used in the version Matlab add-on. Both the commands used, Matlab's `balred` and Slicot's `fwbred` always keeps the unstable part. Since those are not important here, they are removed manually prior to the use of those commands, according to Section 8.3.1. It would also be possible to run the general reduction first, and remove the unstable part afterwards. This solution is not chosen, since it is easier to decide how many states to leave when the model reduction commands are used as the last step.

Matlab's Build-In Function

There is a build-in function in Matlab that is called `balred`, described in Section 8.1. This has been used in the version that removes states by truncation, for the same reason as described in Section 8.3.1.

Reduction Using Balanced Realization Using Slicot Subroutine Library

There is a function in Slicot that is called `fwbred`, described in Section 8.1. This has been used in the version that removes states by truncation, for the same reason as described in Section 8.3.1.

Weighting filters are used to tell the reduction command what is important to keep after the reduction. There are both input and output weighing filters.

1. Input weighing: Weight 1 is used for control inputs, and 0 for disturbances. That is, the effects of the disturbances have been disregarded during the reduction.

2. Output weighing: For the acceleration outputs the comfort filter for the vertical direction, see Section 2.3, is used. For the deflection outputs a band pass filter, H_{bp}, with gain is used. This filter is chosen as

$$H_{\mathrm{bp}} = K \cdot \frac{\frac{s}{\omega_1}}{(1+\frac{s}{\omega_1}) \cdot (1+\frac{s}{\omega_2})}, \tag{8.15}$$

where $K = 317$, $\omega_1 = \frac{1}{2} \cdot 2 \cdot \pi$, and $\omega_2 = 40 \cdot 2 \cdot \pi$. The gain K has been chosen in the same way (to the same number) as the relative importance of the deflection compared to the acceleration was chosen in Section 8.3.2 (normalization of C matrix).

8.4 Comparisons and Conclusions

8.4.1 Bode Plot Comparisons

For each representation of the model (such as the full model or one of the reduced models), there are $4 \cdot 8 = 32$ transfer functions from the control inputs to the outputs, and $12 \cdot 8 = 96$ transfer functions from the disturbances to the outputs. That is, 128 transfer functions in total, each of which can be represented by its own Bode plot. Here, only a selection of those are shown. The Bode plots are plotted in Matlab. Note that Matlab has a tendency to sometimes plot the phase wrong with $n \cdot 360$ degrees, and/or with 180 degrees. The latter can usually be seen as a steep change of 180 degrees in the phase curve. In all plots with acceleration outputs, the plots are frequency weighted according to Section 2.3.

In Figure 8.5–Figure 8.6, the tailored algorithm in the form that disregards the disturbances, is compared to the two commercial methods `fwbred` and `balred`. In both cases those also disregard the disturbances. For all cases, there has been a reduction from 330 states to 21 states. It is clear that for the Matlab function `balred`, this reduction is too big. The Bode plots for the reduced models show no resemblance to the Bode plots of the full, unreduced, model. The other methods both work better, but it is clear that the tailored algorithm produces a result closer to the unreduced model.

In Figure 8.7–Figure 8.11, the two versions of the tailored algorithm is compared. In the first version, it is the same reduction, to 21 states, as above. In the second version, the same 21 states are kept, plus another 4 selected by using Equation 8.13. In the first 2 Bode plots, representing actuator-to-output relationships, the differences between the two versions are small. In the following 3 Bode plots however, the differences are larger, in favor of the method taking disturbances into account. Those 3 Bode plots represent disturbance-to-output relationships. This is as expected, since the additional 4 states were those, not already included, that were influencing the states most according to Section 8.3.2.

In Figure 8.12–Figure 8.15 it is shown how the reduced model is getting further away from the original, full, model, with increased reduction (to 21, 15, and 9 states). They also show the differences between the transfer functions in the front and rear part of the vehicle.

8.4.2 Advantages with Each Method

All methods used have their advantages. Note however, that although Matlab's algorithm has some advantages, it is useless for this application.

Advantages of tailored algorithm:

- Flexible. It is for instance possible to set up conditions that will take several factors into account at once.
- Transparent. For instance, the influences from different states can be studied, before a limit for when a state should be removed, is set.
- Complex conjugated pairs can easily be kept as they are. (For other methods number of states left has to be specified.)
- For this particular model and inputs to the algorithms, this is the method that yields best results.

Advantages of Matlab command `balred`:

- Very easy to use.
- Included in Control System Toolbox.
- Size of remaining model can be explicitly decided.

Advantages of Slicot command `fwbred`:

- Easy to use (at least as an add-on to Matlab).
- Supports weighing of inputs and outputs, including frequency weighting.
- Size of remaining model can be explicitly decided.

The influences from the disturbances can be taken into account both when using the tailored algorithm, and when using Slicot. A major difference though, is that the tailored algorithm can take into account if there is still some control available for a state considered for removal. In the case of Slicot, if disturbances are taken into account, a state that is important to the disturbance-to-output relationship will be kept even if it is completely uncontrollable. This will lead to controllers with unnecessary many states. However, for this application, the need for taking disturbances into account is low. Therefore, generally both methods are used completely without taking disturbances into account.

8.4.3 Concluding Remarks

The higher amount of reduction that is applied to a model, the worse it gets. Thus, there is a trade-off between few states and accurate model. Which model to use depends on the application. In this case the application is control, and different size models are tried for control purposes in a later chapter.

Between the three methods tried: tailored algorithm, Matlab's algorithm, and Slicot's algorithm, there is a clear looser. Matlab's algorithm, which does not take frequency consideration into account, yields unacceptable results for much lesser amount of reduction than the other two. It is more difficult to make a fair comparison between the other two methods. The many possibilities to choose parameters makes it difficult to make any definite conclusions, although an attempt has been made to use similar parameters for both methods. With the author's best attempt to choose parameters for both methods, the tailored algorithm is best for this application.

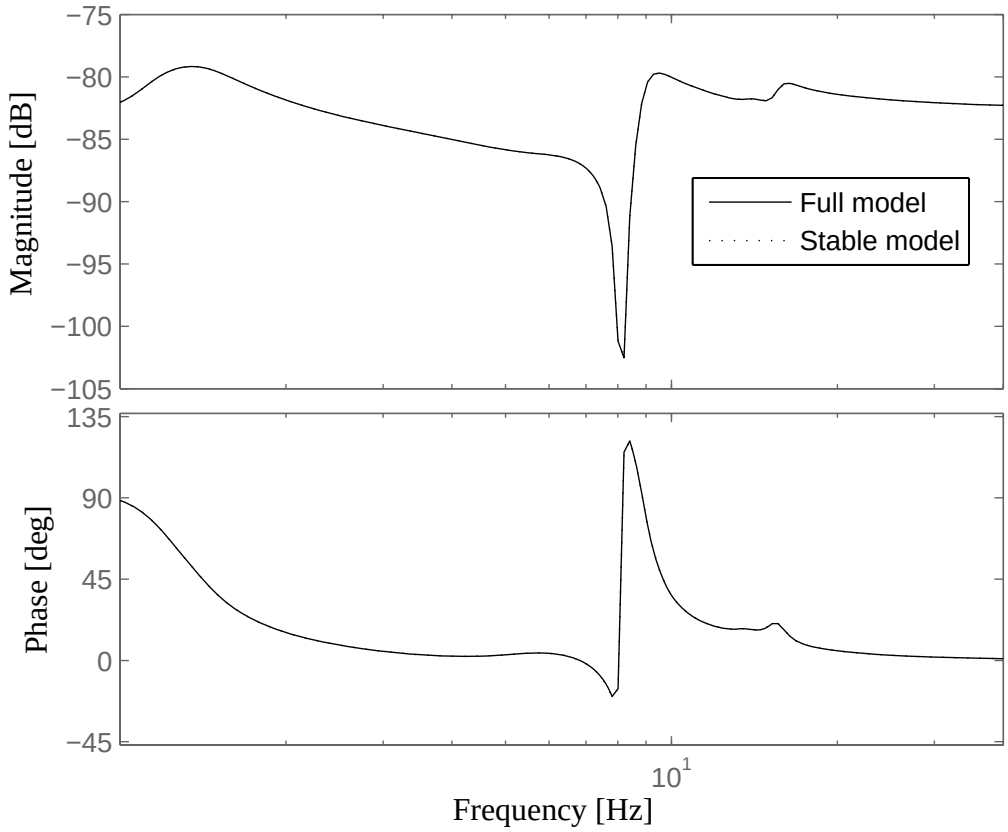

Figure 8.1: Bode plot from control input front right, to car body acceleration front right. Comparison between full model, and model with unstable parts removed. The curves are fully overlapping.

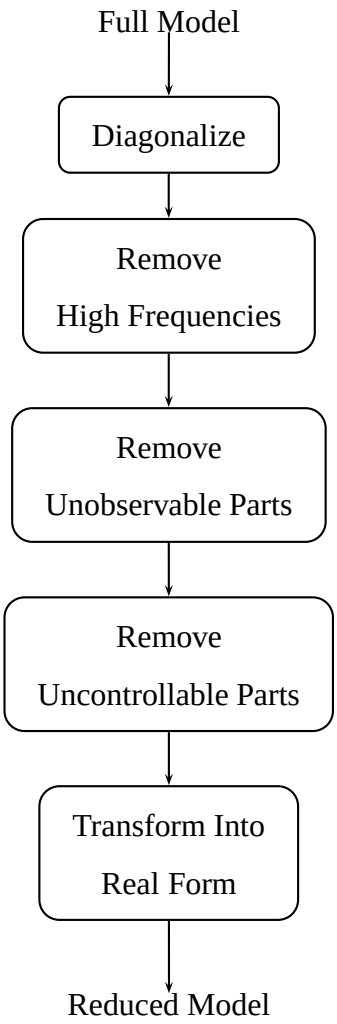

Figure 8.2: Flow chart of main steps in model reduction using tailored algorithm.

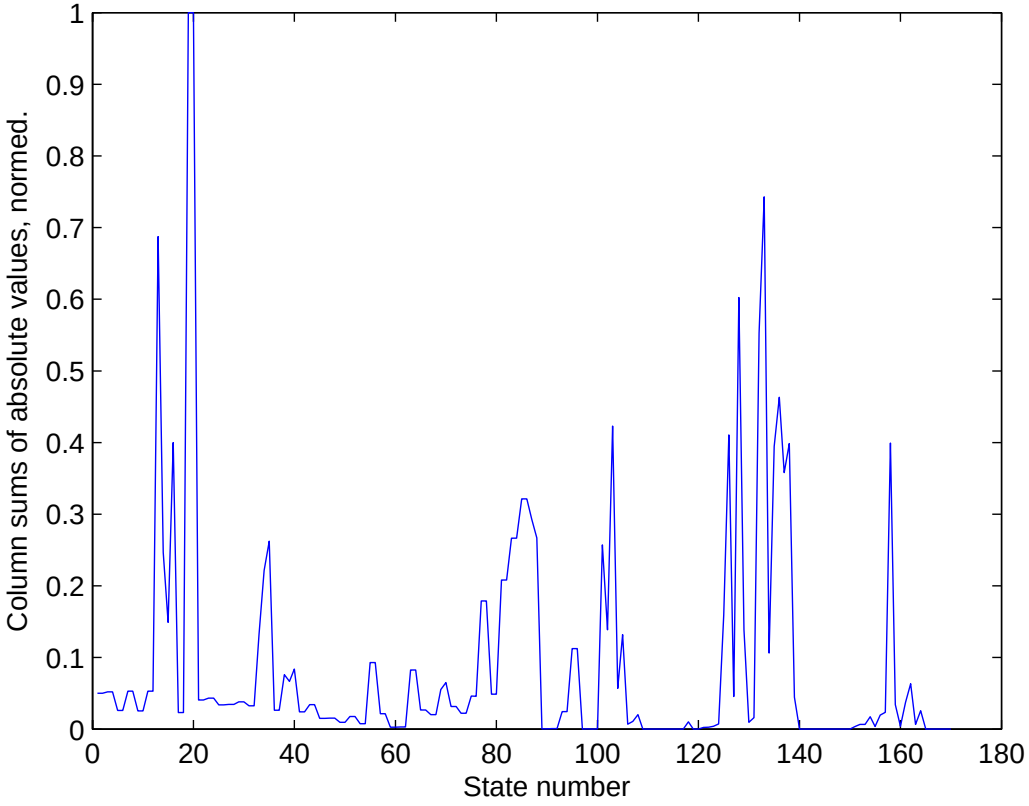

Figure 8.3: Weighted column sums for C matrix, to show observability.

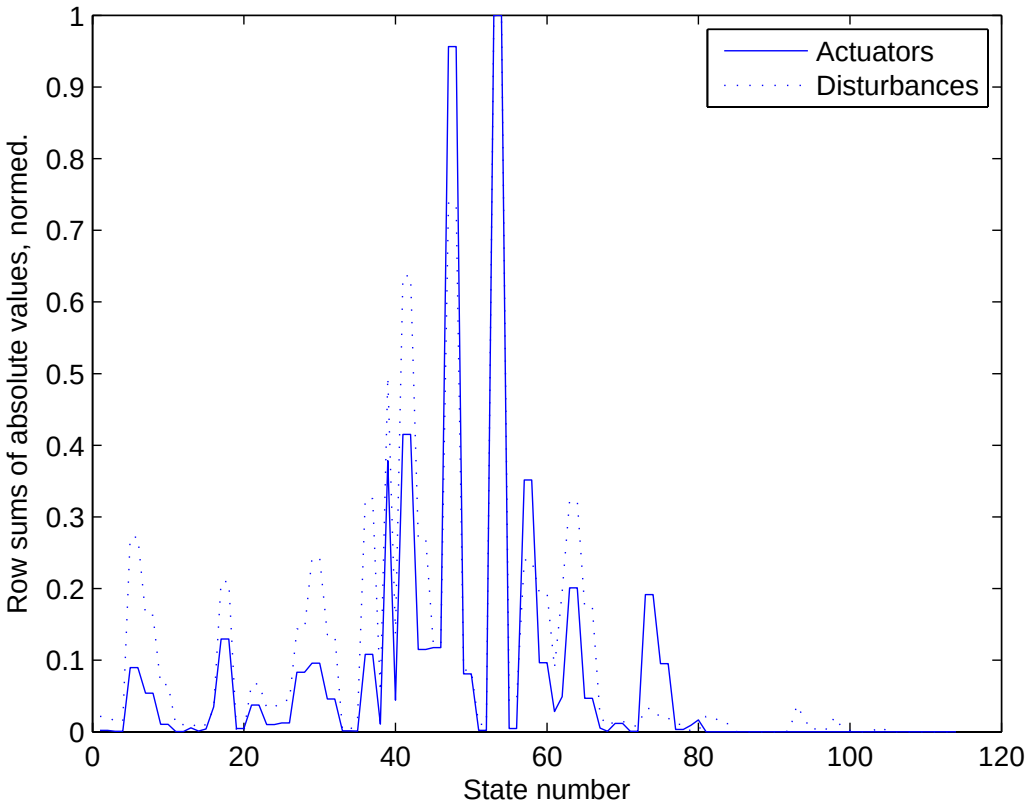

Figure 8.4: Weighted row sums for B and N matrices, to show controllability from actuators and disturbances.

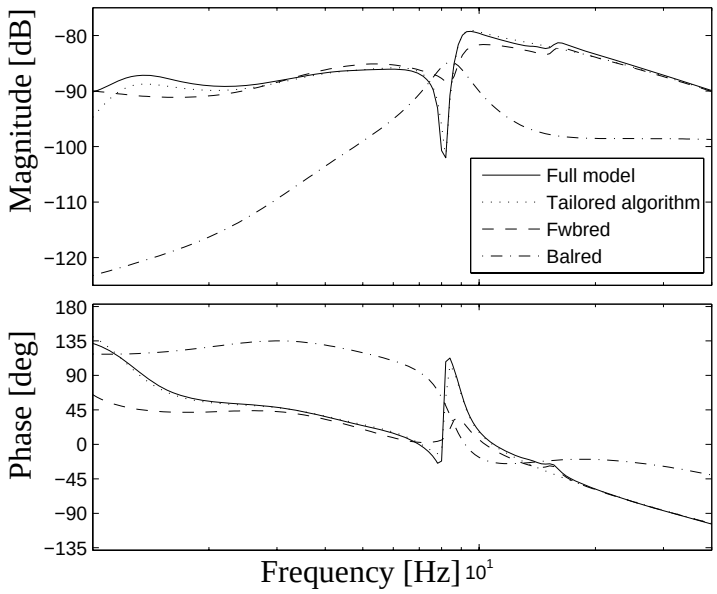

Figure 8.5: Model reduction to 21 states. From control input front right, to frequency weighted acceleration front right.

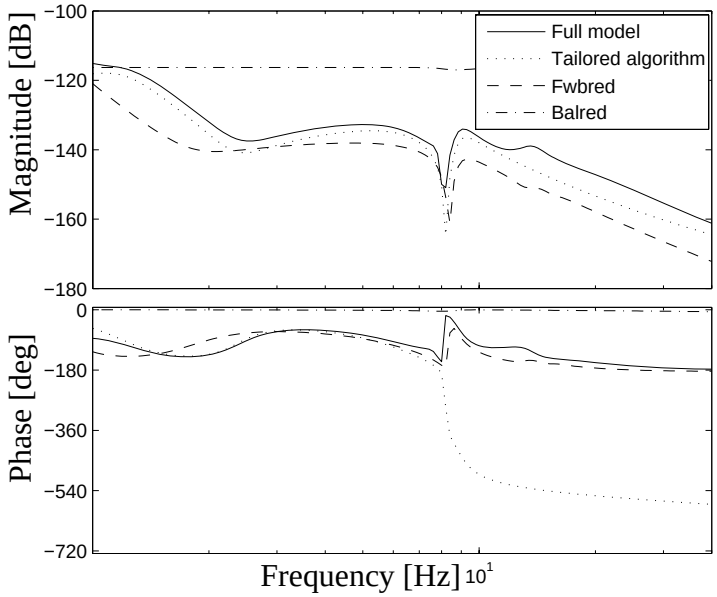

Figure 8.6: Model reduction to 21 states. From control input front right, to deflection front right.

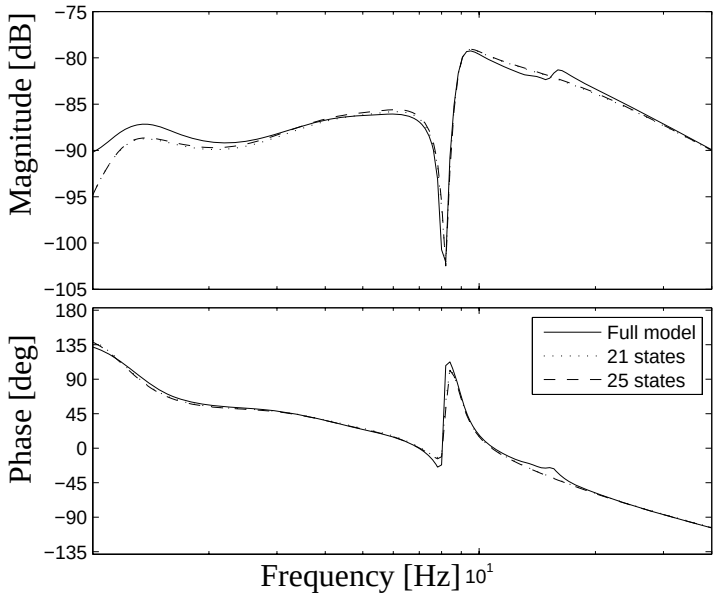

Figure 8.7: Model reduction with and without consideration of disturbances. From control input front right, to frequency weighted acceleration front right.

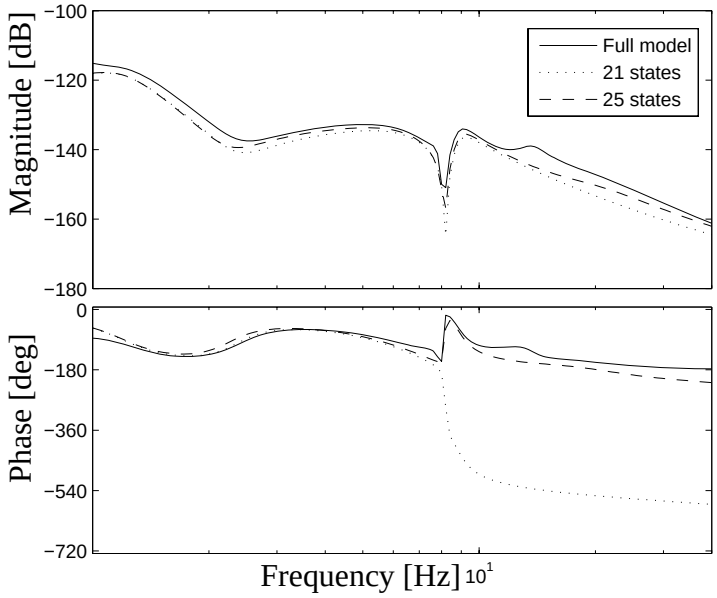

Figure 8.8: Model reduction with and without consideration of disturbances. From control input front right, to deflection front right.

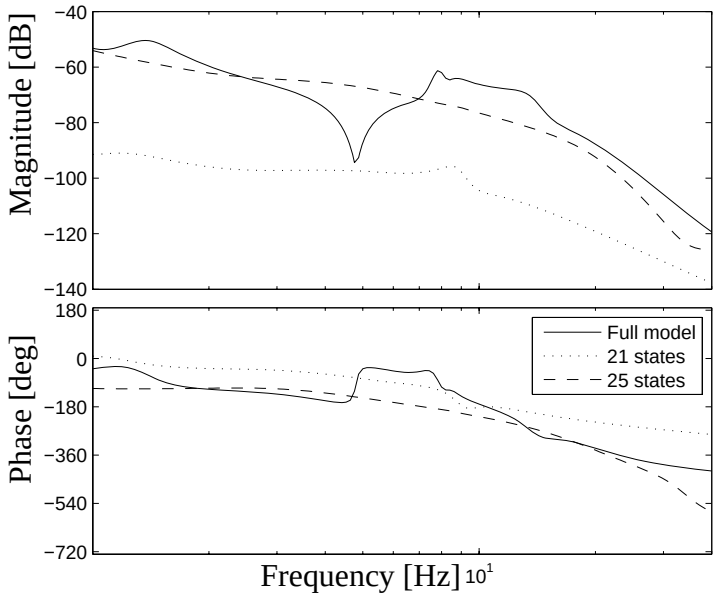

Figure 8.9: Model reduction with and without consideration of disturbances. From lateral disturbance at the front wheelset, to frequency weighted acceleration front right.

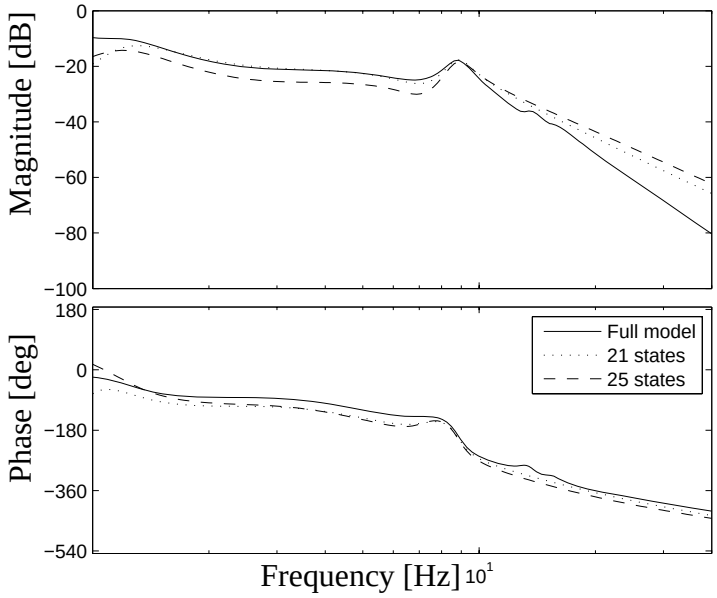

Figure 8.10: Model reduction with and without consideration of disturbances. From vertical disturbance at the front wheelset, to frequency weighted acceleration front right.

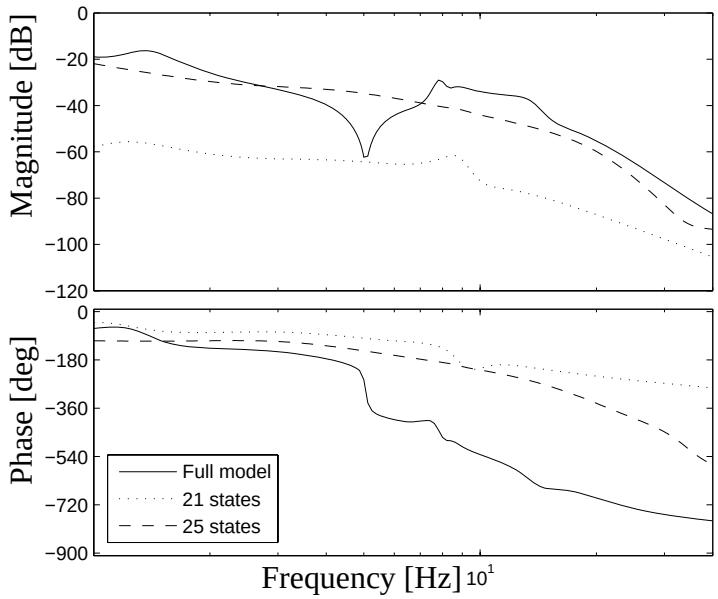

Figure 8.11: Model reduction with and without consideration of disturbances. From roll disturbance at the front wheelset, to frequency weighted acceleration front right.

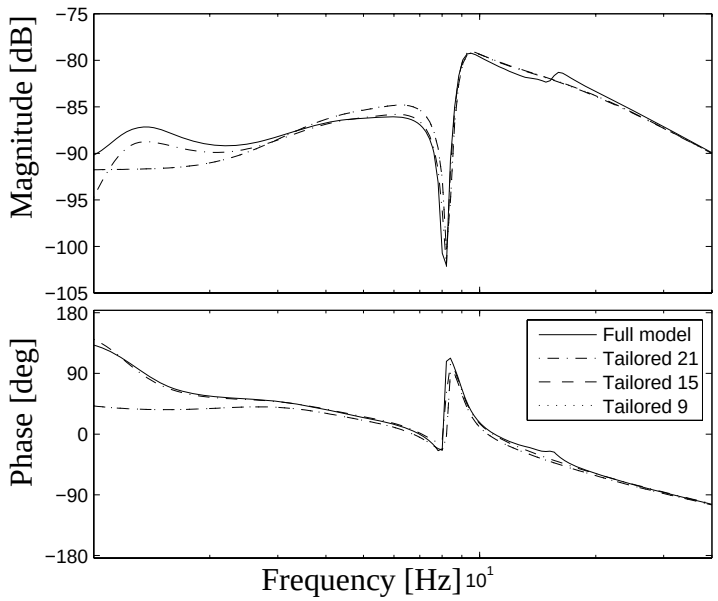

Figure 8.12: Different amount of reduction with tailored algorithm. From control input front right, to frequency weighted acceleration front right. The curves for 9 states and 15 states are difficult to tell apart.

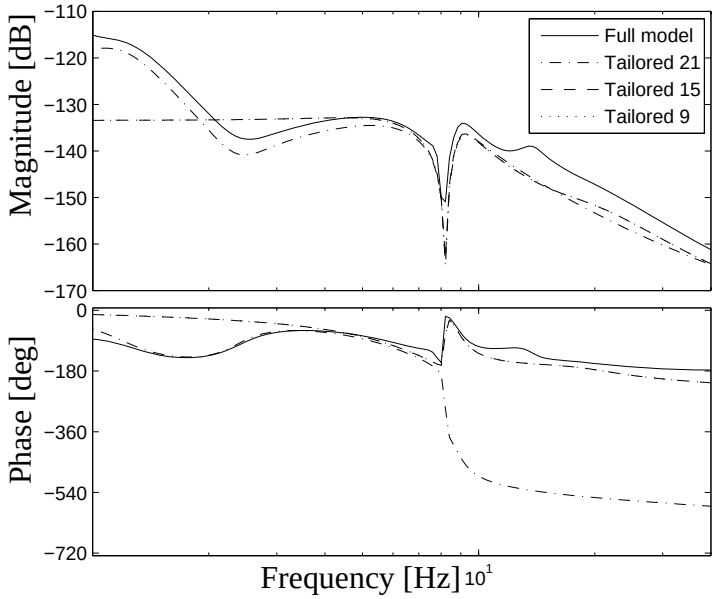

Figure 8.13: Different amount of reduction with tailored algorithm. From control input front right, to deflection front right. The curves for 9 states and 15 states are difficult to tell apart.

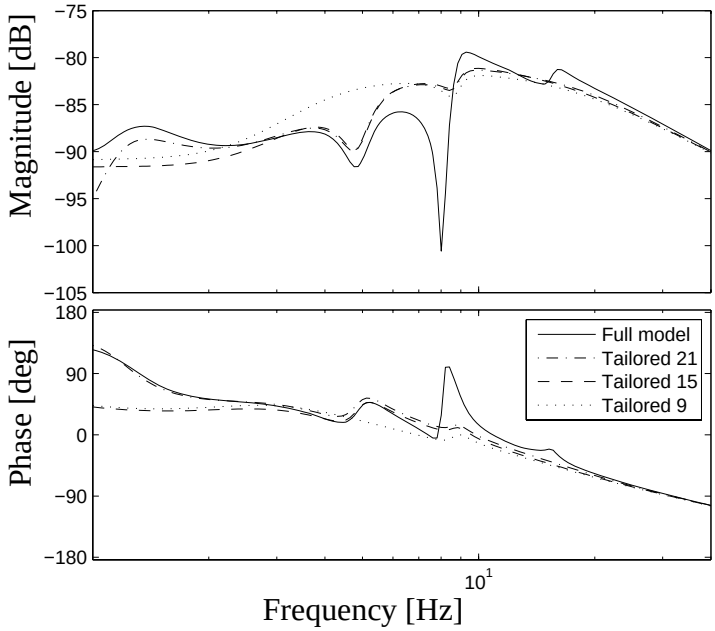

Figure 8.14: Different amount of reduction with tailored algorithm. From control input rear right, to frequency weighted acceleration rear right.

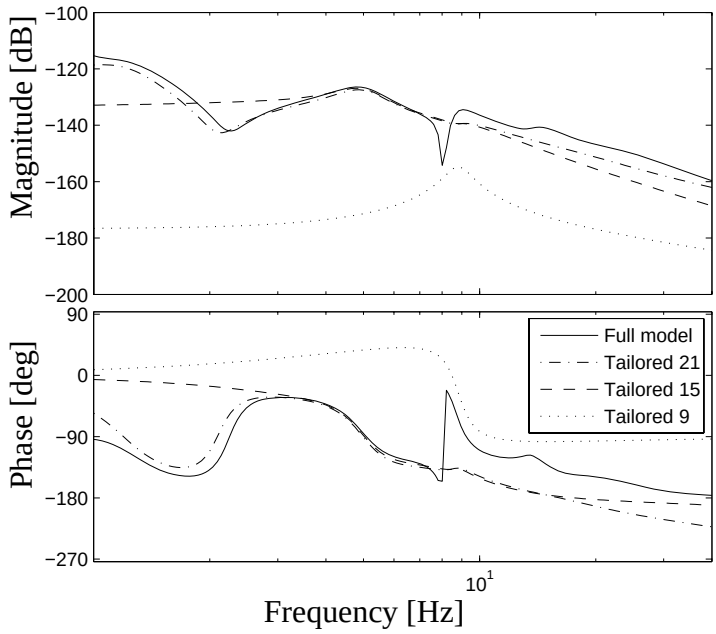

Figure 8.15: Different amount of reduction with tailored algorithm. From control input rear right, to deflection rear right.

chapter ix

linear quadratic (lq) control design

Linear quadratic (LQ) control is a control method that is using state feedback, and that can be used for multiple-input multiple-output (MIMO) systems. Some aspects of linear quadratic control have been studied on a reduced, stable, linear model from Chapter 8, using Matlab/Simulink. Of the reduces models, the one with 9 states has been chosen. All states of the model are assumed to be measurable. This design model is controllable and observable. All simulations and evaluations are made on the reduced model. This is an initial approach to simplify control design. The system is studied in continues time.

9.1 Background Theory

The following notations are used where nothing else is stated:

$$\dot{x} = Ax + Bu \tag{9.1}$$
$$y = Cx + Du, \tag{9.2}$$

where x represents the states, u the control inputs, and y the measured outputs.

9.1.1 Detectability and Stabilizability

A system is *stabilizable* if there exists a matrix L, such that $A - BL$ is stable. It is *detectable* if there exists a matrix K, such that $A - KC$ is stable, (Glad and Ljung 2000).

9.1.2 Linear Quadratic Control

Linear quadratic optimization is used to find a linear, causal feedback law that minimizes the criterion

$$V = \|z\|_{Q_1}^2 + \|u\|_{Q_2}^2 , \tag{9.3}$$

for a positive definite matrix Q_2 and a positive semi-definite matrix Q_1. (It is also possible to have a cross term in the criterion.) z is the controlled variable, and u is the control signal. This is solved with the algebraic Riccati Equation. For more details, see (Glad and Ljung 2000). The evaluation criterion can also be chosen as

$$V = \int (x^T(t)Q_1x(t) + u(t)^TQ_2u(t))dt. \tag{9.4}$$

Let $Q_1 = SS^T$. Then, for the infinite-time, time-invariant problem, there exists a stable closed-loop optimal system with finite performance index V, if and only if (A, B) is stabilizable and (A, S) is detectable, (Anderson and Moore 1989).

LQ and Matlab

Matlab has 2 different build-in commands to calculate a controller by linear quadratic methods (plus some for state estimation), (The MathWorks 2007). Those are:

- `lqr`
  For a continuous-time state-space model, `lqr` calculates the optimal gain matrix L, such that the state-feedback law $u = -Lx$ minimizes the cost function

  $$V(L) = \int (x^T(t)Qx(t) + u(t)^T Ru(t))dt + 2x^T(t)Nu(t))dt. \tag{9.5}$$

  It is sufficient to provide the A and B matrices of the state-space model. Of course also the penalty weighting matrices Q, R, and N has to be provided.

- `lqry`
  `lqry` is similar to `lqr`, but uses output weighting. In this case it is necessary to provide the state-space matrices A, B, C, and D. In this case cost function is

  $$V(L) = \int (y^T(t)Qy(t) + u(t)^T Ru(t))dt + 2y^T(t)Nu(t))dt. \tag{9.6}$$

9.1.3 State Observer

LQ control uses state feedback. If not all states are measurable, there is a need to estimate the states. There are techniques to do this using measured outputs and known (measured) inputs. The states are normally estimated by a so called *observer*, (Glad and Ljung 2000). Under some conditions, described in (Glad and Ljung 2000), the optimal observer, which minimizes the error in the estimation, is the Kalman filter. Among other things, the noise is assumed to be white, (Glad and Ljung 2000).

9.2 Inputs and Outputs

This section describes the disturbances that has been chosen to excite the system, as well as the evaluation of the control.

9.2.1 Disturbances (Inputs)

For simplifying reasons, disturbances have been used only in the vertical direction. The disturbances are based on those described in Section 4.1. However, as can be seen in that same chapter, disturbance inputs are position, velocity, and acceleration. The data is only given for position. The simulation program Simpack, which the original model is modeled in, calculates velocity and acceleration disturbances from position measurements, using partial differential equations. Those have been exported and used also for the simulations in Matlab/Simulink.

The disturbances are given as track disturbances. When simulating the model there are disturbance inputs at each wheelset. Those are obviously not in the same position on the track. Therefore, the disturbances have been entered directly in the first wheelset, but delayed with the times it takes to traverse the distances between the first wheelset and each of the following. A velocity of 72 km/h has been used. With this velocity, the inputs suffice for simulating 12.5 seconds.

9.2.2 Evaluation (Outputs)

The outputs from the model are car body acceleration, and deflection between car body and bogie, see Section 4.1. The accelerations have been used to calculate comfort according to Section 2.3. For the deflection, the maximum of the absolute value has been used, to design the control to keep the bodies within the allowed space. For comparison, all those evaluation parameters have been calculated also for a passive simulation of the same reduced system with the same disturbances. Then, the quotient between the active and the passive system has been calculated. If all those quotients are smaller than 1, the performance has been improved by the control. The maximum of the absolute values of the control signal is also studied, to make sure it is within reason.

In addition to the variables interesting for control (above), the criterion $V(L)$ is calculated, see Section 9.1. The purpose is to see that the optimization works. $V(L)$ has been calculated over the simulation time, and integrated numerically using the trapezoid method.

Note that the criterion minimized by linear quadratic control, and the criteria that are desired, are not the same. However, they have in common that they want the error to be small.

9.3 Control

The overall method used to find a control law has been to combine output weighting with the selection of penalty weighting matrices for linear quadratic control. All states have been measured. Therefore, no observer has been used.

Since the model (process) is stable, it is fulfilling the requirements on detectability and stabilizability in Section 9.1. If the weighting matrices are chosen according to Section 9.1, an LQ controller is expected to be found. It will however be seen that it is not quite that simple to find a satisfactory control law for this application.

9.3.1 Outputs as Criterion Based on State Space Matrices

If the size of the control signals are not considered of major importance, as long as they don't grow towards infinity, it would be a natural approach to concentrate on the outputs in the criterion to be minimized. Since there is a direct term between the control and the output, and all control signals are used for this, there are some penalty on the control signal anyway.

If the criterion to be minimized by LQ is chosen as

$$V(L) = \int_0^\infty y^T(t)y(t)dt, \tag{9.7}$$

then, with

$$y(t) = Cx(t) + Du(t) \tag{9.8}$$

we get

$$V(L) = \int_0^\infty (Cx(t) + Du(t))^T (Cx(t) + Du(t))dt. \tag{9.9}$$

This can be rewritten as

$$V(L) = \int_0^\infty (x^T(t)C^T Cx(t) + 2x^T(t)C^T Du(t) + u(t)^T D^T Du(t))dt. \tag{9.10}$$

Unfortunately, the rank of $D^T D$ is only 3, although it is a 4×4 matrix. Thus, the penalty weighing function that is wished to be used with $u(t)^T u(t)$, is not positive definite, and therefore this criterion cannot be used. Two approaches, described below, have been studied to compensate for this.

Removal of One Control Input

Physical insight has led to the idea to remove one control input. The motivation is as follows: The car body is modeled as a rigid body. Originally, there are 4 force inputs in the vertical direction. Those control the motions of the car body in the vertical, pitch, and roll directions. That is only 3 directions, which are controlled with 4 inputs. The fourth direction that the inputs is attempting to control, is flexing the car body by for instance pushing the front left and rear right corners upwards, while at the same time pulling the front right and rear left corners downwards. Since the car body is modeled without flexibility here, this is not possible. There are possibilities to affect the bogies though, since the front and rear bogie are separate.

The control input has been removed by removal of the corresponding parts in the state space models. What is left is a model with 3 control signals and 8 outputs.

Adding Penalty on Control Input

Another approach is to keep all 4 control signals, but to add a small penalty on them by modifying Equation 9.7 into

$$V(L) = \int_0^\infty (y^T(t)y(t) + \delta u^T(t)u(t))dt, \tag{9.11}$$

Weighing of Outputs

The outputs are of different size orders. To make the outputs equally important during the control design, which uses either the criterion in Equation 9.7 or in Equation 9.12, the model has been modified prior to the control design. If the output of the process is the vector y_p, then the output of the design model can be written $y = Wy_\mathrm{p}$, where W is a weighing matrix. W has been chosen as a diagonal matrix, which means that each output can be written as $y_i = w_{ii}y_{\mathrm{p}i}$.

As an initial guess, the outputs have been roughly scaled to make the gain in the bode plots of similar size order. Further tuning has been made by iterations. A design model is decided upon, a feedback is calculated, the model is simulated, and finally evaluated. Then, the weighing matrix W is altered in order to make the quotients of the passive and active evaluation parameters as close to each other as possible.

Simulation Results

None of the methods above have produced adequate control laws. That is, no control law that produces better results than the passive system, according to the criteria in Section 9.2, has been found. All of the control laws that are discussed in this chapter has negative eigenvalues for the closed loop system, which indicates stability.

For control with 4 actuators, all output criteria are getting worse at the same time. Even the LQ criterion $V(L)$ is getting worse, which it shouldn't. However convergence is not guaranteed for finite time. Also, $V(L)$ has only been calculated approximately, as described in Section 9.2. With weights that makes $D^T D$ of the order of magnitude 10^{-8} and δ selected as 10^{-10}, the results are those in Table 9.1–Table 9.3.

Table 9.1: Output weights for case with 4 actuator forces.

	Front right	Front left	Rear right	Rear left
Output weight, deflection	100	100	2000	2000
Output weight, acceleration	1	1	0.2	0.2

Table 9.2: Results for case with 4 actuator forces.

	Front right	Front left	Rear right	Rear left
$\mathrm{Wz}_{\mathrm{active}}/\mathrm{Wz}_{\mathrm{passive}}$	1.0210	1.0190	1.2816	1.2832
$\mathrm{Defl}_{\mathrm{active}}/\mathrm{Defl}_{\mathrm{passive}}$	1.1317	1.1295	1.0450	1.0505
Control signal [N]	805	606	1593	1411

Table 9.3: LQ criterion for case with 4 actuator forces.

	Open loop	Closed loop
$V(L)$	0.1494	0.1722

When the rear left of the control inputs have been removed, and the outputs of design model weighted prior to control design, the best results are similar to that of the passive system. There is no point in using control if there is no improvement, even if it doesn't get worse either. For control with 3 actuators the results are those in Table 9.4–Table 9.6.

Table 9.4: Output weights for case with 3 actuator forces.

	Front right	Front left	Rear right	Rear left
Output weight, deflection	200	200	1700	1700
Output weight, acceleration	0.7	0.8	0.3	0.3

Table 9.5: Results for case with 3 actuator forces.

	Front right	Front left	Rear right	Rear left
$\mathrm{Wz}_{\mathrm{active}}/\mathrm{Wz}_{\mathrm{passive}}$	1.0221	0.9940	0.9998	0.9728
$\mathrm{Defl}_{\mathrm{active}}/\mathrm{Defl}_{\mathrm{passive}}$	1.0095	1.0028	1.0086	1.0098
Control signal [N]	420	770	634	0

9.3.2 Altering Output Penalty

Further studies have been made with other penalties. A diagonal weighing matrix has been added as follows:

$$V(L) = \int_0^\infty (y^T(t)Qy(t) + \delta u^T(t)u(t))dt, \tag{9.12}$$

which can also be written

$$V(L) = \int_0^\infty (x^T(t)C^TQCx(t) + 2x^T(t)C^TQDu(t) + u(t)^T(D^TQD + \delta I)u(t))dt, \tag{9.13}$$

since Q is diagonal, and thus $Q = Q^T$. In practice though, the Matlab command `lqry`, described in Section 9.1, has been used in an attempt to find an adequate controller. The penalty weighing matrices Q and R have been chosen as diagonal, and N as 0. That is, no cross terms have been considered. For the design, a combination of scaling of the model prior to the design, as in Section 9.3.1, and the penalties Q and R, has been used. The model was scaled roughly to avoid numerical difficulties, then Q and R was used for tuning. The outputs and control signals were studied. Large penalties have been used where the output (or control signal) were too big, and small where there were room for improvement. However, despite extensive searches, no adequate controller was found. There were problems with that after a while further increases of the penalties did not change the controller.

9.3.3 LQ With Optimal Feed Forward

The wheelsets will be affected by the the same disturbances, with a time delay. If the disturbances can be measured, there might be a possibility to compensate for them be use of feed forward. A simple way to estimate if this could lead to a satisfactory design, is to simply set all disturbances at all but the first wheelset to 0. This corresponds to perfect feed forward.

Table 9.6: LQ criterion for case with 3 actuator forces.

	Open loop	Closed loop
$V(L)$	0.0700	0.0652

Although is not reasonable to assume this can be implemented, it can be assumed that nothing better can be achieved. If disconnecting disturbances does not give a satisfactory result, there is no use trying feed forward.

With the same output weighing as with 3 actuators without feed forward, see Table 9.4, the results in Table 9.7–Table 9.8 are obtained. The control signals are not included, since part of the control has been faked. Here both comfort and deflection were improved. If

Table 9.7: Results for case with 3 actuator forces and feed forward.

	Front right	Front left	Rear right	Rear left
$\mathrm{Wz}_{\mathrm{active}}/\mathrm{Wz}_{\mathrm{passive}}$	0.8316	0.8030	0.8124	0.8132
$\mathrm{Defl}_{\mathrm{active}}/\mathrm{Defl}_{\mathrm{passive}}$	0.6250	0.6111	0.4886	0.4903

Table 9.8: LQ criterion for case with 3 actuator forces and feed forward.

	Open loop	Closed loop
$V(L)$	0.0705	0.0194

the output weights are changed to keep deflection at today's level, there is room to improve comfort further, see Table 9.9–Table 9.11.

9.4 Concluding Remarks

LQ design have proved complicated for this model. Either more thorough studies have to be made, or a different design method need to be chosen. No satisfactory control have been found, even disregarding the size of the control signals. Although the LQ criterion is usually made smaller by using control, it is not sufficient to make the output errors smaller by the desired criteria. It is possible to make *some* of the criteria smaller, but no controller has been found that makes *all* criteria smaller at the same time, when using the measured disturbances.

If an optimal feed forward could be constructed, there seem to be some possibilities to improve comfort and decrease deflection. But although this looks promising, it is important to keep in mind that this is a theoretical upper bound, that in practice might be difficult to even get close. One major challenge in reality is to measure or estimate the disturbances during the ride. Another challenge is to approximate the feed forward design. It would

Table 9.9: Output weights for case with 3 actuator forces and feed forward, optimized for comfort.

	Front right	Front left	Rear right	Rear left
Output weight, deflection	10	10	100	100
Output weight, acceleration	0.7	0.8	0.3	0.3

Table 9.10: Results for case with 3 actuator forces and feed forward, optimized for comfort.

	Front right	Front left	Rear right	Rear left
$\mathrm{Wz}_{\mathrm{active}}/\mathrm{Wz}_{\mathrm{passive}}$	0.3214	0.3760	0.5024	0.5077
$\mathrm{Defl}_{\mathrm{active}}/\mathrm{Defl}_{\mathrm{passive}}$	0.7492	0.7465	0.9440	0.9467

include an approximate plant inversion, as well as model reduction. Still, this idea could be interesting for future research.

Another approach could be to try design on another reduced model. However, smaller models will be less accurate and thus a control designed on those are less likely to work on the original model. Larger models, on the other hand, are prone to cause problems with simulations and numerics. Also, although all reduced models are designed to be controllable and observable, somewhat larger models are not considered controllable or observable by Matlab. For larger models the simulation times are significantly increased.

It is not reasonable to assume that all states can be measured in reality, as done here. Therefore, an observer will be needed. All states have been measured during simulations to isolate the control problem from the state estimation problem. Before implementation, the control law with state estimator needs to be verified on the original model. However, first a controller that works sufficiently well on the design model, with known states, has to be found.

Table 9.11: LQ criterion for case with 3 actuator forces and feed forward, optimized for comfort.

	Open loop	Closed loop
$V(L)$	0.0118	$1.1077 \cdot 10^{-4}$

chapter x

concluding remarks

Concluding remarks can be found in the end of Chapter 5–Chapter 9. In this chapter, a summary of those can be found, along with more general comments and recommendations.

Although it would be challenging for the actuators, it is reasonable to design a vertical active suspension, when adding the actuators in parallel with passive springs. The model at hand is not adequate for linear studies of motion sickness. Comfort studies, on the other hand, could be feasible. However, there are nonlinearities, and those are more pronounced at higher frequencies, which makes the linear model less reliable for high frequencies.

The coupling between the different inputs and outputs are high. Also, to decouple the system to make single-input single-output (SISO) control possible, does not look promising. It is not surprising that there are problems with coupling. The car body is stiff, and the corners cannot be controlled independently. Also, the number of inputs is lower than the number of outputs, which means some outputs could not be used. To make multiple-input multiple-output (MIMO) design possible, model reduction is needed. The model can be reduced in different ways, to different extents. Which models that are sufficient for control design cannot be know until a control design is found and is tested on the original model. However, if a too big model is chosen for control design, there are numerical issues. Linear quadratic control have been attempted with no success. A problem is that the LQ criterion is not the same as the criteria used in this thesis.

Generally, the problem is numerically challenging, which should be kept in mind.

10.1 Future Work

There are room for further improvements in each of the areas studied. However, it is not necessarily refining those techniques that will lead to a satisfactory active suspension. A list of suggested things to study follows here.

- Study the model with more simplified assumptions, such as symmetry of vehicle and / or disturbances.
- Improve model simplification, for instance by combining different techniques.
- Generate a model by physical modeling or system identification, instead of by using model reduction.
- An attempt could be made on designing the control on a model using flexible bodies. That would mitigate the problem that there are more control inputs than there are

degrees of freedom that can be controlled in the car body. On the other hand this would make the model even more complicated.

- Change the positions of the actuators. Also, the number of actuators used can be reconsidered.
- Improve control design.
- Evaluate the control design on the original model.
- Model actuator dynamics.
- Calculate forces from passive components that are wished to be removed, and include them in the control law. This could also be done without adding any further control.
- Model measurement noise.

appendices

appendix a

passenger model

When simulations are run with full load, passengers are modeled as masses, springs, and dampers, according to ISO 5982-1981 (E), (*Mechanical vibration and shock - Vibration and shock – Mechanical driving point impedance of the human body* 1981). The ISO-standard describes how to model a seated or standing person in the vertical direction with two masses, two springs, and two dampers, each. The seated and standing human is not modeled in the same way. The standard also includes information about a human in supine position, but there are no people laying down in this model, so that is not used here. To model the lateral direction, the spring and damper values from the ISO-standard have been divided by two. The choice of model for the lateral direction is rather random. Different ways to model the lateral direction will alter the simulation results, but not severely, according to simulations. Since the car body of the vehicle is modeled as rigid instead of flexible, there will be errors anyway, and to model the passengers very well is therefore not motivated. The humans are modeled with only translational degrees of freedom, and the I-tensors of the masses have been neglected. In order to reduce the amount of modeling, the humans have been lumped together in six lumps: four with seated people and two with standing. The placements in the car body are as follows: In the longitudinal direction, the length of the car body was reduced by 10%, and the remaining length was divided by 4. An equal amount of both standing and sitting people were then placed at that distance from the center in both directions. In the lateral direction, all standing people were placed in the middle. For the seated people, the maximum width of the car body was divided by 4. The seated people was then placed that distance away from the center, in both directions. See Figure 1.

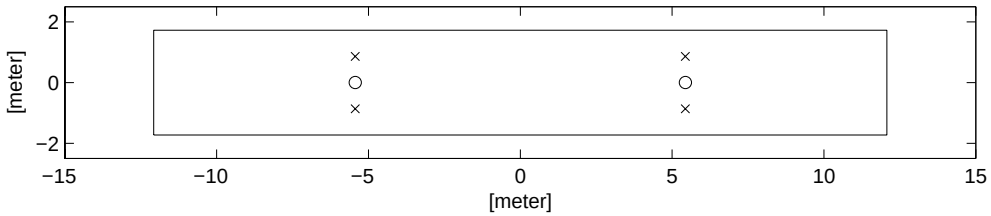

Figure 1: Placement of passengers. x denotes sitting and o denotes standing passengers.

In the vertical direction, the standing passengers are connected to the floor, with center of gravity 1.00 m above the floor. The sitting passengers have been connected to a point 0.45 m above the floor, with center of gravity 0.20 m above the point of connection. There are 100 seated people in the model, each weighing 75 kg. Then there are 43.68 standing

people. The weight of one passenger is according to ISO 5982-1981 (E), which is not the same weight as Bombardier uses for one passenger. The number of standing passengers have however been increased to reach the same total payload.

appendix b

disturbance dynamics modeling by state expansion

There are dynamic dependencies between the disturbances from the rail. The disturbance inputs are acceleration, velocity, and position displacements of the rail, as experienced by the moving railway vehicle. When sending disturbances into the model, those dynamic dependencies must be taken into account, for the disturbances to be physically correct. Those dependencies can, however, also be incorporated in the model. Starting from the acceleration, it is possible to calculate the velocity and positions by integrations. (Assuming the starting point is at rest.) Such a modeling will reduce the number of disturbance inputs, but also leads to more states. The modeling to incorporate the disturbance dynamics into the model is described in this appendix.

Assume the original model is expressed with the state space model

$$\dot{x}_o = A_o x_o + B_o u + N_o w_o \tag{B.1}$$

$$y = C_o x_o + D_o u + M_o w_o, \tag{B.2}$$

where x_o are the original states, w_o are the original disturbances, and the outputs y and control inputs u will stay the same before and after incorporating the disturbance dynamics into the model.

Let the number of original states be J, and the number of original disturbances K, of which there are $K/3$ each of positions, velocities, and accelerations. Then Equation B.1–Equation B.2 can be written as

$$\dot{x}_o = A_o x_o + B_o u + \begin{pmatrix} N_{o,1} & N_{o,2} & N_{o,3} & \cdots & N_{o,K} \end{pmatrix} \begin{pmatrix} w_{o,1} \\ w_{o,2} \\ w_{o,3} \\ \vdots \\ w_{o,K} \end{pmatrix} \tag{B.3}$$

$$y = C_o x_o + D_o u + \begin{pmatrix} M_{o,1} & M_{o,2} & M_{o,3} & \cdots & M_{o,K} \end{pmatrix} \begin{pmatrix} w_{o,1} \\ w_{o,2} \\ w_{o,3} \\ \vdots \\ w_{o,K} \end{pmatrix}. \tag{B.4}$$

Let the input order of the disturbances be first position, then velocity, then acceleration, repeated for each physical disturbance. Then $w_{o_2} = \dot{w}_{o,1}$, $w_{o,3} = \dot{w}_{o,2} = \ddot{w}_{o,1}$, $w_{o,5} = \dot{w}_{o,4}$, $w_{o,6} = \dot{w}_{o,5} = \ddot{w}_{o,4}$, etc. Add new states as

$$\begin{aligned} x_{J+1} &= w_{o,1} \\ x_{J+2} &= w_{o,2} \\ x_{J+3} &= w_{o,4} \\ x_{J+4} &= w_{o,5} \\ &\vdots \\ x_{J+2K/3} &= w_{o,K-1} \end{aligned} \tag{B.5}$$

Now, the state vector can be written as

$$x = \begin{pmatrix} x_o \\ x_{J+1} \\ x_{J+2} \\ x_{J+3} \\ x_{J+4} \\ \vdots \\ x_{J+2K/3} \end{pmatrix}. \tag{B.6}$$

The remaining disturbances will be kept as disturbance inputs for the modified system. The disturbances for the modified system can now be written as

$$w = \begin{pmatrix} w_1 \\ w_2 \\ \vdots \\ w_{K/3} \end{pmatrix} = \begin{pmatrix} w_{o,3} \\ w_{o,6} \\ \vdots \\ w_{o,K} \end{pmatrix}. \tag{B.7}$$

The derivatives of the new states can now be expressed in other states and disturbance inputs as

$$\begin{aligned} \dot{x}_{J+1} &= x_{J+2} \\ \dot{x}_{J+2} &= w_1 \\ \dot{x}_{J+3} &= x_{J+4} \\ \dot{x}_{J+4} &= w_2 \\ &\vdots \\ \dot{x}_{J+2K/3} &= w_2 \end{aligned} \tag{B.8}$$

Now, the full new model can be written as

$$\dot{x} = Ax + Bu + Nw \tag{B.9}$$
$$y = Cx + Du + Mw, \tag{B.10}$$

where

$$A = \begin{pmatrix} A_o & N_{o,1} & N_{o,2} & N_{o,4} & N_{o,5} & \cdots & N_{o,K-2} & N_{o,K-1} \\ 0 & 0 & 1 & 0 & 0 & \cdots & 0 & 0 \\ 0 & 0 & 0 & 0 & 0 & \cdots & 0 & 0 \\ 0 & 0 & 0 & 0 & 1 & \cdots & 0 & 0 \\ 0 & 0 & 0 & 0 & 0 & \cdots & 0 & 0 \\ \vdots & \vdots & \vdots & \vdots & \vdots & \ddots & \vdots & \vdots \\ 0 & 0 & 0 & 0 & 0 & \cdots & 0 & 1 \\ 0 & 0 & 0 & 0 & 0 & \cdots & 0 & 0 \end{pmatrix}, \tag{B.11}$$

$$B = \begin{pmatrix} B_o \\ 0 \\ 0 \\ \vdots \\ 0 \end{pmatrix}, \tag{B.12}$$

$$N = \begin{pmatrix} N_{o,3} & N_{o,6} & \cdots & N_{o,K} \\ 0 & 0 & \cdots & 0 \\ 1 & 0 & \cdots & 0 \\ 0 & 0 & \cdots & 0 \\ 0 & 1 & \cdots & 0 \\ \vdots & \vdots & \ddots & \vdots \\ 0 & 0 & \cdots & 0 \\ 0 & 0 & \cdots & 1 \end{pmatrix}, \tag{B.13}$$

$$C = \begin{pmatrix} C_o & M_{o,1} & M_{o,2} & M_{o,4} & M_{o,5} & \cdots & M_{o,K-2} & M_{o,K-1} \end{pmatrix}, \tag{B.14}$$

$$D = \begin{pmatrix} D_o & 0 & 0 & \cdots & 0 \end{pmatrix}, \tag{B.15}$$

and

$$M = \begin{pmatrix} M_{o,3} & M_{o,6} & \cdots & M_{o,K} \end{pmatrix}. \tag{B.16}$$

appendix c

single transfer function derived from a diagonal mimo system

For a system represented on state space form,

$$\dot{x} = Ax + Bu \tag{C.1}$$
$$y = Cx + Du, \tag{C.2}$$

the transfer functions can be written as

$$G(s) = C(sI - A)^{-1}B + D, \tag{C.3}$$

where I is the identity matrix, (Glad and Ljung 1989).

If A is diagonal, so is $(sI - A)$. Therefore, block inversion can be used, with each element on the diagonal being a block of size 1×1, (Råde and Westergren 1998). With N states we get:

$$(sI - A)^{-1} = \begin{pmatrix} \frac{1}{s-a_{11}} & & & 0 \\ & \frac{1}{s-a_{22}} & & \\ & & \ddots & \\ 0 & & & \frac{1}{s-a_{NN}} \end{pmatrix}. \tag{C.4}$$

Inserting Equation C.4 into Equation C.3 yields, with J number of inputs and K number of outputs:

$$G(s) = \begin{pmatrix} c_{11} & \cdots & c_{1N} \\ \vdots & \ddots & \vdots \\ c_{K1} & \cdots & c_{KN} \end{pmatrix} \begin{pmatrix} \frac{1}{s-a_{11}} & & 0 \\ & \ddots & \\ 0 & & \frac{1}{s-a_{NN}} \end{pmatrix} \begin{pmatrix} b_{11} & \cdots & b_{1J} \\ \vdots & \ddots & \vdots \\ b_{N1} & \cdots & b_{NJ} \end{pmatrix} + D(s) = \quad \text{(C.5)}$$

$$= \begin{pmatrix} \frac{c_{11}}{s-a_{11}} & \frac{c_{12}}{s-a_{22}} & \cdots & \frac{c_{1N}}{s-a_{NN}} \\ \frac{c_{21}}{s-a_{11}} & \frac{c_{22}}{s-a_{22}} & \cdots & \frac{c_{2N}}{s-a_{NN}} \\ \vdots & \vdots & \ddots & \vdots \\ \frac{c_{K1}}{s-a_{11}} & \frac{c_{K2}}{s-a_{22}} & \cdots & \frac{c_{KN}}{s-a_{NN}} \end{pmatrix} \begin{pmatrix} b_{11} & \cdots & b_{1J} \\ \vdots & \ddots & \vdots \\ b_{N1} & \cdots & b_{NJ} \end{pmatrix} + D(s) = \quad \text{(C.6)}$$

$$= \begin{pmatrix} \sum_{n=1}^{N} \frac{c_{1n}b_{n1}}{s-a_{nn}} & \cdots & \sum_{n=1}^{N} \frac{c_{1n}b_{nJ}}{s-a_{nn}} \\ \vdots & \ddots & \vdots \\ \sum_{n=1}^{N} \frac{c_{Kn}b_{n1}}{s-a_{nn}} & \cdots & \sum_{n=1}^{N} \frac{c_{Kn}b_{nJ}}{s-a_{nn}} \end{pmatrix} + D(s). \quad \text{(C.7)}$$

Thus, the transfer function from input number j to output number k can be written:

$$g_{kj} = \sum_{n=1}^{N} \frac{c_{kn}b_{nj}}{s - a_{nn}} + d_{kj}. \quad \text{(C.8)}$$

appendix d

numerical results from feasibility chapter

Here, the full numerical results from the feasibility studies in Chapter 5, are listed. The cases are defined in Section 5.3.1. In the following tables the parts of the variables stands for:

F	Force
P	Power
Wz	Comfort number (Wz)
Z	Vertical deflection (between car body and bogie)
Al	Roll angle α (between car body and bogie)
ARB	Anti-roll bar
VD	Vertical damper
B1	Bogie 1
B2	Bogie 2
R	Right
L	Left
C	Center
x	Longitudinal
y	Lateral
z	Vertical

D.1 Forces in Anti-Roll Bar and Damper

The following table shows the mean and maximum forces in the anti-roll bar and damper, separately. The mean is the mean value taken on the absolute value,

$$\mathrm{F\_mean} = \frac{1}{N}\sum_{i=1}^{N}|F_i|.$$

	Case 1	*Case 2*	*Case 3*	*Case 4*	*Case 5*
F_mean_ARB_B1_R [kN]	5.0467	23.002	32.009	6.2134	7.6153
F_max_ARB_B1_R [kN]	29.329	31.359	40.662	24.165	26.852
F_mean_ARB_B1_L [kN]	5.0463	23.013	32.024	6.2136	7.6148
F_max_ARB_B1_L [kN]	29.336	31.338	40.749	23.953	26.883
F_mean_ARB_B2_R [kN]	4.0703	22.941	31.898	5.8434	7.5232
F_max_ARB_B2_R [kN]	20.832	33.092	41.204	21.158	24.067
F_mean_ARB_B2_L [kN]	4.0667	22.962	31.929	5.8408	7.5227
F_max_ARB_B2_L [kN]	20.861	33.166	41.211	21.172	24.063
F_mean_VD_B1_R [kN]	0.6280	0.3610	0.3577	0.4107	0.4065
F_max_VD_B1_R [kN]	6.1157	2.1355	2.1413	3.9358	3.1779
F_mean_VD_B1_L [kN]	0.6279	0.3661	0.3632	0.4119	0.4108
F_max_VD_B1_L [kN]	5.7143	1.7129	1.6909	3.6121	3.8905
F_mean_VD_B2_R [kN]	0.6268	0.3504	0.3406	0.4275	0.4391
F_max_VD_B2_R [kN]	4.7412	2.0226	2.2793	3.1899	3.5197
F_mean_VD_B2_L [kN]	0.6187	0.3559	0.3412	0.4283	0.4379
F_max_VD_B2_L [kN]	5.2267	1.8157	1.6817	2.8551	2.9135

The following table shows the sum of the forces in the anti-roll bar and damper. The forces are added with sign. The total forces are evaluated in each time sample, before calculating mean and maximum forces.

	Case 1	*Case 2*	*Case 3*	*Case 4*	*Case 5*
F_mean_B1_R [kN]	5.0988	23.002	32.008	6.2315	7.6347
F_max_B1_R [kN]	28.378	32.035	41.232	25.025	27.198
F_mean_B1_L [kN]	5.0990	23.013	32.025	6.2309	7.6325
F_max_B1_L [kN]	27.897	31.330	40.717	24.894	26.955
F_mean_B2_R [kN]	4.1173	22.940	31.897	5.8655	7.5468
F_max_B2_R [kN]	21.333	33.407	41.605	21.524	26.484
F_mean_B2_L [kN]	4.1125	22.961	31.928	5.8620	7.5453
F_max_B2_L [kN]	21.072	33.161	41.291	21.227	26.341

D.2 Ideal Power Dissipation in Anti-Roll Bar and Damper

The following table shows the mean and maximum powers in the anti-roll bar and damper, separately.

	Case 1	*Case 2*	*Case 3*	*Case 4*	*Case 5*
P_mean_ARB_B1_R [kW]	0.1843	0.4187	0.5817	0.1352	0.1624
P_max_ARB_B1_R [kW]	4.3051	2.5907	3.6525	3.0065	2.7924
P_mean_ARB_B1_L [kW]	0.1842	0.4583	0.6361	0.1382	0.1649
P_max_ARB_B1_L [kW]	3.5521	3.1055	4.0418	2.4493	2.1020
P_mean_ARB_B2_R [kW]	0.1483	0.4163	0.5628	0.1366	0.1780
P_max_ARB_B2_R [kW]	3.7406	2.3567	3.2387	2.0719	2.7155
P_mean_ARB_B2_L [kW]	0.1494	0.4424	0.5853	0.1362	0.1750
P_max_ARB_B2_L [kW]	4.3637	2.2949	2.8302	1.9171	2.3432
P_mean_VD_B1_R [kW]	0.0362	0.0108	0.0105	0.0152	0.0151
P_max_VD_B1_R [kW]	1.8701	0.2280	0.2293	0.7745	0.5050
P_mean_VD_B1_L [kW]	0.0360	0.0107	0.0105	0.0155	0.0153
P_max_VD_B1_L [kW]	1.6327	0.1467	0.1430	0.6524	0.7568
P_mean_VD_B2_R [kW]	0.0346	0.0102	0.0097	0.0159	0.0168
P_max_VD_B2_R [kW]	1.1240	0.2046	0.2598	0.5088	0.6194
P_mean_VD_B2_L [kW]	0.0342	0.0101	0.0092	0.0160	0.0168
P_max_VD_B2_L [kW]	1.3659	0.1648	0.1414	0.4076	0.4244

The following table shows the sum of the powers in the anti-roll bar and damper.

	Case 1	*Case 2*	*Case 3*	*Case 4*	*Case 5*
P_mean_B1_R [kW]	0.1838	0.4187	0.5817	0.1357	0.1616
P_max_B1_R [kW]	3.8135	2.7557	3.7976	2.7751	2.5880
P_mean_B1_L [kW]	0.1904	0.4585	0.6363	0.1395	0.1671
P_max_B1_L [kW]	4.0718	3.0722	4.0144	2.5590	2.3745
P_mean_B2_R [kW]	0.1508	0.4168	0.5632	0.1368	0.1760
P_max_B2_R [kW]	3.6918	2.3257	3.1737	2.0725	2.5205
P_mean_B2_L [kW]	0.1549	0.4422	0.5851	0.1389	0.1794
P_max_B2_L [kW]	4.5930	2.2715	2.7850	2.0006	2.6840

D.3 Passenger Comfort

This section lists the passenger comfort in the positions on the vehicle defined in Section 2.3, and for the cases defined in Section 5.3.1.

	Case 1	*Case 2*	*Case 3*	*Case 4*	*Case 5*
Wz_y_B1_C	2.8493	2.2937	2.2873	2.5062	2.3832
Wz_z_B1_C	2.4543	1.8947	1.8726	2.1225	2.0727
Wz_y_C_C	2.3194	1.8242	1.7905	2.0218	1.8486
Wz_z_C_C	1.9032	1.5526	1.5157	1.6690	1.6382
Wz_y_B2_C	2.8697	2.3652	2.2744	2.5071	2.3595
Wz_z_B2_C	2.4539	1.9386	1.8972	2.1519	2.1266
Wz_y_B1_R	2.8491	2.3008	2.3013	2.5334	2.4127
Wz_z_B1_R	2.4985	1.9824	1.9586	2.1624	2.1109
Wz_y_B1_L	2.8495	2.2982	2.2829	2.4789	2.3534
Wz_z_B1_L	2.4865	2.0140	2.0139	2.1582	2.1099

In the table below, the crest factors are stated. The time functions are mirrored in both ends before the filtering, in order to avoid transient errors. The mirroring does seem to be important in the beginning, but not in the end.

	Case 1	*Case 2*	*Case 3*	*Case 4*	*Case 5*
Crest_y_B1_C	4.7939	3.8523	3.6553	5.0996	5.2834
Crest_z_B1_C	6.4267	4.4509	4.1142	7.0556	5.9739
Crest_y_C_C	3.5844	4.8900	5.2593	3.5981	3.7331
Crest_z_C_C	5.2837	3.3719	3.9696	4.6705	5.2262
Crest_y_B2_C	5.3261	4.2478	4.3107	5.2438	5.0243
Crest_z_B2_C	6.2292	3.9855	3.8089	6.2513	5.3738
Crest_y_B1_R	4.7892	3.9592	3.5864	5.1634	5.3198
Crest_z_B1_R	6.4282	4.8932	4.6656	7.2541	5.6871
Crest_y_B1_L	4.7986	4.0145	3.7796	5.0266	5.2401
Crest_z_B1_L	6.7945	3.8018	3.8720	6.7957	5.6693

From the table the conclusion is drawn that the ride index, Wz, is calculated with sufficient accuracy.

D.4 Secondary Suspension Deflection

This table shows the deflection in the secondary suspension from the model setup. The deflections are presented at both the air-springs and the point half-way between the air-springs. Regarding the deflections at the air-springs, only the largest deflection is presented for each bogie. The deflection at any air-spring is labelled ”Side”. The deflections from the mean of the measured values are sometimes higher, sometimes lower, then the deflection from model setup.

	Case 1	*Case 2*	*Case 3*	*Case 4*	*Case 5*
Z_max_B1_C [mm]	20.6	10.6	10.9	15.4	16.0
Z_max_B1_Side [mm]	22.3	30.2	32.5	17.8	17.3
Z_max_B2_C [mm]	22.9	11.0	10.8	16.8	18.7
Z_max_B2_Side [mm]	26.5	25.8	23.6	18.0	21.1

D.5 Secondary Suspension Roll

	Case 1	*Case 2*	*Case 3*	*Case 4*	*Case 5*
Al_max_B1 [mrad]	12.3	32.5	34.6	9.8	11.2
Al_max_B2 [mrad]	8.7	27.1	23.5	8.8	10.0

references

bibliography

Ågren, J. (2004–2005). Private communication. Bombardier Transportation.

Anderson, B. and Moore, J. (1989). *Optimal control – linear quadratic methods*, Prentice-Hall, Englewood Cliffs, NJ, USA.

Andersson, E. and Berg, M. (1999). *Järnvägssystem och spårfordon*, Railway Group KTH, Stockholm, Sweden.

Andersson, E., Berg, M. and Stichel, S. (2004). *Rail Vehicle Dynamics*, Railway Group KTH, Stockholm, Sweden.

Bengtsson, V. and Weisstein, E. (2008). Diagonalizable matrix.
*http://mathworld.wolfram.com/DiagonalizableMatrix.html

Benner, P., Mehrmann, V., Sima, V., Huffel, S. V. and Varga, A. (1998). Slicot — a subroutine library in systems and control theory.
*citeseer.ist.psu.edu/benner97slicot.html

Breitholtz, C. (2009). Private communication. Chalmers University of Technology.

Glad, T. and Ljung, L. (1989). *Reglerteknik – Grundläggande teori*, Studentlitteratur, Lund, Sweden.

Glad, T. and Ljung, L. (2000). *Control Theory – Multivariable and Nonlinear Methods*, Studentlitteratur, Lund, Sweden.

Goodall, R. and Mei, T. (2006). Active suspensions, *in* S. Iwnicki (ed.), *Handbook of Railway Vehicle Dynamics*, pp. 327–357.

Intec GmbH (2003). Simpack training, Educational material.
*http://www.simpack.com/

Intec GmbH (2005). *SIMDOC 8.704*, Intec GmbH, Wessling, Germany.
*http://www.simpack.com/

Kjellqvist, P. (2002). *Modelling and design of electromechanical actuators for active suspension in rail vehicles*, PhD thesis, KTH Electrical Machines and Power Electronics, Stockholm, Sweden.

Lennartson, B. (2002). *Reglerteknikens grunder*, 4:th edn, Studentlitteratur, Lund, Sweden.

Mechanical vibration and shock - Evaluation of human exposure to whole-body vibration – Part 1: General requirements (1997). ISO 2631/1-1997(E).

Mechanical vibration and shock - Vibration and shock – Mechanical driving point impedance of the human body (1981). ISO 5982-1981(E).

Niconet (2005). *Slicot Manual*, Niconet.
*http://www.slicot.org/

Nordling, C. and Österman, J. (1996). *Physics Handbook for Science and Engineering*, 5:th edn, Studentlitteratur, Lund, Sweden.

Orlova, A. and Boronenko, Y. (2006). The anatomy of railway vehicle running gear, *in* S. Iwnicki (ed.), *Handbook of Railway Vehicle Dynamics*, pp. 39–84.

Råde, L. and Westergren, B. (1998). *Mathematics Handbook for Science and Engineering*, 4:th edn, Studentlitteratur, Lund, Sweden.

Roos, B. (2005). Private communication. Bombardier Transportation.

Sedra, A. and Smith, K. (1998). *Microelectronic Circuits*, 4:th edn, Oxford University Press.

Shinskey, F. (1996). *Process Control Systems – Application, Design, and Tuning*, McGraw-Hill.

Skogestad, S. and Postlethwaite, I. (1996). *Multivariable Feedback Control – Analysis and Design*, John Wiley & Sons.

The MathWorks (2007). *Matlab Manual*, The MathWorks.
*http://www.mathworks.com/

Varga, A. (2000). Model reduction software in the slicot library.
*citeseer.ist.psu.edu/varga00model.html

Zolotas, A., Pearson, J. and Goodall, R. (2006). Modelling requirements for the design of active stability control strategies for a high speed bogie, *Multibody System Dynamics* **15**: 51–66.